# Quantum Correlation And Decoherence In Quantum Computation

*by*

Hyungjun Lim

A dissertation submitted in partial fulfillment of
the requirements for the degree of

Doctor of Philosophy
(Physics)

*at the*
University of Wisconsin – Madison
2014

Defended on 30 July 2014
Dissertation approved by the following members of the Final Oral Committee:

Robert Joynt · Professor of Physics
Mark Friesen · Senior Scientist of Physics
Susan Coppersmith · Robert E. Fassnacht and Vilas Professor of Physics
Lisa Everett · Associate Professor of Physics
Mark A. Eriksson · Professor of Physics
Materials Science and Engineering

## Abstract

In this thesis, I will investigate the correlations in the noise source and in the qubit system. Although noise correlation is generally thought to be harmful, in a classical noise correlation model that I will suggest, it will be shown that the correlation of classical telegraph noise might actually lead to improved performance. On the other hand, quantum correlation between qubits seems to be a crucial part of quantum speed-up. The minimal involvement of quantum entanglement in certain quantum algorithms [1] led to the suggestion of the new type of quantum correlation, quantum discord. I will show that the calculation of the geometric global quantum discord is an NP-hard problem. For the states of the special form, I will suggest a numerical method to calculate geometric global quantum discord. It was shown that quantum discord persists longer under noisy environment than quantum entanglement and it suddenly changes its behavior and starts to decay faster (sudden transition) [2, 3]. The condition for this behavior had been shown for two-qubit Bell diagonal states[2], and I will show that the similar condition holds for the more general multi-partite state and randomly chosen 2-qubit states have only a small chance to observe the sudden transition and it becomes exponentially rarer as the number of qubits increases. Finally, I will investigate a two-qubit operation that induces quantum coherence using capacitive coupling. I will suggest that two-qubit operation based on capacitive coupling might be done more efficiently in a parameter regime previously not explored. But after considering more realistic restrictions such as slow quasi-static $1/f$ noise and finite pulse rise-time, I will show the two-qubit operation is not expected to perform sufficiently well.

## Acknowledgements

Over the past five years in Madison, Wisconsin, I have received support and encouragement from a great number of individuals. Firstly, I appreciate my advisor, Prof. Robert Joynt, for his guidance and support throughout my study. He always provided objective feedbacks to my work steering me away from logical leaps and mistakes in my research. He was always incredibly gentle and allowed me freedom to explore variety of topics before I jumped in more depth into one. And it was a rare support to receive as a theory student to be granted the research assistantship for the entire time. Also, I would like to thank my dissertation committee of Prof. Sue Coppersmith, Mark Friesen, Lisa Everett and Mark Eriksson for their support over the past years. Especially I would like to show my special gratitude to Prof. Lisa Everett for giving the wonderful quantum mechanics lectures during my first year. I thank Prof. Michael Ramsey-Musolf for being my supervisor for my high energy theory research. I appreciate Prof. Charlse Dyer and Jude Shavlik in computer science department for their superb machine learning courses and willingly writing a reference letter for my job search in software industry. I also thank Prof. Eric Bach in computer science department as well for his time he shared to discuss NP-hardness of the quantum discord calculation. I appreciate the physics department staffs who are working behind the curtain to keep this department in the best shape as one of the top research institutions in the country, especially I would like to show my gratitude to Renee Lefkow for being such a nice coordinator for graduate students (and it was always nice to visit her office as she keeps extra heaters there).

Eunsong Choi, Younghee Shin, Wittawat Saenrang and Xian Wu started the graduate study together here in Madison and it was such a huge support to see each other moving toward the finish of the degree programs in the one's perspective field of study. I appreciate Nga Nguyen, who is now in Los Alamos National Laboratory, for her comradeship as a post-doctoral researcher in the quantum computing theory group and a number of meaningful discussions we had together. I thank Jianjia who is sharing the same office to have answered my rudimentary questions when I started the quantum dot qubit project. I appreciate Kirit Makwana for being a nice classmate in the quantum field theory class and for the time we

spent discussing our careers and having a nice skiing trip. I appreciate Leonardo Rivera, who had been in Prof. Ramsey-Musolf's group together with whom I had meaningful talks about our research and career perspectives. I appreciate Chien-Yeah Seng and William Cottrel for being nice officemates in the high energy bullpen offices, I would dare to say they are one of the most passionate people I have met in my life-long journey. I appreciate Luca Sabbatini for being a nice classmate and being a support in the department. I appreciate the members of Japanese Karate Club of UW-Madison, of which I am the president, for giving me the opportunity to learn important things outside the classroom. I appreciate coach Corey Wayne who provided invaluable advices to overcome various hardships during my study. Lastly but not the leastly, I appreciate my families in South Korea for being my ultimate supporters and as I move forward further and further in my life, I just realize how strong and great people they are and how much blessed I am to have them in my life.

*"We're the middle children of the history man, no purpose or place, we have no Great war, no Great depression, our great war is a spiritual war, our great depression is our lives."*

Fight club

# Contents

# Chapter 1

# Background

## 1.1 Basic Idea Of Quantum Computation

In 1947, American computer engineer Howard Aiken, who had worked on the Harvard Mark II computer, said that just six digital computers would satisfy the computing needs of the whole United States. However, as we all know, such a prediction could not be further from what we have today. According to Moore's Law which states that the number of the transistors on a microprocessor doubles every 18 months, the circuits on the microprocessor would be on the atomic scale by 2030 from which further improvement of the processors based on traditional principles would be infeasible due to the basic physical limitations.

Quantum computer, on the other thand, is expected to overcome the limitation of digital computers by taking advantage of quantum mechanics. The idea of quantum computation was proposed in 1980's by Yuri Manin[4] and Richard Feynman[5, 6]. Quantum computers represent information using qubits, which can have 'superposed' value of 0 and 1. The point of this superposition can be naively described as following. A system composed of two classical bits can have four possible states (00, 01, 10, 11) of which only one can be chosen. The number of the possible states increases exponentially as the number of bits in the system increases while only one of them can be chosen. In contrast, a system composed of two quantum bits has a superposed state of the four states, where the collection of the

four states is called logical basis. As the size of the system (the number of the qubits) increases, the number of the possible states goes up exponentially as well and so does the number of logical states that can coexist in the superposition. Vaguely speaking, the power of quantum computers, so-called quantum speed-up, is displayed in the exponentially large representation capacity of a quantum system as, for instance, a single operation performed on such state results in the operation done on all the logical states composing the superposition at the same time. This is called quantum parallelism. However, qubits of the system need to be congruently connected to each other in order for such operation to have a meaningful consequence as otherwise each individual qubit would work as separate unit. Such connection, or quantum coherence, has been conjectured as the true resource for quantum computation [7–10]. Quantum entanglement has been investigated for a long time but as quantum algorithms which do not always incur quantum entanglement or involve only the minimum amount were found [1], a new type of quantum correlation, quantum discord, has been receiving much attention recently. Although there are some results relating the performance of the algorithm and the quantum correlations [7, 8, 11], it is generally unclear how quantum correlations can be quantitatively measured as computational resource.

## 1.2 Quantum Algorithms

Various quantum gates designed to perform operations on qubits have been proposed. The gates are described by time-dependent Hamiltonians and they can work as single-qubit gates or multi-qubits gates, and it was shown that single qubit gates (e.g. x-rotation and z-rotation) and C-NOT gates between any pair of qubits are sufficient to implement an arbitrary unitary operation on $N$ qubits [12]. Due to the inherently different nature of qubit and quantum gate from their classical counterparts, the tasks suggested with the quantum computing algorithms are typically very different from those for digital computers. I will look at simple algorithms devised for quantum computers in this section.

On the other hand, there is another approach to quantum computation, called adiabatic quantum computation, based on the adiabatic theorem [13]. In this approach, a Hamiltonian

is prepared such that its ground state describes the solution to the given problem. Additionally, a trivial and easily implementable Hamiltonian is given and the quantum system is initialized to its ground state. Then the simple initial Hamiltonian is adiabatically evolved to the complext Hamiltonian. The adiabatic theorem guarantees that the system remains in the ground state if the transform is slow enough, thus achieving the ground state of the final Hamiltonian, which represents the solution we seek. However, whether this approach conveys the true power of the quantum speed-up is an open question. First, as the size of the problem increases, the energy gap between the ground state and the next one tends to shrink in exponential fashion, thus the operational time, which is inversely proportional to the energy gap, increases exponentially as well. Secondly, as the proposed device only allows the interactions between adjacent pairs of qubits, configuring the final Hamiltonian in a way that can be realized on the device is a difficult challenge on its own. D-Wave Systems, a Canadian company has been working on making adiabatic quantum computer and made about 10 million US dollars deal with Lockheed-Martin in 2011 and Google also purchased a D-wave machine equipped with 512 qubits in 2013. However, as of now, whether the D-Wave computers offer quantum speedup is still unanswered and benchmarks performed by researchers at USC, ETH Zurich, and Google show that there is no strong evidence of a such speedup [14, 15]. In this paper, I will exclude the adiabatic quantum computing from the discussion and focus on the gate based quantum computation.

In this section, I will introduce quantum algorithms that show the idea of quantum parallelism(Deutsch's algorithm, section 1.2) and entanglement(quantum teleportation, section 1.2) in the context of quantum computation.

### Deutsch's Algorithm

Deutsch's Algorithm is a good example to demonstrate the superposition and quantum parallelism. We will have a chance to revisit this algorithm to investigate the role of entanglement in quantum algorithms later in Sec. 3.1. The task is to decide if a given function f that takes a binary number as input is balanced (f(0)=f(1)) or not (f(0)$\neq$f(1)). Obviously,

we need to evaluate the value of f twice (asking the oracle in possession of the function) to answer the question. However, this result can be improved using Deutsch's algorithm.

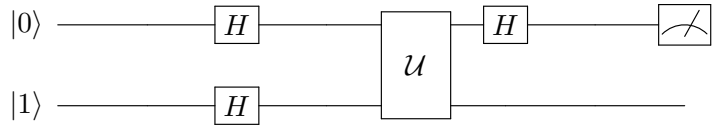


(1.1)

The quantum circuit for the algorithm is described in the diagram above. Two qubits are prepared in $|0\rangle \otimes |1\rangle$ state and Hadamard gates are applied to transform them into $|+\rangle \otimes |-\rangle = \frac{|0\rangle+|1\rangle}{\sqrt{2}} \otimes \frac{|0\rangle-|1\rangle}{\sqrt{2}} = \frac{|00\rangle-|01\rangle+|10\rangle-|11\rangle}{2}$. Here Hadamard gate performs the change of the basis: $|0\rangle \leftrightarrow |+\rangle$ and $|1\rangle \leftrightarrow |-\rangle$. For instance, it can be implemented as

$$U_{Hadamard} = \begin{pmatrix} \frac{1}{\sqrt{2}} & \frac{1}{\sqrt{2}} \\ \frac{1}{\sqrt{2}} & -\frac{1}{\sqrt{2}} \end{pmatrix}$$

Then an unitary operation is performed which takes two qubits as input $x, y$ and ouputs $x, f(x) \oplus y$. Depending on the function f's behavior the result would be either

$$\frac{|0\rangle + |1\rangle}{\sqrt{2}} \otimes \frac{|0\rangle - |1\rangle}{\sqrt{2}}, \textit{ if f(0)=f(1)}$$
$$\frac{|0\rangle - |1\rangle}{\sqrt{2}} \otimes \frac{|0\rangle - |1\rangle}{\sqrt{2}}, \textit{ if f(0)} \neq \textit{f(1)}$$

up to an overall phase factor. Then Hadamard is applied to the first qubit followed by a measurement. The measurement result would be $|0\rangle$ if the function is balanced and $|1\rangle$ otherwise. Thus, by applying the unitary operator just once (once again with the help of the oracle holding the function in her hand), we are able to tell if the function is balanced or not. This is an improvement over the classical case where we are supposed to make two references to the oracle. One may argue how the construction of such unitary operator is even possible without knowing the behavior of the function f itself after all. The rather artificial presence of the function f here is just to demonstrate the advantage of quantum algorithm over classical one, and we delegate the knowledge of the function to the presumed oracle who can evaluate the function and construct the unitary operator. In the algorithm, we can conceptually see how Hadamard gate prepares the superposed states of different input values and the unitary operator evaluates the function on two different values of input in a parallel fashion.

## Quantum Teleportation

In order to demonstrate how quantum entanglement can be involved in quantum algorithm, I would like to demonstrate quantum teleportation algorithm. The task is to transfer a given two level quantum system $|\Psi\rangle = \alpha|0\rangle + \beta|1\rangle$ into another system, possibly located at remote location. The quantum circuit for the algorithm is as following.

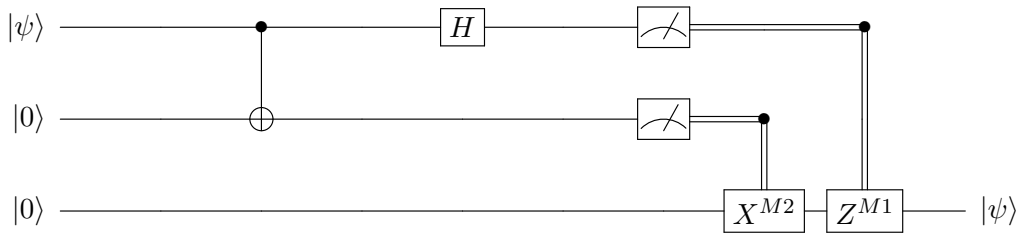


$|\Psi_1\rangle$ $|\Psi_2\rangle$ $|\Psi_3\rangle$

The state is initialized into $|\Psi\rangle \otimes |\Psi_+\rangle = (\alpha|0\rangle + \beta|1\rangle) \otimes \frac{1}{\sqrt{2}}(|00\rangle + |11\rangle)$. Note that here we have $|\Psi_+\rangle$, a maximally entangled Bell state. After a C-NOT gate is applied on the first and the second qubits, we have $|\Psi_1\rangle = \alpha|0\rangle \otimes \frac{1}{\sqrt{2}}(|00\rangle + |11\rangle) + \beta|1\rangle \otimes \frac{1}{\sqrt{2}}(|10\rangle + |01\rangle)$. After a Hadamard gate is applied on the first qubit, we have

$$\begin{aligned} |\Psi_2\rangle = \quad & \frac{1}{2}\alpha(|0\rangle + |1\rangle) \otimes (|00\rangle + |11\rangle) + \frac{1}{2}\beta(|0\rangle - |1\rangle) \otimes (|10\rangle + |01\rangle) \\ = \quad & \frac{1}{2}(|00\rangle \otimes (\alpha|0\rangle + \beta|1\rangle) + |01\rangle \otimes (\alpha|1\rangle + \beta|0\rangle) \\ & + |10\rangle \otimes (\alpha|0\rangle - \beta|1\rangle) + |11\rangle \otimes (\alpha|1\rangle - \beta|0\rangle)) \end{aligned}$$

Now the state of the last qubit depends on the value of the other two qubits. After measurements on the first two qubits are done, we can obtain the original state on the third qubit after applying the appropriate combination of x gate and z gate. By having an entangled pair prepared and 'consuming' it by making measurements, we have created an identical state. One might wonder if this allows transmission of information faster than light, violating the relativistic principle. This is not true as the algorithm involves measurements whose results must be transmitted via a classical channel which is limited by the speed of light.

## 1.3 Decoherence Of Quantum System

The technology to develop a practical quantum computer is beyond our reach for the time being. One of the key issues is the loss of quantum coherence, or so-called decoherence, through which a pure quantum system becomes an mixed ensemble of quantum states. To fight against decoherence, various error correction schemes based on the duplicated representation have been suggested [16] which thus require the presence of additional qubits besides the ones used as logical units of calculation, and it has been suggested that the implementation of interesting quantum algorithm would require about 50 qubits to work coherently to implement quantum algorithms [17]. In Section 1.3, I will talk about how to describe mixed quantum states and in Section 1.3, I will overview how undesirable interaction of the quantum system with its environment can lead to decoherence.

### Mixed Quantum States And Bloch Tensor Representation

In this section, I will talk about how to represent a mix quantum state. A closed quantum state evolves under Schoringer's equation with its time evolution operator written as $U(t) = e^{-iHt}$. The evolution of a closed quantum state described with the state vector can be equivalently described using quantum density operator, $\rho = |\psi\rangle \langle\psi|$, which evolves as $\rho(t) = U(t)\rho(0)U^{\dagger}(t)$. The definition of quantum system can be expanded to include an ensemble of different quantum systems (mixed state). The quantum density operator is the natural description for mixed quantum state with an ensemble being described as $\rho = \sum_k \lambda_k \rho_k$ where $\lambda_k$ is the probability density and $\rho_k$ is a pure quantum state. Pure quantum state corresponds to the case where there is only one state in the ensemble with $\lambda_0 = 1$. One difference between the purely classical probability distribution and ensembled quantum state is that each state in the quantum ensemble might be described in the different basis so that there is no choice of product space basis whose density operator corresponds to a classical distribution with no off-diagonal elements. This character of quantum system motivates the definition of quantum entanglement and quantum discord for multipartite quantum system.

The density matrix of a single qubit system can be written in the following well-known

form: $\rho = \frac{1}{2}(I + \sum_{a=1,2,3} n_a \sigma_a)$ where $\sigma_a$'s are the cartesian products of $N$ Pauli matrices. The condition $Tr(\rho^2) = Tr(\sum_k \lambda_k \rho_k)^2 = \sum_k \lambda_k^2 \leq 1$ requires $\sum_a n_a^2 \leq 1$ so that the three elements of $n_a$ can be well described as a three dimensional vector on or within an unit sphere, and it is called as Bloch vector. The Bloch vector description can be generallized to N qubit systems where

$$\rho = \frac{1}{2^N}( \sum_{a \in \{0,1,2,3\}^{\otimes N}} n_a \sigma_a)$$

with $n_{0^{\otimes N}} = 1$ and $\sum_a n_a^2 \leq 2^N$. In this case, $n_a$ has more than one indices so it is called Bloch tensor. Although the direct visualization of the N-qubit Bloch tensor is not viable, it is still often helpful to use Bloch tensor description as it has a good analogy to the Euclidean geometry of Bloch vector. For single-qubit case, the pure state corresponds to the surface of the Bloch sphere. For two-qubit case, the geometry of Bloch tensor is more involved and entails quantum correlations (entanglement and discord). A detailed analysis was done with respect to quantum correlation[18].

## System-environment Interaction And Decoherence

A closed pure quantum system separated from its environment evolves under its unitary time evolution operator as described above. In cosmological context, it is argued that the whole universe is a closed quantum system [19]. However, in the laboratory setting, it is virtually infeasible to block the system from any interaction with its surroundings and thus an open system that interacts with its environment must be taken into account. Due to the generally undesired interaction with the environment, the quantum system loses some of its information (coherence) and this process is called decoherence.

As a simple example, we can think of a two level quantum system $|\Psi(0)\rangle = |\Psi_{sys}\rangle \otimes |\Psi_{env}(0)\rangle = \alpha_0 |0\rangle \otimes |\Psi_{env}(0)\rangle + \beta_0 |1\rangle \otimes |\Psi_{env}(0)\rangle$ prepared initially separated from the environment ($Tr_{env}(|\rho(0)\rangle) = |\rho_{sys}\rangle$). Over the time, entanglement is formed between the system and the environment $\alpha(t) |0\rangle \otimes |\Psi_{0,env}\rangle + \beta(t) |1\rangle \otimes |\Psi_{1,env}\rangle$ and $Tr_{env}(|\rho(t)\rangle) =$

$$\begin{pmatrix} \alpha^2(t) & \alpha^*(t)\beta(t)\langle \Psi_{0,env} | \Psi_{1,env} \rangle \\ \beta^*(t)\alpha(t)\langle \Psi_{1,env} | \Psi_{0,env} \rangle & \beta^2(t) \end{pmatrix}$$

As the entanglement process proceeds, the entangled parts of the environment would be orthogonal to each other, thus eliminating the off-diagonal terms from the traced out density operator. As a result the quantum state of the system effectively losses quantum coherence and behaves as a mixed ensemble of two states.

As a specific example, the decoherence rate $\Lambda$ in a scattering process in a photon gas at temperature T where off diagonal terms $\langle x_1 |\rho| x_2 \rangle$ are damped by a factor of $e^{-\Lambda \Delta x^2 t}$ has been calculated [20], and shown to be $\Lambda \sim 10^{20}(\frac{T}{K})^9(\frac{a}{cm})^6 \frac{1}{cm^2 s}$ where $a$ is the radius of the object of interest. For an object of size $a = 10^{-6}$cm corresponding to a large molecule at $T =$ 3K (cosmic background radiation), we get $\Lambda \sim 10^6 cm^{-2} sec^{-1}$ and for a small dust particle of $a \sim 10^{-4}$cm, we get $\Lambda \sim 1 cm^{-2} sec^{-1}$ and at $T = 300$K, we get $\Lambda \sim 10^{18} cm^{-2} sec^{-1}$ so it takes subnano seconds for the particle to lose the coherence due to photon collison. In reality, a variety of sources contribute to decoherence making the process even more rapid. For a system at temperature $T = 300$K with mass of $\sim$ 1 g and $\Delta x = 1$ cm, $\tau_{Decoherece}/\tau_{Relaxation} \sim 10^{-40}$. Thus, even if the relaxation rate were of the order of the age of the Universe, quantum coherence would be destroyed in $\tau_{Relaxation} \sim 10^{-23}$sec[21].

It is also argued that the sudden collapse of wave function from quantum measurement can be viewed as the decoherence process[21]. The apparatus for measurement (weather it be instrument or our eyes) causes the entanglement of the system to the environment as described above and they are designed so that the process would take over really quickly and each member of the resulting ensemble corresponds to a measurement outcome. The transition of a pure quantum state into a classical ensemble accounts for the process of quantum measurement, but this description does not remove the probabilistic nature as the resultant state is a statistical ensemble. The collapsing wave function has been hunted by physicist ever since quantum mechanics was formulated in the early 20th century, and alternative explanations involve other hypotheses that are outside the scope of this thesis.

## 1.4 Implementation Of Quantum Computer

Several implementations of quantum gates have been made in the past [16, 22–25]. One promising candidate is electrons in semiconductor quantum dots[26]. The qubit logic might be implemented using the spin property of the electrons (spin qubit) or the location of the electrons in the quantum dots (charge qubit). Recent progress has demonstrated both spin- and charge-like qubit implementations in Si and GaAs. The control of one-qubit such as x-rotation and z-rotation are implemented using magnetic field gradiation and gate voltage control and the fidelity of those controls have been improved greatly recently [22–25]. The implementation of two-qubit gates, however, has not been investigated as much as one-qubit gates and at this moment is yet a more challenging task as its implementation is too complicated[27], the coupling between qubits is not strong enough to overcome decoherence [28].

## 1.5 Outline Of The Thesis

The thesis concerns the quantum correlations and decoherence in systems that are involved in quantum computation. The outline is as follows. Chapter 2 investigates the correlation of different noise sources. Multiple noises can occur concurrently and noise correlation and has been generally considered to do harm to the performance. Noise is described in terms of the interaction with the environment and I will compare environments described by classical and quantum variables. I will suggest a general model for the classical description which leads to the unexpected observation that noise correlation can suppress decoherence. Chapter 3 concerns the correlation between quantum registers, one type of which is quantum entanglement. This chapter focuses on recently suggested type of correlation called quantum discord, investigating methods for its calculation, which turns out to be NP-hard in general. Chapter 4 takes the investigation further to look at the dynamics of quantum discord under noise. Quantum discord was shown to have significantly different dynamics from quantum entanglement in certain condition[2], and I will suggest the condition of such behavior for

more general cases. Chapter 5 focuses on the experimental implementation of two-qubit operations in a double-quantum dot qubit system. I will suggest optimal point of operation based on the behavior of capacitive coupling between two qubits. But due to the large charge-noise decoherence rate and the weakness of the coupling, the optimal operation is not estimated to provide enough performance to lead to scalable implementation of qubits system. Chapter 6 summarizes the points of the thesis and provides the perspectives of the future works.

# Chapter 2

# Noise Correlation

## 2.1 Introduction

It is argued that about 50 $\sim$ 100 qubits are required to implement interesting quantum algorithms[17]. However, the complete isolation of the quantum system from the external environment is virtually unachievable due to the nearly unavoidable interaction with the environment, resulting in the system suffering from the decoherence of its quantum property[21]. In order to remedy the decoherence problem, various quantum error correction (QEC) schemes have been devised [16]. The simplest schemes fix only independently occurring single-qubit errors. Even the most sophisticated schemes fix errors that occur on a finite number of qubits. Therefore, the correlation of the noise source between different qubits is likely to cause more harm to the system than in the uncorrelated case as it is more likely to cause concurrent errors beyond the error correction scheme's capability. In this chapter, I will first use a leading-order approximation, in which noise correlation does indeed worsen decoherence. I then proceed to an exact solution, which gives an unexpected result: sometimes noise correlation reduces decoherence.

## 2.2 Fidelity To The Leading Order After Quantum Error Correction

We design a quantum algorithm so that the system composed of N qubits to be in the state $\rho_0$ in the absence of noise. But due to the inevitable interaction with the environment, the actual system would be $\rho_{err}$. To be specific, I will consider phase flip noise: $\rho_{err} = \sum_{a,b} p_{ab}\sigma_{z,a}\rho_0\sigma_{z,b}$, with $a, b \in \{0, z\}^N$. To protect the system from such errors, we might apply the error correction procedure. The procedure involves measurements (syndrome measurements) that provide the information to lead the following steps accordingly, and they remove the terms with unidentical operators on left and right side of $\rho$ ($a \neq b$). For instance, assuming all qubits are equivalent for simplicity, the density operator after the measurements is divided into the intact part, the terms with one-qubit error, with two-qubit errors, and so on: $\rho_{err,measured} = p_0\rho_0 + p_1\sum_i \sigma_{z,i}\rho_0\sigma_{z,i} + p_2\sum_{i,j(\neq i)} \sigma_{z,ij}\rho_0\sigma_{z,ij} + \cdots$. Further I will assume that the errors happen independently from each other with the chance of one qubit error p, $p_0 = (1-p)^N, p_1 = p(1-p)^{N-1}$, $\ldots$, $p_k = p^k(1-p)^{N-k}$. If, for instance, the error correction can fix one qubit error, we restore the terms involving the one qubit error, $p_1\sum_i \sigma_{z,i}\rho_0\sigma_{z,i} \to Np_1\rho_0$: $\rho_{cor} = (p_0 + Np_1)\rho_0 + p_2\sum_{i,j(\neq i)} \sigma_{z,ij}\rho_0\sigma_{z,ij} + \cdots$. I will use the fidelity measure from the ideal state $\rho_0$ in order to measure the impact of the error and the error correction. The fidelity between two states $\rho$ and $\sigma$ is defined as $F^2(\rho,\sigma) \equiv Tr(\sqrt{\rho}\sigma\sqrt{\rho})$, $0 \leq F \leq 1$, where $F = 1$ for two identical states[16, 29]. For one qubit case, $F^2$ has the simple interpretation using the inner product of the Bloch vectors of the two states that $F^2(\rho,\sigma) = \frac{1}{2}(1+\vec{v}_\rho\cdot\vec{v}_\sigma)$ where $\vec{v}_\rho$ and $\vec{v}_\sigma$ are the Bloch vectors of the states $\rho$ and $\sigma$. We would like $F$ from $\rho_0$ to be close enough to 1 for the practical implementation of quantum computing. It was shown that there is the critical point of the fidelity over which it can be improved with arbitrary precision by cascading quantum circuits[30]. We will assume the ideal state $\rho_0$ is a pure state $\rho_0 = |\psi\rangle\langle\psi|$. In this case, the fidelity between the ideal state $\rho_0$ and another state $\sigma$ is calculated simply by $F(|\psi\rangle\langle\psi|, \sigma) = \sqrt{\langle\psi|\sigma|\psi\rangle}$.

For $\sigma = p_0\rho_0 + p_1 \sum_i \sigma_{z,i}\rho_0\sigma_{z,i} + p_2 \sum_{i,j} \sigma_{z,ij}\rho_0\sigma_{z,ij} + \cdots$ with $\sum_{i=0}^{N} \begin{pmatrix} N \\ i \end{pmatrix} p_i = 1$,

$$F^2(|\psi\rangle\langle\psi|, \sigma) = \langle\psi|\sigma|\psi\rangle = p_0 + ANp_1 + A' \begin{pmatrix} N \\ 2 \end{pmatrix} p_2 + \cdots$$
$$= 1 - (1-A)Np_1 + O(p_2) \tag{2.1}$$

For instance, $F^2(\rho_0, \rho_{cor}) = 1 - (1-A) \begin{pmatrix} N \\ 2 \end{pmatrix} p_2 + O(p_3)$. The values of $0 \leq A, A', \cdots \leq 1$ depend on the property of the physical code used and represent the overlap of the ideal state and the uncorrected part. Now I will remove the assumption that errors on different qubits are independent from each other and investigate correlated noise.

### Quantum Error Correction And Bloch Tensor

The Bloch tensor is helpful to display the quantum error correction scheme. Let's assume as an example that we have a simple three-qubit repetition code where logical qubits are $|0_L\rangle = |000\rangle$ and $|1_L\rangle = |111\rangle$. This code can fix one qubit errors by measuring $\sigma_{1,z}\sigma_{2,z}$ and $\sigma_{2,z}\sigma_{3,z}$ and flipping appropriate qubits[16]. Now we have the state $|\Psi\rangle = \cos(\frac{\theta}{2})|000\rangle + e^{i\phi}\sin(\frac{\theta}{2})|111\rangle = \cos(\frac{\theta}{2})|0_L\rangle + e^{i\phi}\sin(\frac{\theta}{2})|1_L\rangle$. The Bloch tensor of this state can be grouped into four types as following:

$$\vec{n}_{xxx} \equiv (n_{xxx}, -n_{xyy}, -n_{yxy}, -n_{yyx}) = (1,1,1,1)\sin(\theta)\cos(\phi)$$
$$\vec{n}_{yyy} \equiv (-n_{yyy}, n_{yxx}, n_{xyx}, n_{xxy}) = (1,1,1,1)\sin(\theta)\sin(\phi)$$
$$\vec{n}_{III} \equiv (n_{III}, n_{Izz}, n_{zIz}, n_{zzI}) = (1,1,1,1)1$$
$$\vec{n}_{zzz} \equiv (n_{zzz}, n_{zII}, n_{IzI}, n_{IIz}) = (1,1,1,1)\cos(\theta)$$

After phase flip errors[16] are introduced to the system, the state becomes

$$\rho_{error} = p_0\rho + p_1(\rho_1 + \rho_2 + \rho_3) + p_2(\rho_{12} + \rho_{13} + \rho_{23}) + p_3\rho_{123} + \cdots$$

where $\cdots$ are the terms to be removed after the syndrome measurements, $p_i$ is the probability of $i$ errors occuring and $\rho_k$ is the state suffering from errors on the qubit $k$ ($\rho_k = \sigma_{k,z}\rho\sigma_{k,z}$).

Due to the nature of the phase flip error, only $\vec{n}_{zzz}$ vector is altered by the error and the way it changes depends on which qubits get influenced by the error.

$$1st : \vec{n}_{zzz} \to (-1,-1,1,1)\cos(\theta)$$

$$2nd : \vec{n}_{zzz} \to (-1,1,-1,1)\cos(\theta)$$

$$3rd : \vec{n}_{zzz} \to (-1,1,1,-1)\cos(\theta)$$

$$2nd, 3rd : \vec{n}_{zzz} \to (1,1,-1,-1)\cos(\theta)$$

$$1st, 3rd : \vec{n}_{zzz} \to (1,-1,1,-1)\cos(\theta)$$

$$1st, 2nd : \vec{n}_{zzz} \to (1,-1,-1,1)\cos(\theta)$$

$$1st, 2nd, 3rd : \vec{n}_{zzz} \to (-1,-1,-1,-1)\cos(\theta)$$

Thus, $\vec{n}_{zzz}$ vector after the error becomes

$$\vec{n}_{zzz} = \cos(\theta)((p_0 - p_3)(1,1,1,1) + (p_1 - p_2)(-1,-1,1,1) + (p_1 - p_2)(-1,1,-1,1) + (p_1 - p_2)(-1,1,1,-1))$$

where two terms in the same parenthesis are for the errors with the same syndrome result. (this error correction scheme can not tell the difference between one qubit error on the first qubit and two qubit errors on the second, third qubits). It is worth noting that the $\vec{n}_{zzz}$ vectors with different syndrome profiles are orthogonal to each other in the 4 dimensional Euclidean space.

For instance, let's assume that the syndrome measurement of $\sigma_{1,z}\sigma_{2,z}$ and $\sigma_{2,z}\sigma_{3,z}$ turns out to be $+,-$ (the same signs on the first measurement, and the opposite signs on the second). It means either one qubit error occurred on the first qubit or two qubits errors occurred on the second and the third qubits. Then we have $\vec{n}_{zzz,\pm} = \frac{r_1 - r_2}{r_1 + r_2}(-1,-1,1,1)$. What the error correction scheme does is to take $(-1,-1,1,1)$ back to $(1,1,1,1)$. But the state influenced by two or three qubits errors are rotated to the opposite direction $(-1,-1,-1,-1)$ so the final Bloch tensor is not fully recovered. Due to the multi-qubit error, we can not fully recover the state and instead we have $\vec{n}_{zzz,\pm,corrected} = \frac{r_1 - r_2}{r_1 + r_2}(1,1,1,1)$.

### Fidelity Calculation To The Leading Order

In order to see the impact of the error correlation, I will take a look at the leading order terms in the fidelity calculation. In order to see meaningful physics, I will introduce environment and its interaction with the system into the picture. The environment can be modeled using either quantum operators or classical variables. With the quantum operators, the Hamiltonian under consideration now includes the environment part: $H = \sum_i H_{sys,i} + H_{env} + \sum_i V_i$ where $V_i$ is the interaction term of the i'th qubit and $H_{sys,i}$ and $H_{env}$ are for the system and the environment without interaction. With the classical variables, Hamiltonian includes the interaction terms but does not describe the time evoluion of the environment and the time evolution of the classical variables is separately described. In both cases, the interaction term is written as $V_i = -\frac{1}{2} g_i s_i(t) \sigma_{z,i}$ where $s_i(t)$ could either be classical variable or quantum operator. We would use the interaction picture with $\sum_i H_{sys,i} = \sum_i -\vec{B}_i \cdot \vec{\sigma}_i$ and assume the initial time $t_0 = 0$. Then the time evolution operator for the system is $U(t) = T(e^{-i \int_{t_0=0}^{t} V_I(s) ds})$ where $V_I(s)$ is the interaction part of the Hamiltonian in the interaction picture and $T$ is the time ordering operator [31].

### Classical Model: Telegraph Noise Model

In classical models, $s_i(t)$ is a classcial variable and

$$U(t) = \Pi_i U_i(t) = \Pi_i \exp(i\theta_i(t)\frac{g_i t}{2}\sigma_{z,i}) = \Pi_i \left( \cos(\theta_i(t)\frac{g_i t}{2}) + i \sin(\theta_i(t)\frac{g_i t}{2})\sigma_{z,i} \right)$$

where $\theta_i(t) \equiv \frac{1}{t} \int_{t_0}^{t} s_i(s) ds$ is a unitless quantity. The behavior of the classical variable $s_i(t)$ is stochastic and I will take the average value of it for the description. This averaging is justified in the case where the measurement is performed multiple times to be averaged over or if the variable effectively displays the accumulated value from a large number of independent sources with the identical probabilistic property (self-averaging) thus the difference between a specific time evolution scenario and the averaged evolution is negligibly small. The validity of this assumption needs to be verified for specific models. If an error correction scheme

that can fix up to $t$ qubits error is applied, the state under this environment becomes

$$\rho_{cor} = \Big\langle \sum_{i=0}^{t} \sum_{|a|=i} \Pi_{k,a_k=0} cos^2(\tfrac{\theta_k gt}{2}) \Pi_{k,a_k=z} \sin^2(\tfrac{\theta_k gt}{2}) \rho_0$$
$$+ \sum_{i=t+1}^{N} \sum_{|a|=i} \Pi_{k,a_k=0} cos^2(\tfrac{\theta_k gt}{2}) \Pi_{k,a_k=z} \sin^2(\tfrac{\theta_k gt}{2}) \sigma_{z,a} \rho_0 \sigma_{z,a} \Big\rangle$$

where the first summation includes the corrected terms up to $t$ qubits errors, $a \in \{0, z\}^{\otimes N}$ is a N-dimensional vector, $|a|$ represents the number of z's in the indices of $a$. The second summation is for the terms with more than $t$ errors thus beyond the error correction scheme's restoration capability. The fidelity from the ideal state to this state is described in terms of how far it is from the ideal value of 1 due to the uncorrected terms in the second summation.

$$F^2(\rho_0, \rho_{cor}) = 1 - (1 - A) \sum_{i=t+1}^{N} \sum_{|a|=i} \big\langle \Pi_{k,a_k=0} cos^2(\frac{\theta_k gt}{2}) \Pi_{k,a_k=z} \sin^2(\frac{\theta_k gt}{2}) \big\rangle$$
$$= 1 - (1 - A)(\frac{gt}{2})^{2(t+1)} \sum_{|a|=t+1} \big\langle \Pi_{k,a_k=z} \theta_k^2 \big\rangle + O\Big( (gt)^{2(t+2)} \Big) \tag{2.2}$$

For instance, if we have a three-qubit system with the error correction sceheme that can fix one qubit errors (t=1),

$$F^2 = 1 - (1 - A)(\frac{1}{2} gt)^4 \big\langle \theta_1^2 \theta_2^2 + \theta_1^2 \theta_3^2 + \theta_2^2 \theta_3^2 \big\rangle + O\big((gt)^6\big) \tag{2.3}$$

As the expansion is written in terms of $\big\langle \theta_i^2 \theta_j^2 \big\rangle$, $(i \neq j)$, I will focus the evaluation of these terms for different environment models. It is also helpful for understanding the framework to take a look at the simple one qubit system without any error correction scheme, where we have $F^2 = \big\langle cos^2(\theta_1(t) \frac{g_1 t}{2}) + A \sin^2(\theta_1(t) \frac{g_1 t}{2}) \big\rangle = 1 - (1 - A) \big\langle sin^2(\theta_1(t) \frac{g_1 t}{2}) \big\rangle$. Assuming $A = 0$ for simplification, we have $F^2 = \frac{1 + \langle \cos(\theta_1(t) gt) \rangle}{2}$. In the limit $\gamma > g$ (non-Markovian limit), the flucuator does not change its value and $\theta(t) = \pm 1$, $\langle \cos(\theta_1(t) gt) \rangle = \cos(gt)$ so that F oscillates between 0 and 1. In the limit $\gamma \gg \frac{1}{t}$ (Markovian limit), the distribution of $\theta_1(t)$ spreads around 0 to the uniformity rapidly so that $F \to \frac{1}{2}$ as $\langle \cos(\theta_1(t) gt) \rangle$ decays to 0.

To be specific, I will investigate telegraph noise model as an example of classical noise model. This model was motivated by the study of 1/f noise which is claimed to be the major source of the dephasing in Josephson qubits where an ensemble of two-level systems

had been suggested as the source of the 1/f noise[32–36]. Here we make the weak coupling assumption that a large number of independent and weakly coupled fluctuators are summed to produce the 1/f spectrum noise. The result is self-averaing, thus it is safe to use the averaged time evolution to properly describe the behavior of the environment[33]. In this model, $s_i(t) = \pm 1$ (thus, $-1 \leq \theta_i(t) \equiv \frac{1}{t}\int_{t_0}^{t} s_i(s)ds \leq 1$) and each fluctuates at rate $\gamma$. As the fluctuator flips its value, it becomes more equally likely to be situated at either value over the time losing its correlation to the initial value. The time evolution of a fluctuator can be described as $\frac{ds(t)}{dt} = \begin{pmatrix} -\gamma & \gamma \\ \gamma & -\gamma \end{pmatrix} s(t)$ where $s(t) = \begin{pmatrix} p_+ \\ p_- \end{pmatrix}$ is two-dimensional vector to show the chance of the fluctuator to have the value of $\pm 1$. It can be readily shown that

$$\left\langle s(t_1)s(t_2)\right\rangle = \begin{pmatrix} 1 & 0 \end{pmatrix} e^{V|t_1-t_2|} \begin{pmatrix} 1 \\ 0 \end{pmatrix} - \begin{pmatrix} 0 & 1 \end{pmatrix} e^{V|t_1-t_2|} \begin{pmatrix} 1 \\ 0 \end{pmatrix} = e^{-2\gamma|t_1-t_2|}$$

and

$$\begin{aligned}
&\left\langle (s(t_1)s(t_2)s(t_3)s(t_4)\right\rangle \\
&= \begin{pmatrix} 1 & 0 \end{pmatrix} e^{V|t_1-t_2|} \begin{pmatrix} 1 \\ 0 \end{pmatrix} (\cdots)_{|t_1-t_2|\to|t_3-t_4|} + \begin{pmatrix} 0 & 1 \end{pmatrix} e^{V|t_1-t_2|} \begin{pmatrix} 0 \\ 1 \end{pmatrix} (\cdots)_{|t_1-t_2|\to|t_3-t_4|} \\
&-(\begin{pmatrix} 0 & 1 \end{pmatrix} e^{V|t_1-t_2|} \begin{pmatrix} 1 \\ 0 \end{pmatrix} \begin{pmatrix} 1 & 0 \end{pmatrix} e^{V|t_3-t_4|} \begin{pmatrix} 0 \\ 1 \end{pmatrix} + (\cdots)_{t_1\leftrightarrow t_3, t_2\leftrightarrow t_4}) \\
&= e^{-2\gamma|t_1-t_2|} e^{-2\gamma|t_3-t_4|}
\end{aligned}$$

where $e^{V|t|}$ is the exponential function of the matrix $V$.

While the time correlation is described using the parameter $\gamma$, we need to consider the spatial correlation between fluctuators interacting with the different qubits. The complete absence of the spatial correlation can be thought of each of independent N fluctuators $s_i(t)$ being coupled to each qubit. In this case $\left\langle \theta_i^2 \theta_{j\neq i}^2 \right\rangle_{ind} = \left\langle \theta_i^2 \right\rangle \left\langle \theta_j^2 \right\rangle$, and each average value

is

$$\langle\theta_i^2\rangle = \frac{1}{t}\int_0^t dt' \frac{1}{t}\int_0^t dt'' \langle s_i(t')s_j(t'')\rangle = \frac{1}{t}\int_0^t dt' \frac{1}{t}\int_0^t dt'' e^{-2\gamma|t'-t''|}$$
$$= \frac{1}{t^2}\int_0^t dt' e^{-2\gamma t'}\int_{t'}^t dt'' e^{-2\gamma t''}\delta_{t''>t'} + (t' \leftrightarrow t'') = \frac{1}{2(\gamma t)^2}\left(2\gamma t - (1-e^{-2\gamma t})\right) \quad (2.4)$$

On the other hand, completely spatially correlated noise can be thought of single fluctuator $s(t)$ coupled to all qubits, thus $s_i(t) \equiv s(t)$. In this case, the correlation function can be evaluated as

$$\langle\theta_i^2\theta_j^2\rangle_{cor} = \langle\theta^4\rangle = \frac{1}{t^4}\int_0^t dt_4 \int_{t_4}^t dt_3 \int_{t_3}^t dt_2 \int_{t_2}^t dt_1 e^{-2\gamma(t_1-t_2)}e^{-2\gamma(t_3-t_4)} \times 4!$$
$$= \frac{3}{2(\gamma t)^4}\left(2\gamma^2t^2 - 4\gamma t - e^{-2\gamma t}(2\gamma t+3)+3\right) \quad (2.5)$$

In comparison, $\langle\theta_i^2\theta_j^2\rangle_{ind} < \langle\theta_i^2\theta_j^2\rangle_{cor}$ and equivalently $F_{ind} > F_{cor}$. The result is expected as the correlated noise is reasoned to be more harmful because the correlated errors are more likely to occur simultaneously and go beyond the error correction scheme's capacity than when noise on individual qubit behaves independently. However, this is valid only when $gt$ is small and it deserves more detailed analysis which I will discuss in the later section.

It needs to be noted that the expansion of the $F^2$ has to be given in the power of $gt$ and $\gamma t$, instead of $t$ because $F^2$, $gt$ and $\gamma t$ are all unitless quantities. $\left\langle\theta_i^2\theta_j^2\right\rangle$ itself is a function of $\gamma t$ and as $\gamma = 0$ means no fluctuation ($\theta_i^2 = 1$), the expansion of $\langle\theta_i^2\theta_j^2\rangle$ in $\gamma t$ should be of the form $1+O(\gamma t)$. Therefore, if $F^2$ is expanded in $t$, we miss the fidelity difference between the correlated and the uncorrelated noises [37]. Indeed, $\langle\theta_1^2\theta_2^2\rangle_{ind} = 1 - \frac{4t\gamma}{3} + \frac{10t^2\gamma^2}{9} + O\left((\gamma t)^3\right)$ and $\langle\theta_1^2\theta_2^2\rangle_{ind} = 1 - \frac{4t\gamma}{5} + \frac{2t^2\gamma^2}{5} + O\left((\gamma t)^3\right)$ and they are simply 1 when $\gamma \to 0$.

## Quantum Model: Spin Boson Model

A bosonic bath (e.g. phonons, photons) environment in thermal equilibrium with temperature $\tau$, coupled to the qubits of the system is described using spin boson model. Now the Hamiltonian operator includes the environment part $H_{env} = \sum_{\mathbf{k}}(b_{\mathbf{k}}^\dagger b_{\mathbf{k}})\omega_{\mathbf{k}}$ where $b_{\mathbf{k}}^\dagger, b_{\mathbf{k}}$ are creator and annihilator operators of the mode $k$ of the bosonic environment, and the interaction part is $V = -\sum_i \sigma_{z,i}s_{Q,i}(t)$ with $s_{Q,i}(t) = \sum_{\mathbf{k}}\left(g_{\mathbf{k},i}e^{i\omega_{\mathbf{k}}t}b_{\mathbf{k}}^\dagger + g_{\mathbf{k},i}^* e^{-i\omega_{\mathbf{k}}t}b_{\mathbf{k}}\right)$ where

$g_{\mathbf{k},i}$ is the coupling constant between the bath mode $k$ and the qubit $i$ and $g_{\mathbf{k},i} = g_{\mathbf{k}} e^{i\mathbf{k}\cdot\mathbf{r_i}}$. We would evalute the time evolution operator $U(t) = T(e^{-i\int_{t_0=0}^{t} V_I(s)ds})$ where $V_I$ is the interaction part in interaction picture and $T$ is time ordering operator [31].

We might be tempted to do the calculation in the similar way as in the classical case, but the calculation is more involved as quantum operator does not commute in general. For instance, with one qubit error correction, $F^2 = 1 - (1-A)\left\langle \theta_1^2\theta_2^2 + \cdots \right\rangle$ does not lead to the correct result as now $s_i(t)$ consists of quantum operators $a_{\mathbf{k}}^\dagger$ and $a_{\mathbf{k}}$ which do not commute, so $U(t) = \exp(-i\int_{t_0}^{t}\sum_i V_{I,i}(s)ds) \neq \Pi_i \exp(-i\int_{t_0}^{t} H_{I,i}(s)ds)$ and special care should be taken to deal with this. According to Reina *et al.*[38, 39] (detailed derivation is given in Appendix A), with $\Phi(t) \equiv \sum_{m,n}\sum_k g_{\mathbf{k}}^2 2\cos(\mathbf{k}\cdot r_{mn})\sigma_{z,m}\sigma_{z,n}\frac{\omega_{\mathbf{k}}t - \sin(\omega_{\mathbf{k}}t)}{\omega_{\mathbf{k}}^2}$, and $A_{\mathbf{k}} \equiv g_{\mathbf{k}}\phi_{\mathbf{k}}^* b_{\mathbf{k}}\sigma_{z,\mathbf{k}}$, $\phi_{\mathbf{k}}(t) \equiv \frac{1-e^{i\omega_{\mathbf{k}}t}}{\omega_{\mathbf{k}}} = \frac{1}{i}\int_{t_0}^{t} e^{i\omega_{\mathbf{k}}t'}dt'$ and $B_n(t) = \sum_{\mathbf{k}}(-i)g_{\mathbf{k}}(\phi_{\mathbf{k}}(t)b_{\mathbf{k}}^\dagger e^{-i\mathbf{k}\cdot\mathbf{r_n}} - \phi_{\mathbf{k}}^* b_{\mathbf{k}} e^{i\mathbf{k}\cdot\mathbf{r_n}})$,

$$\begin{aligned} U_I &= e^{i\Phi(t)} e^{\sum_{\mathbf{k}}(A_{\mathbf{k}}^\dagger(t) - A_{\mathbf{k}}(t))} \\ &\equiv e^{i\Phi(t)} e^{i\sum_n B_n(t)\sigma_{z,n}} \end{aligned}$$

where $m, n$ indices stand for qubits. The commutator of $iB$'s is,

$$[iB_m(t), iB_n(t)] = -\sum_{\mathbf{k}} g_{\mathbf{k}}^2 |\phi_{\mathbf{k}}|^2 2i\sin(\mathbf{k}\cdot\mathbf{r_{mn}})$$

and applying the Baker-Campbell-Hausdorff formula $e^{A+B} = e^A e^B e^{-\frac{1}{2}[A,B]}$, it can be rewritten as

$$\begin{aligned} U_I &= e^{i\Phi(t)} e^{i\sum_n B_n(t)\sigma_{z,n}} \\ &= e^{i\sum_{m<n} D_{mn}(t)\sigma_{z,m}\sigma_{z,n}} \times \Pi_n e^{iB_n(t)\sigma_{z,n}} \end{aligned} \tag{2.6}$$

where $D_{mn}$ is given in Appendix A. Thus due to the bosonic part operator commutation relation, we have the extra factor $e^{i\sum_{m,n} D_{mn}(t)\sigma_{z,m}\sigma_{z,n}}$ in addition to the classical case of $U(t) = \Pi_n U_n(t)$. For instance, if we have three-qubit system with one qubit error correction, the fidelity is

$$F^2 = 1 - (1-A)\left\langle D_{12}^2 + D_{13}^2 + D_{23}^2 + B_1^2 B_2^2 + B_1^2 B_3^2 + B_2^2 B_3^2 \right\rangle + O\left((gt)^6\right) \tag{2.7}$$

The average values can be evaluated as,

$$\begin{aligned}
\left\langle B_m^2 B_n^2 \right\rangle &= \left\langle \left( \int_{t_0}^{t} s_{Q,m}(t')dt' \right)^2 \left( \int_{t_0}^{t} s_{Q,n}(t')dt' \right)^2 \right\rangle \\
&= (i)^4 \big\langle (\textstyle\sum_{\mathbf{k_1}} g_{\mathbf{k_1}} (e^{-i\mathbf{k_1}\cdot\mathbf{r_m}} \phi_{\omega_{\mathbf{k_1}}}(t) b^\dagger_{\mathbf{k_1}} - e^{i\mathbf{k_1}\cdot\mathbf{r_m}} \phi^*_{\omega_{\mathbf{k_1}}}(t) b_{\mathbf{k_1}})) \times \\
&\quad (\textstyle\sum_{\mathbf{k_2}} g_{\mathbf{k_2}} (e^{-i\mathbf{k_2}\cdot\mathbf{r_m}} \phi_{\omega_{\mathbf{k_2}}}(t) b^\dagger_{\mathbf{k_2}} - e^{i\mathbf{k_2}\cdot\mathbf{r_m}} \phi^*_{\omega_{\mathbf{k_2}}}(t) b_{\mathbf{k_2}})) \times \\
&\quad (\textstyle\sum_{\mathbf{k_3}} g_{\mathbf{k_3}} (e^{-i\mathbf{k_3}\cdot\mathbf{r_n}} \phi_{\omega_{\mathbf{k_3}}}(t) b^\dagger_{\mathbf{k_3}} - e^{i\mathbf{k_3}\cdot\mathbf{r_n}} \phi^*_{\omega_{\mathbf{k_3}}}(t) b_{\mathbf{k_3}})) \times \\
&\quad (\textstyle\sum_{\mathbf{k_4}} g_{\mathbf{k_4}} (e^{-i\mathbf{k_4}\cdot\mathbf{r_n}} \phi_{\omega_{\mathbf{k_4}}}(t) b^\dagger_{\mathbf{k_4}} - e^{i\mathbf{k_4}\cdot\mathbf{r_n}} \phi^*_{\omega_{\mathbf{k_4}}}(t) b_{\mathbf{k_4}}))\big\rangle
\end{aligned}$$

which can be written using Wick's theorem[12] as,

$$\begin{aligned}
&= \left( \sum_{\mathbf{k}} g_{\mathbf{k}}^2 |\phi_{\omega_{\mathbf{k}}}(t)|^2 \big\langle \{b_{\mathbf{k}}, b^\dagger_{\mathbf{k}}\} \big\rangle \right)^2 \\
&+2 \times \left( \sum_{\mathbf{k},\mathbf{k'}} g_{\mathbf{k}} g_{\mathbf{k'}} \delta_{\mathbf{k},\mathbf{k'}} \big\langle (e^{-i\mathbf{k}\cdot\mathbf{r_m}} \phi_{\mathbf{k}}(t) b^\dagger_{\mathbf{k}} - e^{i\mathbf{k}\cdot\mathbf{r_m}} \phi_{\mathbf{k}}(t)^* b_{\mathbf{k}}) \right. \\
&\left. (e^{-i\mathbf{k'}\cdot\mathbf{r_m}} \phi_{\mathbf{k'}}(t) b^\dagger_{\mathbf{k'}} - e^{i\mathbf{k'}\cdot\mathbf{r_m}} \phi_{\mathbf{k'}}(t)^* b_{\mathbf{k'}}) \big\rangle \right)^2 \\
&= \left( \sum_{\mathbf{k}} g_{\mathbf{k}}^2 |\phi_{\omega_{\mathbf{k}}}(t)|^2 \big\langle \{b_{\mathbf{k}}, b^\dagger_{\mathbf{k}}\} \big\rangle \right)^2 \\
&+2 \times \left( \sum_{\mathbf{k}} g_{\mathbf{k}}^2 |\phi_{\omega_{\mathbf{k}}}(t)|^2 (\cos(\mathbf{k}\cdot\mathbf{r_{mn}}) \left\langle \{b_{\mathbf{k}}, b^\dagger_{\mathbf{k}}\} \right\rangle + \sin(\mathbf{k}\cdot\mathbf{r_{mn}}) \left\langle [b_{\mathbf{k}}, b^\dagger_{\mathbf{k}}] \right\rangle) \right)^2
\end{aligned}$$

Here we have $\big\langle \{b_{\mathbf{k}}, b^\dagger_{\mathbf{k}}\} \big\rangle = 2\coth(\frac{\omega_k}{\tau})$ [35, 39, 40]. Also, if we take the continuum limit of the momentum $\mathbf{k}$, the sum over $\mathbf{k}$, $\sum_{\mathbf{k}}$ becomes integration $\int dk \int d\Omega_{\mathbf{k}}$. The angular part of the integral eliminates $\sin(\mathbf{k}\cdot\mathbf{r_{mn}})$ and turns $\cos(\mathbf{k}\cdot\mathbf{r_{mn}})$ into $4\pi\frac{\sin(kr_{mn})}{kr_{mn}}$. And the integration over the radial part $\int dk$ can be replaced by the integration over $\omega$ with spectral density given as $\frac{A(\omega)}{4\pi}\omega^s$. Thus, the average value becomes

$$\begin{aligned}
\left\langle B_m^2 B_n^2 \right\rangle &= \left( \int d\omega A(\omega)\omega^s 2 \frac{1-\cos(\omega t)}{\omega^2} 2\coth(\frac{\omega}{2\tau}) \right)^2 + 2 \times \\
&\left( \int d\omega A(\omega)\omega^s 2 \frac{1-\cos(\omega t)}{\omega^2} 2\coth(\frac{\omega}{2\tau}) \frac{\sin(k_\omega r_{mn})}{k_\omega r_{mn}} \right)^2 \qquad (2.8) \\
&\equiv \Gamma_0^2 + 2\Gamma_{r_{mn}}^2 \qquad (2.9)
\end{aligned}$$

We also have additional contribution from $D_{mn}(t)$,

$$\left\langle D_{mn}^2 \right\rangle = \left( \int d\omega A(\omega)\omega^s \frac{\omega_k t - \sin(\omega_k t)}{\omega_k^2} \frac{\sin(k_\omega r_{mn})}{k_\omega r_{mn}} \right)^2 \equiv \Gamma'^2_{r_{mn}} \qquad (2.10)$$

All things together Eq. 2.7 becomes

$$F^2 = \quad 1-(1-A)\Big(3\Gamma_0^2+2\big(\Gamma_{r_{12}}^2+\Gamma_{r_{13}}^2+\Gamma_{r_{23}}^2\big) \\ +\big(\Gamma_{r_{12}}'^2+\Gamma_{r_{13}}'^2+\Gamma_{r_{23}}'^2\big)\Big)+O\left((gt)^6\right) \tag{2.11}$$

Note that $\Gamma_r'$ from $D_{mn}(t)$ is independent on the temperature thus it is a pure quantum mechanical quantity.

In this model, the noise correlation between qubit $m$ and $n$ is described by the distance between them, $r_{mn}$. Larger noise correlation (with smaller $r_{mn}$ value) lowers the fidelity. As we have seen from both classical spin fluctuator model and quantum spin boson model, noise correlation is harmful in leading order approximation limit. It is worthwhile mentioning that as in the spin fluctuator model, the expansion has to be made in the order of $gt$, instead of $t$ as the leading order terms in the expansion with t would miss $\Gamma_r'$ for $\Gamma_0 \sim \Gamma_r \sim O(g^2t^2)$ and $\Gamma_r' \sim O(g^2t^3\omega)$.

## 2.3 Non-perturbative Fidelity Calculation

In this section we show how to analyze the sensitivity of the decoherence to the extent of correlation in classical model for a simple but non-trivial model. This model has the virtue that the correlation strength can be measured by a single parameter.

### Multiqubit Asymptotic Behavior

Let's assume a simple error model for the $N$-qubit system where we have an error correction scheme that can correct up to $t$ qubits errors and errors occur on each qubit independently with probability $p$. The fidelity of Eq. 2.1 (with $A = 0$ for simplicity) becomes

$$F^2 = \sum_{k=0}^{t} \begin{pmatrix} N \\ k \end{pmatrix} p^k (1-p)^{N-k} \tag{2.12}$$

In $N \to \infty$ limit,

$$F^2 = \begin{cases} 1, & \text{if } p < q(\equiv \frac{t}{N}) \\ 0, & \text{if } p \geq q \end{cases} \tag{2.13}$$

The probability distribution for the number of errors spreads with a standard deviation that scales as $\sim \sqrt{N}$ while the gap between the bound of the summation and the peak of the probability distribution $|t - Np|$ scales as $\sim N$ so as $N$ becomes large the summation either covers the whole range of non-zero probability around the average value $Np$ or does not cover it at all. The limit of the large number of qubits is worth investigating as the practical quantum computer is expected to need at least $50 \sim 100$ qubits[17]. I will proceed to the analytic solution of the telegraph noise model for the in detail analysis in this large $N$ limit.

### Analytic Solution of Telegraph Noise Decoherence

We can obtain the analytical solution for the dynamics of a qubit system coupled to a single fluctuator. One approach is the transfer matrix method[41–43] (Appendix B) where the state density matrix and fluctuator state together are regarded as a vector and linear differential equation is solved for the system and fluctuator. In another approach, the solution can be obtained by tossing a coin to decide the value of fluctuator at each time step (telegraph process [34, 35]) and the probability distribution of $\theta$ can be obtained and used to get the solution. I will take the random walk approach. Bergli *et al.*[34, 35] have shown the distribution function

$$\begin{aligned} Pr(\theta) &= \int \frac{dk}{2\pi} e^{ik\theta} e^{-\gamma t} \Big[ \cos\left(\gamma t \sqrt{\left(\frac{k}{\gamma t}\right)^2 - 1}\right) \\ &+ \frac{1}{\sqrt{\left(\frac{k}{\gamma t}\right)^2 - 1}} \sin\left(\gamma t \sqrt{\left(\frac{k}{\gamma t}\right)^2 - 1}\right) \Big] \\ &= \frac{1}{2}\gamma t e^{-\gamma t}\left(\frac{I_1(\gamma t\sqrt{1-\theta^2})}{\sqrt{1-\theta^2}} + I_0(\gamma t\sqrt{1-\theta^2})\right)\delta(|\theta| < 1) \\ &+ \frac{1}{2} e^{-\gamma t}(\delta(\theta - 1) + \delta(\theta + 1)) \end{aligned} \tag{2.14}$$

where $I_n$'s are the modified Bessel functions of the first kind. Then $\rho_{error} = \sum_k prob_k U_k \rho U_k^\dagger = \int_{-\infty}^{\infty} d\theta Pr(\theta) e^{i\theta(t)\frac{gt}{2}\sigma_z} \rho e^{-i\theta(t)\frac{gt}{2}\sigma_z}$. Using this, for qubits coupled to a single fluctuator, we

have $\rho'_{\mu\nu} = \rho_{\mu\nu}\zeta_{\mu\nu}$, with

$$\begin{aligned}\zeta_{\mu\nu} &= e^{-\gamma t}\big[\cos(\sqrt{{g_{\mu\nu}}^2-\gamma^2}t) + \frac{\sin(\sqrt{{g_{\mu\nu}}^2-\gamma^2}t)}{\sqrt{(\frac{g_{\mu\nu}}{\gamma})^2-1}}\big] \\ &= e^{-\gamma t}\big[\cosh(\sqrt{\gamma^2-{g_{\mu\nu}}^2}t) + \frac{\sinh(\sqrt{\gamma^2-{g_{\mu\nu}}^2}t)}{\sqrt{1-(\frac{g_{\mu\nu}}{\gamma})^2}}\big]\end{aligned} \tag{2.15}$$

where $\mu, \nu \in \{-1, +1\}^N$ are indices in the z spin basis, and $g_{\mu\nu} = g(\sum_i \delta_{\mu_i,(+1)} - \sum_i \delta_{\nu_i,(+1)})$[34, 35, 44].

In Gaussian limit ($\gamma t > 1$), $Pr(\theta) \cong \frac{1}{\sqrt{2\pi(\frac{1}{\gamma t})}} e^{-\frac{\theta^2}{2\frac{1}{\gamma t}}}$ using $I_n(x >> 1) \cong \frac{1}{\sqrt{2\pi x}e^x}$. It is worth noting that Gaussian approximation $\gamma t > 1$ is applicable only when Markovian approximation $\gamma > g$ condition is met. Markovian approximation applies when $\gamma > g$ where the decoherence behaviros is display in the monotonic exponential decay. On the other hand, Gaussian approximation applies when $\gamma t > 1$ where we can assume $Pr(\theta)$ to be a Gaussian distribution function. The decay rate of $\zeta$ is $\gamma\sqrt{1-\sqrt{1-(\frac{g}{\gamma})^2}}$ and it approaches $\frac{\gamma}{2}(\frac{g}{\gamma})^2$ in the Markovian limit, which is the decay rate in the Gaussian appoximation. Bergli *et al.* made an observation that the size of $\delta$ function part (which is not part of Gaussian distrubution) of $Pr(\theta)$ diminishes to negligible size when $\gamma > g$ and thus $\gamma > g$ condition is required for Gaussian approxomation. However, the $\delta$ function part is actually, independent of $g$, of the size $e^{-\gamma t}$ thus I find the argument not convincing. Instead, in non-Markovian, Gaussian regime, the decay function $\zeta \sim e^{-\gamma t}$ is already substantially diminished from 1, so that the decay rate should be decided in the regime where Gaussian approximation is not valid. On the other hand, in Markovian regime $\frac{g}{\gamma}$ factor offsets $\gamma t$ and $\zeta \sim e^{-\frac{\gamma t}{2}(\frac{g}{\gamma})^2} \sim O(1)$ even in Gaussian regime $\gamma t > 1$ so the decay rate can be calculated with the Gaussian approximation. Therefore, the Gaussian approximation decay rate is applicable only in Markovian regime.

In order to investigate the impact of error correlation, I will propose a classical noise correlation model: $Pr(\vec{\theta}) = \int_{-\infty}^{\infty} d\theta Pr(\theta)\Pi_i \left(r\delta(\theta-\theta_i) + (1-r)Pr(\theta_i)\right)$. Each $\theta_i$ is independent and has identical problabilty density distribution to $\theta$ with average value $\langle\theta\rangle = 0$

and $0 \leq r \leq 1$. The parameter $r$ is our measure of how correlated the noises. This way we can handle neither completely correlated nor completely independent noise correlation. This model satisfies the linear cross approximation[45], meaning the correlation between two environment variables has the linear dependence on $r$.

$$\begin{aligned}
&\langle \theta_i \theta_{j\neq i} \rangle = \int Pr(\vec{\theta}) \theta_i \theta_j d\vec{\theta} \\
&= \int_{-\infty}^{\infty} d\theta Pr(\theta) \int_{-\infty}^{\infty} d\theta_i \theta_i (r\delta(\theta - \theta_i) + (1-r) Pr(\theta_i)) \\
&\int_{-\infty}^{\infty} d\theta_j \theta_j (r\delta(\theta - \theta_j) + (1-r) Pr(\theta_j)) \\
&\Pi_{k\neq i,j} \int_{-\infty}^{\infty} d\theta_k (r\delta(\theta - \theta_k) + (1-r) Pr(\theta_k) = 1) \\
&= \int_{-\infty}^{\infty} d\theta Pr(\theta) (r\theta + (1-r)\langle \theta \rangle)(r\theta + (1-r)\langle \theta \rangle) \\
&= r\langle \theta^2 \rangle
\end{aligned}$$

and

$$\begin{aligned}
&\langle \theta_i \theta_i \rangle = \int_{-\infty}^{\infty} Pr(\theta) \\
&\int_{-\infty}^{\infty} d\theta_i \theta_i^2 (r\delta(\theta - \theta_i) + (1-r) Pr(\theta_i)) = \langle \theta^2 \rangle
\end{aligned}$$

With the suggested noise correlation model, the state under the influence of the noise can be written

$$\rho_{error} = \sum_{\nu,\nu'} r_{\nu,\nu'} \sigma_\nu \rho \sigma_{\nu'}$$

with

$$\begin{aligned}
r_{\nu,\nu} \quad &= \int d\vec{\theta} Pr(\vec{\theta}) \Pi_{i,\nu_i=1} \left( \frac{1 - \cos(\theta_i g t)}{2} \right) \Pi_{i,\nu_i=0} \left( \frac{1 + \cos(\theta_i g t)}{2} \right) \\
&= \int d\theta Pr(\theta) p'(\theta)^{|\nu|} (1 - p'(\theta))^{N - |\nu|}
\end{aligned}$$

with $p' \equiv r\frac{1-\cos(\theta g t)}{2} + (1-r)p_0 > q$ where $p_0$ is the value for the independent noise case ($r = 0$). Note the resemblence to the simple noise case Eq. (2.12). If I introduce a t-qubit

error correction scheme, the fidelity becomes

$$F^2(\rho,\rho_{cor}) = \sum_{k=0}^{t} \begin{pmatrix} N \\ k \end{pmatrix} r_{\nu\nu,|\nu|=k}$$
$$= \sum_{k=0}^{t} \int d\theta \begin{pmatrix} N \\ k \end{pmatrix} p'(\theta)^{|\nu|}(1-p'(\theta))^{n-|\nu|}$$

In the $N \to \infty$ limit, the only non vanishing terms are those for which $p' > q$ where $q = \frac{t}{N}$ is defined in Eq. 2.13

$$F^2 \xrightarrow[N\to\infty]{} \int_{p'<q} d\theta Pr(\theta)$$

As $p'$ can be thought of as effective error probability, we can think only the $\theta$ value that does not cause the error probability to exceed the error correction capacity $q$, contributes to the fidelity. If the interaction coupling and time period t are small enough $gt\theta < gt << 1$, the $p' \equiv r\frac{1-\cos(\theta gt)}{2} + (1-r)p_0 < q$ condition becomes

$$\frac{1-\cos(\theta gt)}{2} \cong (\theta\frac{gt}{2})^2 < \frac{q-(1-r)p_0}{r} \tag{2.16}$$

In the Gaussian limit $\gamma t > 1$, $\theta$ has Gaussian distribution $N(0,\frac{1}{\sqrt{\gamma t}})$. Finally,

$$1-F^2 = Pr(\frac{2}{gt}\sqrt{\frac{q-(1-r)p_0}{r}} < |\theta| < 1)$$
$$\equiv Pr(1-\epsilon < |\theta| < 1) \tag{2.17}$$

It is worthy noting that if $p_0 > \frac{q}{1-r}$, the inequality Eq.(2.16) is never fulfilled that the fidelity becomes 0. On the other hand, as $|\theta|$ is bounded by 1, if $p_0 < \frac{q-r(\frac{gt}{2})^2}{1-r}$, the inequality Eq.(2.16) is always met so the fidelity becomes 1. Figure 2.1 shows these two limits for varying correlation $r$ parameter. One very surprising point is that the noise correlation can actually be beneficial. As shown in the leading order approximation, the noise correlation is harmful for the performance. But in my error correlation model, it is shown in Figure 2.1 that increasing $r$ value allows larger $p_0$ value from which the fidelity vanishes and also larger $p_0$ value to have the ideal fidelity of 1. This happens because, with the correlated noise ($r > 0$), $p_0 > q$ does not lead to $p' > q$ as $(\frac{gt\theta}{2})^2 < \frac{q-(1-r)p_0}{r} (> 0)$ unless $p_0 > \frac{q}{1-r}$,

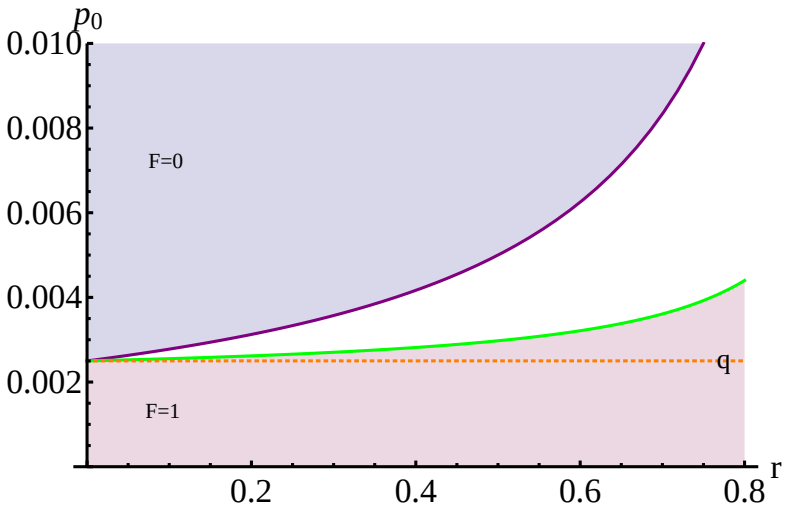


Figure 2.1: $p_0$ is the uncorrelated error probability on individual qubit. $0 < r < 1$ is the noise correlation parameter. Increasing $r$ value allows larger $p_0$ value from which the fidelity vanishes and also larger $p_0$ value to have the ideal fidelity of 1. The fidelity is loast only when the error probability $p_0$ is larger than the chance of correcting error $q \equiv \frac{t}{N}$ where $t$ is the number of errors that the error correction scheme can fix. The result was obtained with Gaussian approximation $\gamma t \gg 1$ and $gt \ll 1$ so $\frac{1-\cos(\theta gt)}{2} \sim (\frac{\theta gt}{2})^2$.

so some value of $\theta$ satisfies the above inequality contributing positive fidelity $F^2 > 0$. Part of the qubits starts behaving as one unit to some degree due to correlation, so that for the environment that would fail the individual qubit, there exists chance for the group of the qubit to remain coherent. It needs to be noted that as it was shown as a particular choice of classical model, it is not clear if this is the general behavior. One should note this beneficial effect of noise correlation in quantum environments as been noted in some previous work [46] as well, and can be due to the existence of decoherence-free subspaces (DFS). However, that does not appear to true in our case, since DFS effects would normally show up at all orders

## 2.4 Summary

I investigated the classical telegraph noise model and the quantum spin boson model environments and showed that the noise correlation lowers the fidelity measure from the ideal

case in the leading order calculation for both models. It is important to expand in the parameter gt instead of $t$ for the correct comparison. However, it appears that the general conclusion that correlation always destroys coherence is an artifact of the approximations in the calculation. In an exactly solvable model of correlated telegraphic noise, I showed that correlations could actually preserve coherence.

# Chapter 3

# Quantum Discord

## 3.1 Introduction

The term quantum entanglement was coined by Erwin Schrodinger who called it "the characteristic trait of quantum mechanics". Conceptually, quantum entanglement arises when the "joint" events states get superpositioned. For instance, the two-qubit state $|\psi\rangle = \frac{1}{\sqrt{2}}(|00\rangle + e^{\imath\phi}|11\rangle)$ involves the maximum amount of quantum entanglement. Entanglement is a unique property of composite quantum systems and it is known to be essential for certain quantum communication protocols [7, 8].

I will discuss an example to show Entanglement gives quantum systems the non-classical property that classical system does not have indeed. In 1935, Albert Eignstein, Boris Podolsky, and Nathan Rosen (collectively referred to as EPR) authored a paper where they reasoned that a valid physical theory must entail the locality and realism[47]. The paper suggests a quantum system whose momentum and position are entangled and argues that as the entangled quantities are real physical quantities but have correlation of a seemingly non-local character, the quantum mechanical description is an incomplete description of nature. Although the debate over the validity and the interpretation of the quantum mechanics continues until today, a number of experiments have verified the existence of entanglement. In 1964, John Bell suggested spin measurements on a pair of entangled electrons [48]. Based

on EPR's criteria for the locality that a choice of measurement at a position is not supposed to affect the outcome of a measurement in the remote position, he suggested the cases that would contradict the result of quantum mechanics which can be described as following[16]. Imagine an experiment where Charlie prepares two systems and sends one to Alice and the other to Bob. Once Alice receives the system, she performs a measurement on it. She has two choices as to which measurement apparatus to use, Q or R and she flips a fair coin to make the decision. Similarly, Bob flips a coin to decided which apparatus to use, S or T. Each apparatus can have the outcome value of either $\pm 1$ which would be denoted as q, r, s, t. The timing of the measurements is arranged so that two measurements are causally disconnected in the relativistic context. Now let's take a look at the quantity

$$qs + rs + rt - qt = (r + q)s + (r - q)t$$

which is supposed to have either the value of $\pm 2$ as $p, q, s, t = \pm 1$. Therefore, the average value of the quantity satisfies the following

$$\begin{aligned} &E(QS + RS + RT - QT) = E(QS) + E(RS) + E(RT) - E(QT) \\ &= E((R + Q)S + (R - Q)T) \leq 2 \end{aligned} \tag{3.1}$$

which is called Bell's inequality and it should be satisfied if Q, R, S and T are classical variables.

Now assume that Charlie prepares a two-qubit quantum state $|\psi\rangle = \frac{|01\rangle - |10\rangle}{2}$ and sends the first qubit to Alics and the second to Bob. The measurements for Alice and Bob are $Q = \sigma_{1,z}$ and $R = \sigma_{1,x}$, $S = \frac{-\sigma_{2,z} - \sigma_{2,x}}{\sqrt{2}}$, $T = \frac{\sigma_{2,z} - \sigma_{2,x}}{\sqrt{2}}$. It can be readily shown that

$$E(QS) = \frac{1}{\sqrt{2}}, E(RS) = \frac{1}{\sqrt{2}}, E(RT) = \frac{1}{\sqrt{2}}, E(QT) = -\frac{1}{\sqrt{2}}$$

and thus

$$E(QS + RS + RT - QT) = 2\sqrt{2}$$

which violates the Bell's inquality (Eq. 3.1). The reason Bell's inequality (Eq. 3.1) fails in the quantum case is that some assumptions made to establish it turn out to be invalid. Here are two assumption the inequality is based on.

1. The assumption of realism: The physical properties Q, R, S, T have definite values q, r, s, t which exist independent of observation.

2. The assumption of locality: Alice performing her measurement does not influence the result of Bob's measurement.

Although these assumptions make sense as to how they fit our every day experience, they are not the accurate descriptions of nature when it comes to handle subatomic objects where quantum mechanics rules. The reason we do not feel this quantum effect in our daily experience is that as our focus shifts toward the macroscopic world, the quantum effects of the scale $\hbar$ fades away and the macroscopic object loses its quantum coherence extremely rapidly due to its macroscope exposure to its environment. For the same reason, it is practically infeasible to keep the coherently quantum state of a cat in a box.

The reason the assumption of locality is violated is that the quantum systems of Alice and Bob are entangled. Quantum entanglement is known to be essential for certain quantum communication protocols [7, 8], and it is generally considered to be an essential resource of the exponential speedup of quantum algorithms [9, 10]. For instance, the Deutsch-Josza algorithm (DJA) (the simplest of all quantum algorithms) [49] is designed to figure out if a given function is balanced or not. As I will show in the later section, quantum entanglement is unavoidable in the DJA as the number $N$ of qubit increases [50], since the total number of balanced functions scales doubly exponentially: $B(2^N, 2^{N-1}) \sim 2^{2^N}$, while the number of separable states scales as $2^N$. Thus, in order to represent all the balanced function with $N$ qubits, we inevitably introduce entanglement.

On the other hand, there have been questions concerning whether entanglement is the only resource of the power of quantum algorithms [51, 52]. And the quantitative measure of quantum entanglement as quantum calculation resource is generally not available. For instance, the DJA for the 2- and 3- qubit cases have an advantage over classical algorithm but they do not involve much more than simple interference, which is not usually thought of as quantum correlation. Moreover, the Gottesman-Knill theorem [16] states that certain of quantum algorithms involving only pure states can be simulated on classical computer

without exponential overload, demonstrating the entanglement is far from sufficient for exponential speedup [1].

Therefore, we come to the idea that quantum entanglement is missing certain 'quantum' feature of quauntum systems and are thus motivated to seek for alternative types of quantum correlation not accounted for by quantum entanglement, especially in the case involving mixed state quantum state. For that matter, quantum discord has been introduced as another type of quantum correlation [53]. Quantum discord catches the 'missing' element of quantum entanglement as quantum discord can be present even in separable states. It might be an additional resource of quantum algorithms giving computational advantages over classical calculation. Evidence for this point of view comes from the existence of an algorithm (DQC1) that computes the trace of a unitary matrix[1, 54, 55]. It uses only one pure qubit and exhibits discord but little entanglement [1, 54, 55], and still appears to be more powerful than classical algorithms for the same problem. Also, it was shown that quantum discord between bipartite systems can be consumed to encode information that can only be accessed by coherent quantum interactions [11]. Since quantum discord is more robust against decoherence than entanglement there is the hope that quantum algorithms dependent only on quantum discord might be more feasible to implement physically than those dependent on the more fragile entanglement. The true physical resource of quantum computation still has many open issues.

The structure of the chapter is as follows. I will look at quantum algorithms which unavoidably involve quantum entanglement as the number of qubits $N$ increases. However, in order to stress the view that quantum entanglement might not be necessary for quantum speedup, I will investigate the DQC1 algorithm in Section 3.2 to demonstrate the involvement of the quantum correlation other than quantum entanglement. Although the original quantum discord was introduced for bipartite systems, as my focus in this chapter is on multipartite systems, the extended definition of quantum discord for multipartite system, the global geometric quantum discord (GGQD) [56], will be introduced in Section 3.3. The distance can be defined either by the relative entropy measure [57], or by means of the met-

ric derived from the Hilbert-Schimdt inner product [58–60]. We will use the latter form in this work. It facilitates the calculations by removing the nonpolynomial log function from the definition, but at the cost of muddying the information-theoretic interpretation. Then in Section 3.4 I will proceed to give an interpretation of quantum discord in terms of Bloch vector geometry, providing with a proof that computing GGCD is NP-hard in the number of qubits, and also treats the problem of 2,3, and N qubits from an algebraic point of view. Then I will describe a relatively simple heuristic method to calculate GGQD for certain highly symmetric but important classes of multiqubit states.

### Deutsch-Josza Algorithm

I will introduce Deutsch-Josza algorithm[49], the extended version of the Deutsch's algorithm of Section 1.2. Similarly to Deutsch's algorithm, the task again is to figure out if the given function is balanced (half of the inputs lead to 0) or constant but now the function has the inputs of $N$-digit binary numbers instead of the simple 1 digit of Deutsch's algorithm. The idea is to prepare the superposed state by applying N Hadamard gates and use the unitary oracle gate to change the state depending on the value of the function for each of the superposed part. The quantum circuit for the algorithm is shown at the diagram 3.2.

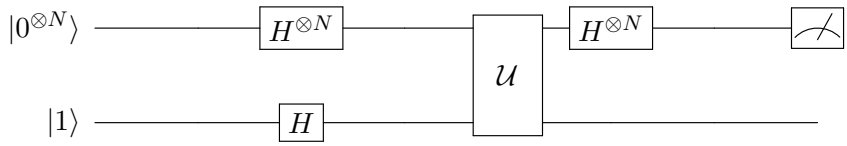


(3.2)

While a classical protocol must require at least $2^{N-1}+1$ oracle calls to perform the task, it suffices to perform the unitary operation only 1 time with Deutsch-Josza scheme thus obtaining the exponential speedup.

Unlike the Deutsch algorithm where the state stays separated, Deutsch-Josza algorithm might involve non-separable, entangled state[50]. The total number of balanced functions is the number of ways to pick up the half of the input values ($\times\frac{1}{2}\times 2$ as choosing the half excludes choosing the other half and we have two ways of parity for each choice) and it scales doubly exponentially in the number of the digit of the input $N$: $\begin{pmatrix} 2^N \\ 2^{N-1} \end{pmatrix} \sim 2^{2^N}$.

On the other hand, the unitary operator for the first N qubits part can be described as $|x\rangle \rightarrow (-1)^{f(x)}|x\rangle$. Applying this to the initial state after the Hadamard is $\frac{1}{\sqrt{2^N}}\sum_{x=0}^{2^N-1}|x\rangle$, we have

$$\frac{1}{\sqrt{2^N}}\sum_{x=0}^{2^N-1}(-1)^{f(x)}|x\rangle \tag{3.3}$$

If f is constant, the state is obviously separable. Or if f is balanced, the state is separable only when it can be written as

$$\frac{1}{\sqrt{2^N}}\sum_{x=0}^{2^N-1}(-1)^{a\cdot x}|x\rangle \tag{3.4}$$

($a$ is a $N$-digit binary number and the multiplication is done in the modulo of 2). The number of the functions that lead to the separable form scales only as $2(2^N-1)$ (the number of ways to choose a binary value for each digit of a, multiplied by 2 to count for two choices of the parity, excluding the constant case when $a = 0^{\otimes N}$). In comparison, $\lim_{N\rightarrow\infty}\frac{2(2^N-1)}{2^{2^N}} = 0$. Therefore, the involvement of quantum entanglement in Deutsch-Josza algorithm becomes unavoidable as N, the number of qubits, increases.

### Grover's Searching Algorithm

The task of Grover's algorithm [16, 61] is to find an element (called a solution) in the given list of the size $2^N$ where there are $M$ solutions. Again, we assume the presence of the oracle who can tell if an entry is a solution. Obviously, classical protocol must involve checking each entry of the list which should require on average of $\frac{N}{M}$ oracle calls to find a match. In Grover's algorithm, we prepare the initial state $|0^{\otimes N}\rangle$ and apply $N$ Hadamard operators $H^{\otimes N}$as in Deutsch Josza's algorithm to get $|\psi_I\rangle \equiv \frac{1}{\sqrt{N}}\sum_{x=0}^{2^N-1}|x\rangle$. Then a series of the identical unitary operators $U_G$, called Grover's operator is applied. The first step of the Grover's operator is the identical unitary operator involving oracle $U_O$ used in Deutsch Josza's algorithm: $U_O(|x\rangle) \equiv (-1)^{f(x)}|x\rangle$ where $f(x) = 1$ if $x$ is a solution and $f(x) = 0$ otherwise. And it is followed by N Hadamard gates $U_H \equiv H^{\otimes N}$, a phase shift gate $U_P$ of $-1$ except for $|0\rangle$: $U_P(|x\rangle) \equiv (-1)^{\delta_{x>0}}|x\rangle = (2|0\rangle\langle 0| - I)|x\rangle$ and another $H^{\otimes N}$, thus $U_G \equiv U_H U_P U_H U_O$.

Grover's operator can be understood noting that the initial state can be divided to the solution part and the other,

$$\begin{aligned} |\psi_I\rangle = & \quad \frac{\sqrt{N-M}}{\sqrt{N}}\Big(\frac{1}{\sqrt{N-M}}\sum_{x,f(x)=0}|x\rangle\Big) + \frac{\sqrt{M}}{\sqrt{N}}\Big(\frac{1}{\sqrt{M}}\sum_{x,f(x)=1}|x\rangle\Big) \\ \equiv & \quad \frac{\sqrt{N-M}}{\sqrt{N}}|\alpha\rangle + \frac{\sqrt{M}}{\sqrt{N}}|\beta\rangle \end{aligned}$$

and

$$\begin{aligned} U_O(\alpha|\alpha\rangle + \beta|\beta\rangle) \quad & = \alpha|\alpha\rangle - \beta|\beta\rangle \\ U_H U_P U_H \quad & = H^{\otimes N}(2|0\rangle\langle 0| - I)H^{\otimes N} = 2|\psi_I\rangle\langle\psi_I| - I \\ & = |\psi_I\rangle\langle\psi_I| - |\psi_{I\perp}\rangle\langle\psi_{I\perp}| - \cdots \end{aligned}$$

where $\cdots$ stands for the state space not spanned by $\{|\alpha\rangle, |\beta\rangle\}$. Regarding $|\psi_I\rangle = \alpha|\alpha\rangle + \beta|\beta\rangle$ as two level quantum system whose Bloch vector stays on xz plane as $\beta \in Re$: $|\psi_I\rangle = \cos(\frac{\theta}{2})|\alpha\rangle + \sin(\frac{\theta}{2})|\beta\rangle$, the Grover operations work as two reflections as

$$U_O(\cos(\frac{\theta}{2})|\alpha\rangle + \sin(\frac{\theta}{2})|\beta\rangle) = \cos(\frac{\theta}{2})|\alpha\rangle - \sin(\frac{\theta}{2})|\beta\rangle$$

and

$$\begin{aligned} & U_H U_P U_H(\cos(\frac{\theta}{2})|\alpha\rangle - \sin(\frac{\theta}{2})|\beta\rangle) = \\ & (|\psi_I\rangle\langle\psi_I| - |\psi_{I\perp}\rangle\langle\psi_{I\perp}|)(\cos(\frac{\theta}{2})|\alpha\rangle - \sin(\frac{\theta}{2})|\beta\rangle) = \cos(\frac{3\theta}{2})|\alpha\rangle + \sin(\frac{3\theta}{2})|\beta\rangle \end{aligned}$$

The last relation is from the observation that $U_H U_P U_H$ projects the state along $|\psi_I\rangle$ direction but changes the sign along $|\psi_{I\perp}\rangle$ so they do the reflection along $|\psi_I\rangle$ state just as $U_O$ does so along $|\alpha\rangle$. This can be generalized to show $G^k(\cos(\frac{\theta}{2})|\alpha\rangle + \sin(\frac{\theta}{2})|\beta\rangle) = \cos(\frac{2k+1}{2}\theta)|\alpha\rangle + \sin(\frac{2k+1}{2}\theta)|\beta\rangle$. Therefore, repeated application of Grover's operator $G$ would lead the state close to $|\beta\rangle$. Upon making an measurement we would have the high chance of obtaining one of the states in $|\beta\rangle$. The chance would be maximized when $(2k+1)\theta = \pi$. In case $N \gg M$, $\frac{\sqrt{M}}{\sqrt{N}} = \sin(\frac{\theta}{2}) \sim \frac{\theta}{2}$ so that $k = \frac{\pi}{2\theta} - \frac{1}{2} = \frac{\pi}{2\theta} - \frac{1}{2} \sim 4\pi\sqrt{\frac{N}{M}} - \frac{1}{2} = O(\sqrt{\frac{N}{M}})$.

Bruß *et al.* [50] claimed that dominantly many cases of Grover's algorithm must involve non-separable entangled states as $N$ increases. But it needs to be pointed out that the

argument is not based on fully quantitative measure of quantum entanglement. For instance, they counted the number of cases not involving the state in a tensor product form, rendering such state having the full entanglement. But this disregards the different degree of quantum entanglement in quantum states. For instance, the state $\frac{1}{\sqrt{2}}(|000\rangle + |111\rangle)$ is more entangled than

$$\begin{aligned}&\frac{1}{\sqrt{8}}(|000\rangle + |001\rangle + |010\rangle + |011\rangle + |100\rangle + |101\rangle + |110\rangle - |111\rangle)\\ &= \frac{1}{4}(\sqrt{2}\,|0+\rangle + |10\rangle) \otimes |+\rangle + \frac{1}{4}\,|11\rangle \otimes |-\rangle\end{aligned}$$

as the latter contains some overlap on the second qubit in $|0+\rangle$ and $|10\rangle$ although it involves certain degree of quntum entanglement.

## 3.2 Quantum Discord And Quantum Algorithm

The counting argument discussed in the previous section, however, does not give the quantitative measure of quantum entanglement as calculational resource and it ignores the different degree of entanglement induced in the various cases. Moreover, though the cases involving entanglement dominates in number in those algorithms, they still have the cases where states are kept separable the whole time.

In the next sections, I will focus on the new type of quantum correlation, quantum discord, that can exist even in separable states. I will demonstrate Deterministic quantum computing with 1 pure qubit (DQC1) algorithm, that computes the trace of a unitary matrix[1, 54, 55] giving computational advantages over classical calculation. DQC1 was introduced to demonstrate what can be accomplished if the initial state is a highly mixed state[62], which begins with the state with only one pure qubit and little quantum entanglement [1, 54, 55]. The quantum circuit diagram for the algorithm is as follows:

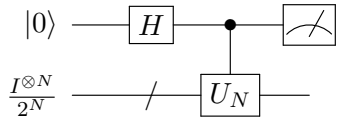

Here $U_N$ is unitary operation on $N$ qubits. Before the measurement, the state is

$$\begin{aligned}\rho = & \quad \frac{1}{2^N}(|0\rangle\langle 0| \otimes I_N + |1\rangle\langle 1| \otimes I_N + |0\rangle\langle 1| \otimes U_N^\dagger + |1\rangle\langle 0| \otimes U_N) \\ = & \quad \frac{1}{2^N}\begin{pmatrix} I_N & U_N^\dagger \\ U_N & I_N \end{pmatrix}\end{aligned}$$

The normalized trace of the operator $U_N$ is encoded in the expectation values of the first qubit as measured by Pauli operators $\sigma_x$ and $\sigma_y$. It can be readily shown that $\langle\sigma_x\rangle = \frac{1}{2^N} Re(\,Tr(U_N))$, $\langle\sigma_y\rangle = -\frac{1}{2^N} Im(\,Tr(U_N))$. Those expectation values can be evaluated by making the measurement repeatedly. As each measurement would be bounded by $-1 < \langle\sigma_x\rangle, \langle\sigma_y\rangle < 1$, the average value of the $M$ repeated measurement values would asymptotically follow the normal distribution with the standard deviation of $\frac{1}{\sqrt{M}}$ so in order to achieve the estimation accuracy $\epsilon$, we need to run the measurements $\frac{1}{\epsilon^2}$ times. On the other hand, classical procedure should require $O(2^{2N})$ inquiries about the unitary operator $U_N$ as an unitary matrix of $m \times m$ dimension has $O(m^2)$ degrees of freedom. Therefore, the number of runs to achieve a given accuracy does not depend on $N$ and DQC1 algorithm provides an efficient means for the trace value of a unitary matrix calculation.

It was shown that although the state of the algorithm generally involves quantum entanglement, the amount is bounded by a constant value regardless of the number of qubits $N$ thus only a vanishingly small fraction of the maximum possible entanglement is involved as $N$ gets large [1]. This result suggests that new quantum character missing in quantum entanglement contributes to the computing power of the algorithm.

## 3.3 Measures Of Quantum Correlation

The original definition of quantum discord was an extension of analogous classical correlation to the quantum systems [53]. A good measure of the classical correlation between two probability distributions $\{p_{1,i}\}, \{p_{2,j}\}$ with $\{p_{12,ij}\}$ as their joint distribution is given by the mutual information

$$I_{classical} = H(\{p_{1,i}\}) + H(\{p_{2,j}\}) - H(\{p_{12,ij}\})$$

where $H(\{p_k\}) \equiv -\sum_k p_k \log_2(p_k)$ is Shannon entropy. Note that $H(\{p_{12,ij}\}) = H(\{p_{1,i}\}) + H(\{p_{2,j}\})$ when two distributions are independent in which case $I_{classical} = 0$. $I_{classical}$ can also be written as

$$\begin{aligned} I_{classical} &= H(\{p_{1,i}\}) + H(\{p_{2,j}\}) - H(\{p_{12,ij}\}) \\ &= H(\{p_{1,i}\}) - (H(\{p_{12,ij}\}) - H(\{p_{2,j}\})) \\ &= H(\{p_{1,i}\}) - \left( -\sum_{ij} p_{12,ij} \log_2 (p_{12,ij}) + \sum_{ij} p_{12,ij} \log_2(p_{2,i}) \right) \\ &= H(\{p_{1,i}\}) - \left( -\sum_{ij} p_{2,j} \left( \frac{p_{12,ij}}{p_{2,j}} \right) \log_2(\frac{p_{12,ij}}{p_{2,j}}) \right) \\ &= H\left(\{p_{1,i}\}\right) - \sum_j p_{2,j} H\left(\left\{p_{1|2=j,i}\right\}\right) \end{aligned} \tag{3.5}$$

Here the conditional probability $p_{1|2=j,i}$ is the probability of event $i$ in system 1, given that event $j$ has been measured in system 2.

This process can be viewed as the partial elimination of uncertainty of system 1 from knowledge of system 2. The classical correlation between two quantum systems can be defined in the light of these equations. In the quantum case, the probability distribution is replaced by the density operator $\rho$, and the Shannon entropy $H$ is replaced by the von Neumann entropy $S(\rho) \equiv H(\{\lambda_{\rho,k}\}) = -\sum_k \lambda_{\rho,k} log_2(\lambda_{\rho,k})$ where $\lambda_{\rho,k}$ are singular values of the density matrix $\rho$. We see that the classical conditional probability distribution $\{p_{1|2=j,i}\}$ is analogous to $\rho_{1|j}$, the state of system 1 after a projective measurement $\Pi_j^{(2)}$ is applied on the second system, thus a reasonable definition of the classical correlation is then given by

$$J_{\{\Pi_j^{(2)}\}} = S(\rho_1) - \left( \sum_j p_{\Pi_j^{(2)}} S(\rho_{1|j} \otimes |j\rangle \langle j|) \right)$$

It has to be noted that this quantity still depends on the measurement choice which is the big difference between quantum and classical mechanics. If we make the best choice to remove the maximum amount of uncertainty from the measurement, then we finally find the *optimized* classical correlation $J_{1|2}$ between two quantum systems:

$$J_{1|2} = \max_{\{\Pi_j^{(2)}\}} J_{\{\Pi_j^{(2)}\}}. \tag{3.6}$$

Quantum discord is defined as the difference of the total correlation $I(\rho) = S(\rho_1) + S(\rho_2) - S(\rho)$, and the optimized classical correlation [53],

$$D_{1|2}(\rho) = I(\rho) - J_{1|2}(\rho)$$

This original definition of quantum discord has certain drawbacks. It is asymmetric between systems 1 and 2 so ambiguity exists as to which to choose. Also it is defined only for bipartite systems so an extension of the definition to multipartite systems is needed. Finally, it involves an optimization which can be challenging to calculate. Girolami *et al.* obtained simplified analytic conditions for the optimal value for the 2-qubit case [63]. However, it needs to be noted that this definition is still asymmetrical and generally requires optimization.

These problems can be alleviated by noting that $D_{1|2}(\rho)$ vanishes in quantum-classical states, defined as all states of the form

$$\{\sum_i p_i \rho_i \otimes |i\rangle \langle i| \, ; p_i \leq 0, \langle i|j\rangle = \delta_{i,j}\} \tag{3.7}$$

The idea of measuring the distance between the given quantum state and its closest state not having a certain property has been investigated by Modi *et al.* [57, 64]. In this picture, the total correlation $I$ is the distance to the closest product state of the form $\otimes_{i=1\cdots N} |\psi_i\rangle$ and quantum discord $D$ is to the closest state of the form Eq. 3.7 and finally, classical correlation $J$ is the distance from the closest quantum-classical state to its nearest product state. But instead of the addivity relation $I = D + J$, the correlations are subadditive $I \geq D + J$. To simplify the calculation, we define the geometric discord[64] of a given state as the square-norm (Hilbert-Schmidt) distance to the nearest quantum-classical state.

Rulli *et al.*[56] suggested that one can make quantum discord into a symmetrical, multipartite quantity by defining the global quantum discord. Its definition is motivated by the observation that using $S(\sum_j p_j \rho_{1|j} \otimes |j\rangle \langle j|) = S(\sum_j p_j |j\rangle \langle j|) + \sum_j p_j S(\rho_{1|j} \otimes |j\rangle \langle j|)$[57, 60], the original quantum discord can also be written as

$$D_{1|2} = \min_{\{\Pi_j^{(2)}\}} \left[ I(\rho) - S(\Pi^{(2)}(\rho) \parallel \rho_1 \otimes tr_1(\Pi^{(2)}(\rho))) \right]$$

where

$$\Pi^{(2)}(\rho) \equiv \sum_j (I \otimes \Pi_j^{(2)})\rho(I \otimes \Pi_j^{(2)}) = \sum_j p_j \rho_{1|j} \otimes |j\rangle \langle j|$$

and

$$S(\hat{x} \parallel \hat{y}) = -tr(\hat{x} \log \hat{y}) - S(\hat{x})$$

For qubit system, the index $j$ has two values $j = 1, 2$ representing the direction (and its opposite direction) of the measurement. So we have $|j = 1\rangle = \cos(\frac{\theta}{2}) |0\rangle + e^{i\phi} \sin(\frac{\theta}{2}) |1\rangle$ and $|j = 2\rangle = \sin(\frac{\theta}{2}) |0\rangle - e^{i\phi} \cos(\frac{\theta}{2}) |1\rangle$.

Based on this observation, we expand the measurement $\Pi^{(2)}$ on the second part, to the measurement $\Pi^{(1,2)}$ on both parts to define the global quantum discord.

$$\begin{aligned} D_G &= \min_{\{\Pi_{i_1}^{(1)}\},\{\Pi_{i_2}^{(2)}\}} \left( I(\rho) - S\big(\Pi^{(1,2)}(\rho) \parallel tr_2(\Pi^{(1,2)}(\rho)) \otimes tr_1(\Pi^{(1,2)}(\rho))\big) \right) \\ &= \min_{\{\Pi_{i_1}^{(1)}\},\{\Pi_{i_2}^{(2)}\}} \big( I(\rho) - I(\Pi^{(1,2)}(\rho)) \big) \end{aligned} \tag{3.8}$$

where

$$\Pi^{(1,2)}(\rho) \equiv \sum_{i_1,i_2} (\Pi_{i_1}^{(1)} \otimes \Pi_{i_2}^{(2)})\rho(\Pi_{i_1}^{(1)} \otimes \Pi_{i_2}^{(2)}) = \sum_{i_1,i_2} p_{i_1,i_2} |i_1\rangle \langle i_1| \otimes |i_2\rangle \langle i_2|$$

and $I(\rho) = S(\rho \parallel tr_2(\rho) \otimes tr_1(\rho))$ was used [57]. Rulli *et al.*[56] performed analytical calculations for the 2-qubit Werner-GHZ state and X. Jianwei[59] applied it to a multiqubit Werner-GHZ state. Furthermore, we can make an observation that if the state is in the set $Cl$ of classical states defined by

$$\{\sum_{i_1,i_2} p_{i_1,i_2} |i_1\rangle \langle i_1| \otimes |i_2\rangle \langle i_2|; p_{i_1,i_2} \leq 0, \langle i_1|j_1\rangle = \delta_{i_1,j_1}, \langle i_2|j_2\rangle = \delta_{i_2,j_2}\}$$

then $D_G = 0$. In this spirit, geometric global quantum discord (GGQD) is defined as the distance to the nearest classical state[59].

$$D_{GG}(\rho) \min_{\chi \in Cl} \ |\rho - \chi|^2 ,$$

where we use the Hilbert-Schmidt metric:

$$|\rho - \chi|^2 = Tr\big( (\rho - \chi)^\dagger (\rho - \chi) \big)$$

It is worthwhile to note that for two-qubit states, the above definition is scaled from the original form by the factor of $\frac{1}{2}$ and we have $1 \geq 2D_{GG} \geq D_G$ [65]. The Hilbert-Schmidt metric has many advantages: it is relatively easy to calculate and since it is related to the Euclidean metric, it has a simple geometrical interpretation, which allows one to use more powerful optimization methods. By contrast, the definition of GQD involves logarithms, which complicates the optimization. As GGQD removes the logarithm, we will instead use it, even though its interpretation as a resource for quantum information processing is less clear.

## 3.4 Calculation Of Quantum Discord

### Bloch Vector For Generalized Bell States

We represent the density matrix $\rho = \frac{1}{2^N} \sum_{a=0}^{2^N-1} n_a \sigma_a$ for an $N$-qubit system using the generalized Bloch vector, Bloch tensor, $n_a$:

$$n_a = Tr(\rho \sigma_a) \tag{3.9}$$

where the subscript $a$ labels the generators $\sigma_a$ of $\mathrm{SU}\big(2^N\big)$, taken as tensor products of the Pauli matrices $\sigma_0 = I, \sigma_{1,2,3} = \sigma_{x,y,z}$. Thus $a \in \{0,3\}^N$, *i.e.*, $a$ is an $N$-digit base-4 number. The trace condition on $\rho$ always gives $n_{\vec{0}} = 1$, so we omit the index $a = \vec{0}$ in what follows. Inverting Eq.(3.9) gives

$$\rho = \frac{1}{2^N}(I_n + \sum_{a=00..01}^{4^N-1} n_a O_a)$$

The $n_a$ are the real components of a $(4^N - 1)$-dimensional vector, which can be thought of as a generalization of the Bloch vector. Positivity requirements on $\rho$ lead to a state space $\mathcal{M}$ that is a subset of $\mathbb{R}^{4^N-1}$. For given $N, \mathcal{M}$ is compact and convex, but its surface has a complicated shape [66, 67].

The Bloch tensor is useful to calculate GGQD and it was shown [60] that GGQD for $N$-qubit state $\rho = \frac{1}{2^N} \sum_{a=0}^{2^N-1} n_a \sigma_a$ can be evaluated as follows:

$$D_{GG}(\rho) = \frac{1}{2^N}(\sum_a n_a^2 - \max_{\{\vec{\Theta}_i\}}(\sum_a n_a \Pi_{i=1}^n \Theta_{i,a_i})^2) \tag{3.10}$$

where the measurement on each qubit is along the qubit direction $\vec{\Theta}_i$ so that $\Pi^{(i)}_{m=1} = |\vec{\Theta}_i\rangle\langle\vec{\Theta}_i|$, with $|\vec{\Theta}_i\rangle = \cos(\frac{\theta(\vec{\Theta}_i)}{2})|0\rangle + e^{i\phi(\vec{\Theta}_i)}\sin(\frac{\theta(\vec{\Theta}_i)}{2})|1\rangle$ where $\theta(\vec{\Theta}_i)$ and $\phi(\vec{\Theta}_i)$ are the polar and azimuthal angles of the unit vector $\vec{\Theta}_i$, and the second angle is parallel but toward the opposite direction $\Pi^{(i)}_{m=2} = |\vec{\Theta}'_i\rangle\langle\vec{\Theta}'_i|$ with $|\vec{\Theta}'_i\rangle = \sin(\frac{\theta(\vec{\Theta}_i)}{2})|0\rangle - e^{i\phi(\vec{\Theta}_i)}\cos(\frac{\theta(\vec{\Theta}_i)}{2})|1\rangle$.

As mentioned in the previous section, GQD introduces a measurement on the all parts of the system and in order to calculate $I(\Pi^{(1,2)}(\rho))$ in Eq.(3.8), we need the eigenvalue spectrum of the state $\Pi^{(1,2)}(\rho)$ after the measurement is applied. In this paper, we focus on a linear subspace of $\mathcal{M}$ (more precisely, the intersection of a $3^N$-dimensional linear subspace of $\mathbb{R}^{4^N-1}$ with $\mathcal{M}$.) This subspace is defined by the condition that $n_a = 0$ if any digit of $a$ is zero. Then the marginal state of any subsystem is maximally mixed: if we take the partial trace over any subset of the qubits, the remaining marginal state is a state whose density matrix is proportional to identity matrix. From that point of view, these $N$-qubit states can be thought of as generalizations of the 2-qubit Bell states. Unlike the 2-qubit Bell states, these states are not known to be maximally entangled in any sense, but they are good candidates for highly entangled states that involve relatively few parameters.

We now perform the measurements along the angles given by $\{\vec{\Theta}_i\}$, a set of unit vectors, given $\rho$ in this described subspace. The eigenvalues of $\rho$ after the measurements are what we need for the calculation of the discord. There are only two distinct eigenvalues given by $2^{-N}[1 \pm C(\{\vec{\Theta}_i\})]$, and each is $2^{N-1}-$fold degenerate. Here $C(\{\vec{\Theta}_i\}) \equiv \sum_{\vec{a}} n_{a_1,\cdots,a_N}\Theta_{1,a_1}\cdots\Theta_{N,a_N}$. The global quantum discord and geometric global quantum discord are, from Eq.(3.8) and Eq.(3.10),

$$\begin{aligned} D_G(\rho) &= I(\rho) + \min_{\{\vec{\Theta}_i\}} H(\{\frac{1}{2}(1+C), \frac{1}{2}(1-C)\}) - (N-1) \\ &= I(\rho) + H(\{\frac{1}{2}(1+\max_{\{\vec{\Theta}_i\}} C), \frac{1}{2}(1-\max_{\{\vec{\Theta}_i\}} C)\}) - (N-1) \end{aligned} \tag{3.11}$$

and

$$D_{GG}(\rho) = \frac{1}{2^n}(\sum_a n_a^2 - \max_{\{\vec{\Theta}_i\}} C^2) \tag{3.12}$$

The Shannon entropy function $H$, the measure of randomness, is larger when the probability is more evenly distributed, so the optimization problem for both GQD and GGQD becomes

the task of finding maximum $C$. $C$ is the contraction of the tensors $n$ and the product of the 1-tensors $\vec{\Theta}_i$ For two qubits, $\max_{\{\vec{\Theta}_i\}} C$ is the operator norm of the matrix $n$ whose calculation is essentially an eigenvalue problem, but even for three qubits, an analytic expression for $\max_{\{\vec{\Theta}_i\}} \sum_{ijk} n_{ijk}\Theta_{1,i}\ \Theta_{2,j}\ \Theta_{3,k}$ is not available in general. This suggests that the problem for $N$ qubits may be very difficult, and we turn to that issue next.

## NP-hardness Of Quantum Discord Calculation

$$\max_{\{\vec{\Theta}_i\}} C(\{\vec{\Theta}_i\}) \equiv \max_{\{\vec{\Theta}_i\}} \sum_{a_1\cdots a_N \in \{1,2,3\}^{\otimes N}} n_{a_1\cdots a_N} \Pi_{i=1}^{N} \Theta_{i,a_i} \tag{3.13}$$

is called the injective tensor norm of the tensor $n_a$ with $N$ indices[68]. There are various ways to define a norm on tensors, the injective tensor norm is the most straightforward generalization of the operator norm, to which it reduces when $N = 2$. Physically one may think of it as the ground state energy of a classical spin glass with unit vector spins, with arbitrary $N$-spin interactions and a Hamiltonian $H = -\sum_a n_a\ \Theta_{1,a_1}\cdots\ \Theta_{N,a_N}$.

For the general state, the geometric global quantum discord (GGQD, Eq.(3.10)) involves the calculation of $\max_{\{\vec{\Theta}_i\}}(\sum_{a\in\{0,\cdots,3\}^{\otimes N}} n_a \Pi_{i=1}^{N}\Theta_{i,a_i})$. It is similar to the injective tensor norm Eq.(3.13), but now $n_a$ is not necessarily zero when some digit of $a$ is zero. It can be shown that GGQD calculation is NP-hard by converting an NP-hard MAX-k-SAT problem to GGQD calculation.

In a MAX-k-SAT problem, we have M clauses, $\{C_i : i = 1,\cdots M\}$ where each clause $C_i$ involves k boolean variables, $V_i \equiv \{v_{c(i,j)} : j = 1,\cdots k, c(i,j) \in \mathbb{N}\}$ and the whole problem involves N variables, $V \equiv \cup_i V_i = \{v_i : i = 1,\cdots,N\}$. For each clause $C_i$, there is a set of assignments for variables in $V_i$ that satisfy $C_i$, $A_i = \{A_{i,l} : A_{i,l} = \{v_{c(i,j)} = a_{c(i,j),l}\}, a_{c(i,j),l} \in \{T,F\}, l = 1,\cdots,|A_i|\}$. The problem is to find an assignment $A^* = \{v_i = a_i^*\}$ of the all variables that maximizes the number of the satisfied clauses: $A^* = \arg\max_A \text{k-SAT}(A)$ where k-SAT$(A)$ is the number of clauses.

To make the connection between the GGQD calculation and MAX-k-SAT problem, define a measurement angle $\vec{\Theta}_i$ for each variable $v_i$ in V. For an assignment of a variable,

we define the corresponding measurement angle such that $\vec{\Theta}(T) = (0,0,1)^T$ and $\vec{\Theta}(F) = (0,0,-1)^T$. For each clause $C_i$, define the corresponding Hamiltonian $H_i$ such that $H_i$ has the value of $-1$ for the assignments that satisfy the clause and 0 otherwise: $H_i = -\sum_l \Pi_{j=1}^k \{\frac{1}{2}(1 + \Theta(a_{c(i,j),l})_z \Theta_{j,z})\}$. The total Hamiltonian is the sum of all $H_i$ and $n_a$ is defined accordingly: $H_{tot} = \sum_{i=1}^N H_i = -\sum_{a\in\{0,\cdots,3\}^{\otimes N}} n_a \Pi_{i=1}^N \Theta_{i,a_i}$. The measurement angles $\{\vec{\Theta}_i^* \equiv \vec{\Theta}(a_i^*) : i = 1,\cdots,N\}$ corresponding to $A^*$ also make $H_{tot}$ to have the lowest value.

As a simple example, for $C_1 = v_1 \vee v_2$, $C_2 = v_1 \vee \neg v_2$, we have

$$H_1 = -\frac{(1+\Theta_{1,z})}{2}\frac{(1+\Theta_{2,z})}{2} - \frac{(1+\Theta_{1,z})}{2}\frac{(1-\Theta_{2,z})}{2} - \frac{(1-\Theta_{1,z})}{2}\frac{(1+\Theta_{2,z})}{2}$$

and

$$H_2 = -\frac{(1+\Theta_{1,z})}{2}\frac{(1+\Theta_{2,z})}{2} - \frac{(1+\Theta_{1,z})}{2}\frac{(1-\Theta_{2,z})}{2} - \frac{(1-\Theta_{1,z})}{2}\frac{(1-\Theta_{2,z})}{2}$$

so that

$$\begin{aligned} H_{tot} \quad &= -2\frac{(1+\Theta_{1,z})}{2}\frac{(1+\Theta_{2,z})}{2} - 2\frac{(1+\Theta_{1,z})}{2}\frac{(1-\Theta_{2,z})}{2} \\ &\quad -\frac{(1-\Theta_{1,z})}{2}\frac{(1+\Theta_{2,z})}{2} - \frac{(1-\Theta_{1,z})}{2}\frac{(1-\Theta_{2,z})}{2} \\ &= -\frac{3}{2} - \frac{1}{2}\Theta_{1,z} \end{aligned}$$

and the ground state is obtained with $\vec{\Theta}_1 = \vec{\Theta}(T)$ which means $\Theta_{2,z}$ can either be $+1$ or $-1$. It corresponds to the assignments of $\{v_1 = T, v_2 = T\}$ or $\{v_1 = T, v_2 = F\}$.

Therefore, by being able to calculate $\max_{\{\vec{\Theta}_i\}}(\sum_{a\in\{0,\cdots,3\}^{\otimes N}} n_a \Pi_{i=1}^N \Theta_{i,a_i})$ which is a part of GGQD calculation, we can solve the NP-hard, MAX-k-SAT problem. The NP-hardness of MAX-k-SAT is in the number of the total variables $N$, which is the number of the measurement angles in the corresponding GGQD calculation. Thus, the GGQD calculation is NP-hard in the number of qubits as well.

As for the (non-geometric) global quantum discord calculation (Eq.(3.8)), we did not get the conclusive proof that its calculation is NP-hard. Nonetheless, we suggest that the injective tensor norm calculation is also NP-hard as the NP-hardness essentially comes from the exponentially large dimension of the space of the measurement angles and the global

quantum discord calculation involves *log* functions which are generally more difficult to calculate than the polynomials which appear in the calculation of the GGQD.

### Two Qubits

For the case of two qubits, the Bloch vector has two indices and thus can be viewed as a matrix. The GQD can be efficiently and exactly calculated via singular value decomposition (SVD).

$$\begin{aligned}\rho &= \frac{1}{4}(I + \sum_{i\neq 0} n_{i0}\sigma_i \otimes I + \sum_{j\neq 0} n_{0j} I \otimes \sigma_j + \sum_{i,j\neq 0} n_{ij}\sigma_i \otimes \sigma_j) \\ &= \frac{1}{4}(I + \sum_{i\neq 0} n_{i0}\sigma_i \otimes I + \sum_{j\neq 0} n_{0j} I \otimes \sigma_j + \sum_{i,j\neq 0, a=1,2,3} \sigma_i \otimes \sigma_j R_{1,ia} R_{2,ja} d_a) \\ &= \frac{1}{4}(I + \sum_{i\neq 0,a} R_{1,ai} n_{i0}\sigma'_a \otimes I + \sum_{j\neq 0,a} R_{2,aj} n_{0j} I \otimes \sigma''_a + \sum_a d_a \sigma'_a \otimes \sigma''_a)\end{aligned} \tag{3.14}$$

where $\vec{\sigma}' \equiv U_{R_1}\vec{\sigma}U_{R_1}^\dagger, \vec{\sigma}'' \equiv U_{R_2}\vec{\sigma}U_{R_2}^\dagger$. This corresponds to a local change of basis via local unitary transformation so it does not change the correlation measure. Since we consider the special case where the marginalized partial states are maximally mixed ($n_{i0} = n_{0j} = 0, i, j \neq 0$), the first two terms are zero, and the state becomes a Bell diagonal state after SVD is applied.

$$\rho = \frac{1}{4}(I + \sum_{i,j\neq 0} n_{ij}\sigma_i \otimes \sigma_j) \tag{3.15}$$

Now with SVD, $n_{ij} = \delta_{ij} d_i$, and the $C$ in Eq.(3.11) is $C = d_1\theta_{1,1}\theta_{2,1} + d_2\theta_{1,2}\theta_{2,2} + d_3\theta_{1,3}\theta_{2,3}$, ordered so that $d_1 \geq d_2 \geq d_3$, ($d_i \in \mathbb{R}$ and $n_{ij} \in \mathbb{R}$). The maximum value of $C$ is attained by choosing the largest $d_i$ and setting the corresponding $\theta_{1,i} = 1$. This is much simpler than other methods that have been used [69, 70].

With $n_{ij} = \delta_{ij} d_i$, the geometric quantum discord as in Eq.(3.12) now simplifies as

$$D_{GG} \quad = \tfrac{1}{4}(d_1^2 + d_2^2 + d_3^2 - \max_i d_i^2) = \tfrac{1}{4}(d_2^2 + d_3^2) \tag{3.16}$$

$D_{GG}$ is the sum of the squares of the singular values *excluding* the largest one [71–73].

The (original) quantum discord is defined as

$$D = I - J = (\textit{total correlation}) - (\textit{classical correlation})$$

This allows us to interpret this expression for the geometric quantum discord as follows. The largest singular value of the Bloch vector quantifies the classical correlation, and the basis vectors that diagonalize the corresponding density matrix give us the measurement direction that teases out this correlation. If the other directions are uncorrelated, as they would be in a classical state, then $D = 0$. In a quantum-correlated state, there is residual correlation over and above this classical correlation in the other directions. This additional correlation is the discord and it is measured by the size of the other singular values. In other words, the other singular values are how large the off-diagonal terms of the density matrix would be in the "classical" basis.

The fact that the geometric quantum discord is a function only of the 2nd and 3rd largest singular values is in sharp contrast to entanglement. For the Bell diagonal states, the entropy of formation $E$ was calculated can be computed analytically [74]. A Bell diagonal state is parametrized by three parameters $c_1, c_2, c_3$, whose physically allowed values (by positivity arguments) form a tetrahedron and the four corners of the tetrahedron are the maximally entangled Bell states $\psi^+, \psi^-, \phi^+, \phi^-$ given by $(c_1, c_2, c_3)_{Bell} = (1, 1, 1), (1, -1, -1), (-1, 1, -1), (-1, -1, 1)$. $E$ is a monotonic function of the distance to the closest corner $E(c_1, c_2, c_3) = (c_1, c_2, c_3) \cdot (c_1, c_2, c_3)_{Bell}$. Unlike geometric quantum discord, entanglement depends mostly on the radius (distance from the fully mixed state). It depends only weakly on the direction in the vector space of the $c_i$. This feature of $E$ is manifests itself in the possibility of entanglement sudden death which is due to the fact that there exists a finite radius within which all states are separable and the entanglement is zero [67, 75–77]. For Bell diagonal states, an octahedron of separable states resides inside the tetrahedron, inside which the state is separable[74]. Thus, $E$ is more fragile: more sensitive to external noise.

### N Qubits

Turning to the $N$-qubit case, Tucker decomposition can be applied to the tensor $n$. For example, for three indices, $n$ may be written as $n_{ijk} = \sum_{abc} D_{abc} R^{(1)}_{ai} R^{(2)}_{bj} R^{(3)}_{ck}$, where $R^{(\alpha)} \in$ SO(3) but $D_{abc}$ is not in any sense diagonal. No simple criterion seems to be available to determine whether $D_{abc}$ is of the form $D_{abc} = D_a \delta_{ab} \delta_{bc}$, in which case the decomposition is called higher order singular value decomposition (HOSVD)[78, 79]. For more than three qubits, HOSVD would be $n_{i_1 \cdots i_N} = \sum_a D_a \Pi_{k=1}^N R^{(k)}_{a i_k}$. In this case, we have three principal values and the GGQD can be calculated as in the two-qubit case, as in Eq.(3.16).

### Numerical Method

In this section we will be considering low-dimensional symmetric $n$'s.

$$\rho = \frac{1}{2^N}(I + \sum_{\vec{a}, a_i \neq 0} n_{\vec{a}} \sigma_{a_1} \otimes \cdots \otimes \sigma_{a_N}) \tag{3.17}$$

In these cases, it is reasonable to employ a heuristic algorithm used in other physical contexts to compute $D$. This algorithm demonstrably works for some simple cases, but we will apply it without proof. We regard $-n_{ijk\ldots}$as an interaction energy among classical spins $\vec{\Theta}_i$ located at sites labeled by $i$. The method starts with a trial set $\left\{\vec{\Theta}_i^{(0)}\right\}$, and uses it to compute a mean field on each of the sites. $\left\{\vec{\Theta}_i^{(1)}\right\}$ is computed by minimizing the energy at each site $i$ individually. $\left\{\vec{\Theta}_i^{(1)}\right\}$ is used to compute a new mean field that determines $\left\{\vec{\Theta}_i^{(2)}\right\}$ and the iteration is repeated to convergence. In practice, the convergence may be improved by introducing a damping factor $\alpha$ with $0 < \alpha < 1$ and computing $\left\{\vec{\Theta}_i^{(j)}\right\}'$, where

$$\begin{aligned}
\left\{\vec{\Theta}_i^{(0)}\right\}' &= \left\{\vec{\Theta}_i^{(0)}\right\}, \\
\left\{\vec{\Theta}_i^{(1)}\right\}' &= (1-\alpha)\left\{\vec{\Theta}_i^{(0)}\right\} + \alpha\left\{\vec{\Theta}_i^{(1)}\right\} \\
\left\{\vec{\Theta}_i^{(2)}\right\}' &= (1-\alpha)\left\{\vec{\Theta}_i^{(1)}\right\}' + \alpha\left\{\vec{\Theta}_i^{(2)}\right\}, \\
&\ldots
\end{aligned}$$

where $\left\{\vec{\Theta}_i^{(2)}\right\}$ is computed by minimizing the energy in the mean field of $\left\{\vec{\Theta}_i^{(1)}\right\}'$, not $\left\{\vec{\Theta}_i^{(1)}\right\}$. This method has been used for spin glasses and it is analogous to calculation methods that have been used for geometric entanglement [80].

As a simple example, consider $n = (n_{11}, n_{22}, ...) = (1, \frac{1}{2}, 0, ...)$ with initial guess $\vec{\Theta}_1^{(0)} = \vec{\Theta}_2^{(0)} = (\frac{1}{\sqrt{2}}, \frac{1}{\sqrt{2}}, 0)$, during the first iteration, update $\vec{\Theta}_1$ to

$$\vec{\Theta}_1^{(1)} = n \cdot \vec{\Theta}_2^{(0)} = (n_{11}\ \vec{\Theta}_{2,1}^{(0)} + n_{12}\ \vec{\Theta}_{2,2}^{(0)} + \cdots,\ n_{21}\ \vec{\Theta}_{2,1}^{(0)} + \cdots,\ \cdots)$$
$$= (\frac{1}{2\sqrt{2}}, \frac{1}{4\sqrt{2}}, 0) \rightarrow (\frac{2}{\sqrt{5}}, \frac{1}{\sqrt{5}}, 0)\ \textit{(normalized)}$$

update $\vec{\Theta}_2$ to

$$\vec{\Theta}_2^{(1)} = n \cdot \vec{\Theta}_1^{(1)} = (n_{11}\ \vec{\Theta}_{1,1}^{(1)} + n_{12}\ \vec{\Theta}_{1,2}^{(1)} + \cdots,\ n_{21}\vec{\Theta}_{1,1}^{(1)} + \cdots, \cdots)$$
$$= (\frac{1}{\sqrt{5}}, \frac{1}{4\sqrt{5}}, 0) \rightarrow (\frac{4}{\sqrt{17}}, \frac{1}{\sqrt{17}}, 0)\ \textit{(normalized)}$$

We can see $\vec{\Theta}_1^{(n)}, \vec{\Theta}_2^{(n)}$ gradually move to the optimal values of (1,0,0), (1,0,0) as $n$ increases.

This mean-field-like method is not as accurate or as general as, say, the branch and bound method[81]. Indeed, the general problem is very similar to the calculation of the ground state of a spin glass, and it is unlikely that mean-field approaches will be effective for very general states. For the relatively symmetrical cases we will consider in the next chapter it seems to be adequate.

## 3.5 Summary

In this chapter, I demonstrated the motivation to consider a type of new quantum correlation, quantum discord besides quantum entanglement. I proposed the use of the generalized Bloch vector for calculation of quantum discord. It makes calculation easier for previously known cases and provides some useful insights on quantum correlation. We showed (under certain weak assumptions) that the calculation of the geometric global quantum discord is an NP-hard problem by considering a certain interesting class of multi-qubit states. It appears to be significantly more difficult to prove corresponding statements for other, non-geometric measures of discord, since they involve more complicated functions. For states of the form of Eq.(3.17), I suggested a numerical method to calculate geometric global quantum discord, which appears to give good results for many interesting models.

# Chapter 4

# Dynamics of Quantum Discord

## 4.1 Introduction

As it was discussed in Chapter 2, a quantum system exposed to the interaction with its environment goes through decoherence process, through which it losses its quantum coherence. The behavior of quantum entanglement under decoherence was studied in detail and it was shown that quantum entanglement suddenly vanishes as decoherence proceeds[2, 3, 67]. As I demonstrated with the geometric global quantum discord (GGQD) in Chapter 3, this peculiar behavior is due to the fact that two-qubit Bell diagonal states have the parameter space of zero entanglement with non-zero volume, while concordant space (with zero quantum discord) has zero volume[65, 82]. Therefore, quantum discord is more robust to noise and it was shown that a class of initial states for which the quantum discord are slowed destroyed (or not destroyed in extreme cases) by decoherence for certain initial period, after which quantum discord starts to drop down and the loss of classical coherence slows down which is called "sudden transition of decoherence". In this chapter, I will investigate the dynamics of quantum discord to find the condition for the sudden transition to be observed for more general choice of initial state. As it turns out, the sudden transition is generally not observed for randomly chosen initial state of the form of Eq. 3.17 and it becomes harder as the number of qubits increases.

## 4.2 Sudden Transitions Of Classical And Quantum Decoherence

### Dynamics Of Discord

Now having achieved some insight into the geometrical structure of quantum discord in Chapter 3, we can make some statements about its dynamics. We define the concordant set as the set of states with zero quantum discord. Sudden death of quantum discord does not occur in a generic system evolution because the concordant space has measure zero and is nowhere dense[65, 82]. Thus a state picked out at random has positive discord with very high probability and an arbitrarily small perturbation can always be found that will take a state with zero discord to a state of strictly positive discord. By the same token, the phenomenon of frozen geometric discord (in which the geometric discord is constant for a finite interval of time) is also not generic. It occurs in highly symmetric situations when the trajectory in state space parallels the nearest surface of the concordant set (of zero quantum discord).

The stronger anisotropy in the state space (as it depends only on the 2nd and 3rd singular value as shown in the previous section) of the quantum discord as compared to the entanglement implies that it can be less sensitive to decoherence than entanglement, if the decoherence takes the trajectory in the proper direction. We now consider these effects as manifested in the observation of sudden transitions in the quantum discord.

The type of sudden transition we consider is when the quantum discord $D_{GG}(t)$ decays at first slowly (classical decoherence) until a certain time $t_c$ when it begins to decay more quickly (quantum decoherence), the transition point being defined by a discontinuous change of the derivative $dD_{GG}(t)/dt$ at $t = t_c$. The sudden transition for two qubits was demonstrated for states of the form:

$$\rho = \frac{1}{4}(I + n_{11}\sigma_{11} + n_{22}\sigma_{22} + n_{33}\sigma_{33})$$

and a dynamical model that included only phase flips: $\rho \to p\rho + (1-p)\sigma_z\rho\sigma_z$, where $p(t)$ is a monotonically increasing function of time. Under these circumstances the $z$-like components

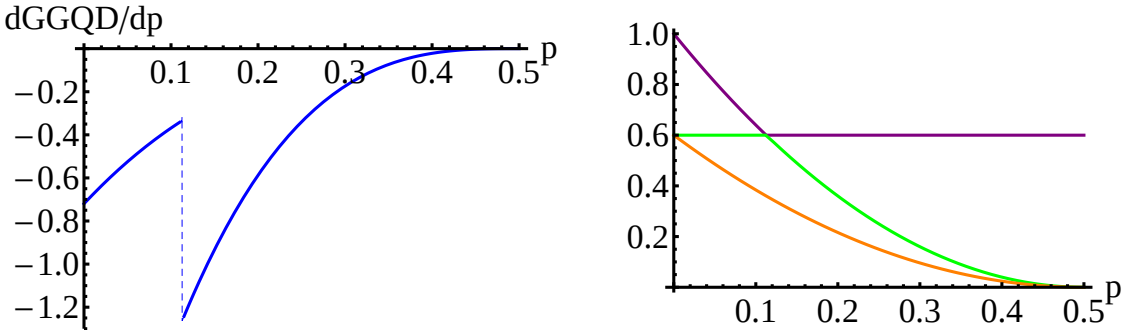


(a) Discontinuous derivative

(b) Level crossing

Figure 4.1: (a) The sudden transition is characterized by a discontinuous change in the time derivative of the discord. Here this phenomenon is shown for a model in which decoherence comes from phase flips. p is the probability that a flip has taken place, so p is a monotonically increasing function of time. (b) The transition may be traced back to the a level crossing of singular values f the density matrix. Here we show the three largest singular values as a function of time.

of the generalized Bloch vector do not decay, while the $x$- and $y$-like components elements do decay. This suggests that the observation of the transition is connected with the existence of decoherence-free subspaces.

It was shown that the condition of the sudden transition with quantum discord for the state of the form $\rho = \frac{1}{4}(I + n_{11}\sigma_{11} + n_{22}\sigma_{22} + n_{33}\sigma_{33})$ is either $|n_{11}(p=0)| \geq |n_{33}(p=0)|$ or $|n_{22}(p=0)| \geq |n_{33}(p=0)|$[2]. We have the identical condition for geometric global quantum discord as is clearly seen from Eq.(3.16). The discontinuous change in the slope of geometric global quantum discord occurs if and only if the first ($d_1$) and second largest ($d_2$) singular values cross as a function of $p$. In this case $d_1$ has a discontinuous derivative as a function of $p$ (or $t$). The discontinuity in the derivative of GGQD and its connection with the behavior of the singular values is shown in Figure 4.1. The crossing is observed because the $n_{33}$, which is supposed to be either the second or the third largest initial singular value, does not change due to the aforementioned symmetry of the system. The same behavior occurs for a state of the form: $\rho = \frac{1}{4}(I + \sum_{i,j=1,2} n_{ij}\sigma_{ij} + n_{33}\sigma_{33})$ where the discontinuous change of derivative is also observed.

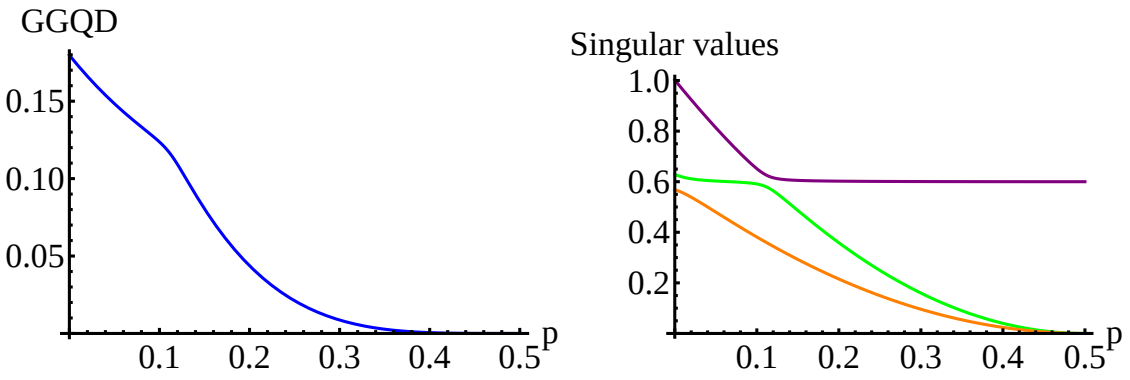


(a) Geometric Global QD (b) Singular values

Figure 4.2: (a) The sudden transition is smoothed when the level crossing is avoided. Here the discord as a function of time shows a smooth crossover from slow to fast decay. (b) The three largest singular values of the density matrix. The crossing of the two largest singular values is now avoided. The symmetry that allowed the level crossing in Figure 1(b) has been removed.

However, when we have non zero $n_{i3}$, $n_{3i}$ $(i = 1, 2)$ elements, the symmetry is violated and the level crossing goes away. The singular value evolution is completely smooth and the crossing does not occur. The contrast between the nearly discontinuous and the smooth behavior is shown in Figure 4.2. Thus the qualitative conclusion is that the sudden transition is due to a level crossing, which is essentially always a consequence of symmetry; level repulsion due to a small symmetry breaking smooths the crossing, giving rise to a smooth but rapid change, and generic level movement without any symmetry destroys the transition entirely. Similar conclusions have been obtained in [83]. It is important to note that if entropic definitions of discord are used, then rapid changes may still be observed, but the behavior of the discord is always continuous, as pointed out in [84]. This allows us to formulate more quantitatively the conditions for the observation of the sudden transition, for which sudden but not discontinuous change in the slope of geometric global quantum discord is observed, i.e., the level crossing is avoided, but the gap is small. It is motivated by observing that each singular value has contributions from various parts of the generalized Bloch vector, of which only the one from the protected part $n_{33}$ is preserved: $d_a = \sum_{ij} n_{ij} R^{(1)}_{ia} R^{(2)}_{ja} = n_{\alpha\alpha} R^{(1)}_{\alpha a} R^{(2)}_{\alpha a} + \sum_{(i,j)\neq(\alpha,\alpha)} n_{ij} R^{(1)}_{ia} R^{(2)}_{ja}$, where

$d_{a,robust} \equiv n_{\alpha\alpha} R^{(1)}_{\alpha a} R^{(2)}_{\alpha a}$ is the contribution to $d_a$ from the conserved part of Bloch vector. Contributions from other parts vanish as decoherence proceeds (with $p$ approaching 1/2). Therefore, we model the behavior of each singular value $d_a$ to monotonically decrease to $d_{a,robust}$ and the heuristic argument for the sudden transition is that the largest singular value crosses a smaller one as $p$ increases. In this picture, the criteria for the crossing of the largest singular value and the one of the smaller ones is either $|d_{2,robust}(p=0)| > |d_{1,robust}(p=0)|$ or $|d_{3,robust}(p=0)| > |d_{1,robust}(p=0)|$. But this model does not accurately describe the actual behavior, as it does not capture that the $R^{(i)}$s change over time as well and the only one singular value has nonzero value of $n_{33}$ at full decoherence ($p = 1/2$). However, if the size of the off-diagonal terms are small enough compared to the other parts, above argument still gives reasonable condition for sudden transition and it converges to the accurate condition as $\epsilon \to 0$. The previously shown condition [2] is a special case for $\epsilon \to 0$ case where $n_{ij}$ is diagonal.

### Probability of Sudden Change Dynamics

In order to estimate the chance of observing the sudden transition from arbitrary states of the form of Eq.(3.15), we assume the axis of each rotation $R^{(i)}$ is uniformly distributed over the unit spheres: $\Pr(\theta = \theta_0, \phi = \phi_0)\ d\theta\ d\phi = \frac{1}{4\pi}\sin(\theta_0)\ d\theta\ d\phi$. It corresponds to the random choice of SU(2) unitary matrix according to Haar measure, and we choose the state at random given the three singular values $d_a, a = 1, 2, 3$. The rotation matrix without nonzero off-diagonal entries corresponds to a rotation in two dimensional space, and the volume of the sets of 2-dimensional rotation matrices in the space of 3-dimentional rotation matrices of course has zero measure. Even if we loosen the condition by allowing a small deviation from the 2-dimensional rotation which results in small probability $\epsilon \ll 1$ for the rotation matrix to have the desired character, the probability of the sudden transition for the 2-qubit system is proportional to $\epsilon^2$. For the three or more qubits case where subsystems are maximally mixed ($\rho = \frac{1}{2^N}(I + \sum_{a_1=1}^{3} \cdots \sum_{a_N=1}^{3} n_{\vec{a}} \sigma_{\vec{a}})$) and HOSVD can be applied to the generalized Bloch vector as mentioned earlier ($n_{i_1 \cdots i_N} = \sum_a d_a \Pi_{k=1}^{N} R^{(k)}_{a i_k}$), each rotation matrix $R^{(i)}$

independently gives a additional factor of $\epsilon$ to the chance of the sudden transition so the chance of the transition decays exponentially as $\epsilon^N$, as $N$, the number of qubits, increases.

## 4.3 Summary

In this chapter, I used singular value decomposition to investigate the dyanamics of quantum discord. When higher-order singular value decomposition is applicable, we proposed a condition to observe the sudden transitions in the geometric global quantum discord, assuming the part preserved by the symmetry of the system and the other parts do not mix significantly. For randomly chosen states, the sharp sudden transition has only a small chance of being observed in the 2-qubit case and it becomes exponentially rarer as the number of qubits increases, because the number of restrictive symmetry conditions needed for this phenomenon to occur increases rapidly with system size.

# Chapter 5

# Decoherence and Entanglement in Multiple Quantum Dot Systems

## 5.1 Introduction

This chapter concerns the physical implementation of qubits in semiconductor quantum dots. Electrons in semiconductor quantum dots[26] are a promising candidate to enable coherent quantum control and the maturity of the semiconductor technology on which it is based gives hope that scaling up will not be difficult. The qubit logic might be implemented using the spin property of the electrons (spin qubit) or the location of the electrons in the quantum dots (charge qubit). Recent progress has demonstrated spin- and charge-like qubit implementations in Si and GaAs [22–25]. Charge qubits can be manipulated quickly (on the sub-nanosecond scale) e.g. by applying a voltage sequence which can be switch on sub-nanosecond scale [25]. However, at the same time they are exposed to the strong noise as they are strongly coupled to the environment which also leads to sub-nanosecond scale $T_2^*$ decoherence time [22, 24, 28]. On the other hand, spin qubits[23] couple weakly to the environment leading to slower $\sim 10$ nanosecond decoherence time. On the flip side, controlling spin qubits requires manipulation of magnetic field which is slow. This correlation between the control time and the decoherence time is not surprising because they both come

from the coupling to external degrees of freedom of the same nature.

Therefore, an ideal implementation would facilitate the best of both worlds with the fast control of the charge qubit and the long decoherence time of the spin qubit. One implementation of semiconductor quantum dots qubit is the singlet-triplet qubit[85] where we keep two electrons in double quantum dots representing the ground state (singlet) as the logical $|0\rangle$ and the one of the triple $\frac{1}{\sqrt{2}}(|\uparrow\downarrow\rangle - |\downarrow\uparrow\rangle)$ as the logical $|1\rangle$. Depending on the setting of the gate the qubit can operate in both charge-like and spin-like fashion. In each regime, the control time and the decoherence time are in competition against each other[86] and it was shown that an optimal point of operation can be chosen to find the 'golden spot' for one qubit operation[87]. Another recent implementation of semiconductor quantum dot qubits is the quantum dot hybrid qubit [88, 89]. In this scheme, three electrons are put into double quantum dots. Different spin states with long coherence times represent logical qubit states, and a transition to the excited state via the exchange coupling controlled by a charge pulse enabling a fast one qubit operation. This approach demonstrated the sub-nanosecond scale control while keeping the relatively long coherence time of spin qubit of $\sim$ 10ns, yielding more than 100 coherent oscillations within a $T_2^*$ time [25].

Most investigations have focused on the one qubit operation but relatively little light has been shed on two qubit operations. In order to make use of the power of quantum computation, it is necessary to implement two-qubit gate operations which involve the conditioning of the operation of one qubit on the state of the other [16]. There are two approaches to implement the two-qubit operation for semiconductor quantum dot qubits. One is to use Heisenberg exchange interaction of the form $H_{i,j} = J_{ij}\vec{S}_i \cdot \vec{S}_j$ between two qubits i, j. It is a strong interaction allowing fast gate operation of sub-nanosecond scale. Also it is short-ranged interaction arising from the spatial overlap of electron wavefunctions allowing on-off ratio of many orders of magnitude by controlling tunnel coupling between dot sites. So only the electrons seated on the adjacent sites are allowed to be coupled and this implies that the implementation of quantum operation depends on the choice of geometry of the quantum dots layout. Several implementations of the qubits in double quantum dots with

three electrons have given the sequence of the interaction control to perform one- and two-qubits operations [27, 89, 90]. One issue with this approach is that there is no general rule for finding the interaction control sequence to perform certain types of operations and it requires optimization calculations and the intuitive meaning of the obtained sequence seems to be purely operational giving little room for physical interpretation.

The other approach is to use the Coulomb interaction between two qubits. In some implementations, for e.g. singlet-triplet qubits, the charge distribution between $|0\rangle$ and $|1\rangle$ is different thus a Hamiltonian with different energy value according to the state of one qubit can be constructed. In recent experiments and numerical simulations, it was shown the energy shift of the scale of $\sim 20\mu eV$ would occur by the different charge setting between two double quantum dot qubits [28, 88, 91]. The strength of the coupling depends on the layout of the quantum dots and some suggestions have been made to increase the strength[92].

In this chapter, I will investigate the implementation of two-qubit operations using the capacitive coupling. In the similar way that the optimal parameters of operation were found for one qubit operations [87], I will suggest the optimal parameters for a two-qubit gate operation. As I will show more detail in later section, the optimal operation point for two-qubit operations is different from that of one-qubit operations due to the different behavior of the couplings. Two-qubit operation has not been implemented with the optimal parameters, which suggests that the performance can be improved. Also, I would estimate the minimum coupling strengh to expect the reasonable performance boost and it turns out that the coupling strengh in the current implementation is not strong enough.

## 5.2 Double Quantum Dot Qubit

Before proceeding to two-qubit gates, I will talk about the singlet-triplet qubit system[85] displaying a single logical qubit consisting of two electrons confined in the two double quantum dots. This allows us to define the appropriate parameters and fix some of the physics in a simplified case. The system, if it is not coupled to another qubit, has the following

Hamiltonian.

$$H_i = \begin{pmatrix} 0 & \Delta B_i & \sqrt{2}g_i \\ \Delta B_i & 0 & 0 \\ \sqrt{2}g_i & 0 & -\epsilon_i \end{pmatrix} \tag{5.1}$$

where $i = 1, 2$ and the Hamiltonian is written in the

$$\begin{aligned} \{|S(1,1)\rangle &= \frac{1}{\sqrt{2}}(|\uparrow_{(1)}\downarrow_{(2)}\rangle - |\downarrow_{(1)}\uparrow_{(2)}\rangle), \\ |T\rangle &= \frac{1}{\sqrt{2}}(|\uparrow_{(1)}\downarrow_{(2)}\rangle + |\downarrow_{(1)}\uparrow_{(2)}\rangle), \\ |S(0,2)\rangle &= \frac{1}{\sqrt{2}}(|\uparrow_{(2)}\downarrow_{(2)}\rangle - |\downarrow_{(2)}\uparrow_{(2)}\rangle)\} \end{aligned}$$

basis where the lower indices of the spins show which dot the electrons reside in. The first and the third states are coupled by the tunnel coupling constant $\sqrt{2}g$. The double occupation of the electrons causes the charge disparity and contributes to the energy splitting for the non-zero voltage detuning $\epsilon$ value. The logical qubits $|0\rangle$ and $|1\rangle$ are defined to be the two lowest energy eigenstates of the Hamiltonian with $\Delta B = 0$. $|1\rangle$ is always $|T\rangle$ and it is coupled to the singlet states with $\Delta B$. In the far left detuning limit $-\epsilon \gg g$, the tunneling $g$ between two singlets becomes negligible and $|0\rangle \sim |S(1,1)\rangle$ and in the far right detuning limit $\epsilon \gg g$, $|0\rangle \sim |S(0,2)\rangle$. The energy spectrum as $\epsilon$ changes is shown in Figure 5.1. In general, the eigenstates of the singlets are mixed and the lower energy state is the logical $|0\rangle$ while the other one becomes the excited, leakage state $|e\rangle$ not included in the logical qubit space,

$$\begin{aligned} |0\rangle &= \cos(\theta)\,|S(1,1)\rangle + \sin(\theta)\,|S(0,2)\rangle \\ |e\rangle &= -\sin(\theta)\,|S(1,1)\rangle + \cos(\theta)\,|S(0,2)\rangle \end{aligned}$$

The mixing angle $\theta$ and the energy eigenvalues (assuming $\Delta B = 0$) are as follows:

$$\begin{aligned} \tan(\theta) &= \frac{2\sqrt{2}g}{-\epsilon + \sqrt{8g^2 + \epsilon^2}}, \\ E_{|0\rangle} &= -\frac{\epsilon}{2} - \sqrt{2g^2 + (\frac{\epsilon}{2})^2} = -\sqrt{2}g\ \tan(\theta), \\ E_{|e\rangle} &= -\frac{\epsilon}{2} + \sqrt{2g^2 + (\frac{\epsilon}{2})^2} = \sqrt{2}g\ \tan(\frac{\pi}{2} - \theta) \end{aligned} \tag{5.2}$$

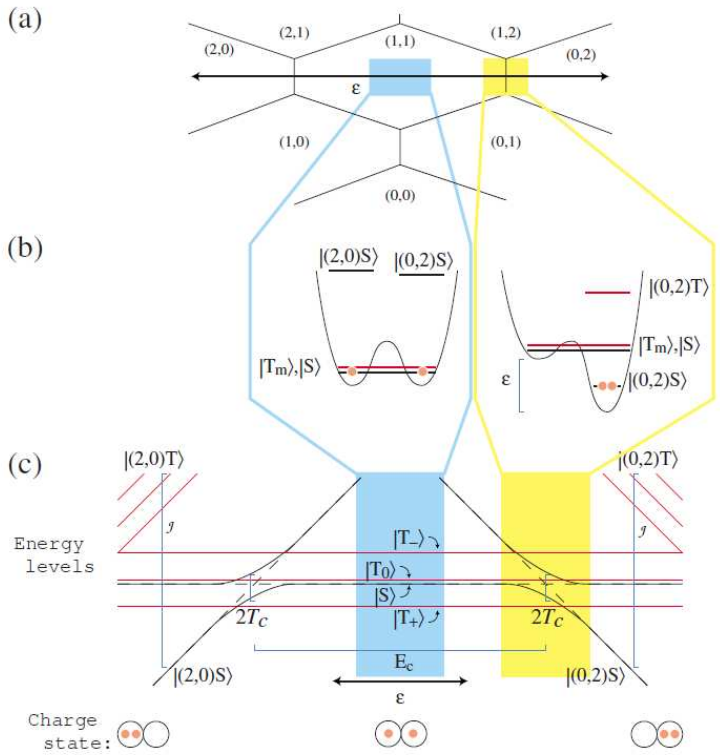


Figure 5.1: (Figure adapted from Taylor *et al.* [85]) (a) Charge stability diagram for a double-dot system. Double-ot occupation is denoted by ($n_l$, $n_r$). The detuning is parametrized by $\epsilon$, and the far-detuned regime (light blue) and charge transition (yellow) are shown. (b) Schematic of the double-well potentials along one axis (x) with tight confinement in the other two axes (i.e., y and z). In the far-detuned regime, the (1, 1) charge states are the ground state, while in the charge transition regime, (0,2) can be the ground state. Triplet states are indicated in red, while electron charges are indicated in orange. (c) Energy-level structure of the double-dot system as a function of detuning. From left to right, the lowest-energy charge state as a function of $\epsilon$ is (2,0), (1,1), and (0,2). The detuning at the middle of the graph corresponds to where $\epsilon = E_c/2$, $E_c$ is the charging energy of a single dot. The three (1,1) triplet states(shown in red) are split by the Zeeman energy.

It is worth noting that $\epsilon$ might be either positive or negative so care needs to be taken to deal with $\epsilon = \pm|\epsilon|$. Also, we can observe that in the far left detuning limit $-\epsilon \gg g$,

$$E_{|0\rangle} \simeq -\frac{2g^2}{|\epsilon|}, E_{|e\rangle} \simeq |\epsilon|.$$

Because the singlet-triplet double quantum dot qubit has different charge layouts for the two logical states, the charge noise is the dominant cause of decoherence. One source of the

charge noise is fluctuation of nearby charge distribution over time, and it changes the barrier which changes the tunneling coefficient between the dots and the detuning voltage of two dots [93]. I will assume the Markovian limit of this noise source which results in exponentially decaying off-diagonal elements of density matrix of a quantum system. Thus, in addition to the unitary time evolution $\frac{d\rho}{dt} = \frac{i}{\hbar}[\rho, H]$, the decoherence introduces an additional term to the equation $\frac{d\rho}{dt} = \frac{i}{\hbar}[\rho, H] + \mathcal{L}(\rho)$. The charge noise eliminates the quantum coherence between two states with the different charge profiles given by the off-diagonal terms:

$$\mathcal{L}(\rho) = \quad -\sum_{k,b} |k\rangle \langle b| \tilde{\Gamma}\delta\big((k(b), b(k)) = (0,1)\big)\rho_{|k\rangle,|b\rangle} \tag{5.3}$$

$\mathcal{L}$ can be described using Lindblad operators [94].

$$\mathcal{L}(\rho) = \sum_k L_k^+ \rho L_k - \frac{1}{2} L_k^+ L_k \rho - \frac{1}{2} \rho L_k^+ L_k \tag{5.4}$$

where $L_1 = \sqrt{\frac{\tilde{\Gamma}}{2}}\sigma_z$. The time evolution with decoherence can also described in Kraus operator-sum representation [16],

$$\rho(t) = \sum_k E_k(t)\rho(0)E_k(t)^+ \tag{5.5}$$

where $E_1(t) = \sqrt{\frac{1+e^{-\tilde{\Gamma}t}}{2}}U(t)$ and $E_2(t) = \sqrt{\frac{1-e^{-\tilde{\Gamma}t}}{2}}\sigma_z U(t)$.

Another source of the charge noise is the low-frequency charge fluctuators that we discussed in Chapter 2, which as an ensemble has the $1/f$ frequency spectrum. Though the slow fluctuators do not evolve over time during each experimental run, each run would have the different charge layout which would result in the varying voltage profiles with Gaussian distribution with the deviation $\sigma_\epsilon$. The time evolution of the off-diagonal part of the density matrix is convolved with the Gaussian distribution giving the $e^{-\frac{1}{2}(\frac{\frac{d\Delta E}{d\epsilon}\sigma_\epsilon t}{\hbar})^2}$ Gaussian decay factor and the $T_2^*$ coherence time of $\frac{\sqrt{2}\hbar}{\frac{d\Delta E}{d\epsilon}\sigma_\epsilon}$ [22]. The experiments have shown that the decoherence rate with the Gaussian envelope from quasistatic slow noise is dominantly larger than fast Markovian noise [22, 24, 87, 95].

The charge noise results in the density matrix of the state being

$$\rho = \begin{pmatrix} \rho_{00} & D\rho_{01} \\ D\rho_{10} & \rho_{11} \end{pmatrix}$$

where $\rho_{01}$ and $\rho_{10}$ are the off-diagonal elements with no decoherence and $D$ is the decaying factor

$$D \equiv e^{-\tilde{\Gamma}_M t} e^{-(\tilde{\Gamma}_G t)^2}$$

for the off-diagonal elements of density matrix of a quantum system. The Lindblad operator in Eq. 5.4 would then be $L_1 = \sqrt{\frac{\tilde{\Gamma}_M + \frac{1}{2}\tilde{\Gamma}_G t}{2}}\sigma_z$ and the Kraus operator in 5.5 would be $E_1(t) = \sqrt{\frac{1+D}{2}}U(t)$ and $E_2(t) = \sqrt{\frac{1-D}{2}}\sigma_z U(t)$. It was observed that the maximum Gaussian decay rate is approximately $\Gamma_{G,max} \sim 10$ GHz [22, 24] and the Markovian decay rate is approximately $\Gamma_{M,max} \sim 1$ GHz [87, 95].

The influence of the charge noise on the system is due to the different charge distributions of the states $|0\rangle$ and $|1\rangle$. The energy shift by the small change of potential gap $\frac{d\Delta E}{d\epsilon}$ is proportional to the charge disparity, so the effective decoherence rate is proportional to the slope of the energy splitting which is maximized at the large detuning limit at far right $\epsilon \gg g$. The slope is $s(\epsilon) = (\epsilon + \sqrt{\epsilon^2 + 8g^2})/(2\sqrt{\epsilon^2 + 8g^2}) = \sin(\theta)^2$ where the mixing angle between single-occupied and double-occupied singlet states is given in Eq.(5.2) and

$$\tilde{\Gamma}_M = \Gamma_{M,max} s(\epsilon) \leq \Gamma_{M,max} \tag{5.6}$$

$$\tilde{\Gamma}_G = \Gamma_{G,max} s(\epsilon) \leq \Gamma_{G,max} \tag{5.7}$$

The lowest energy state $|0\rangle$ approaches $|S(0,2)\rangle$ as the detuning $\epsilon$ is pushed toward right, while the second lowest energy state $|1\rangle$ does not mix with $|e\rangle$ so its charge distribution does not change. As a result, the largest charge disparity is obtained in the $\epsilon \gg g$ limit.

## 5.3 Three Levels vs. Two Levels

We can describe a two-level quantum system using a Bloch vector and it can be generalized to Bloch tensor for multipartite systems as I discussed in Chapter 1.3. But as we consider three-level system described in Eq.(5.1) one of which is the leakage state not included in the logical qubit state, we need a way to extract the two-level equivalent information out of three levels. One option is to disregard the part of the density matrix related to the leakage state. However, care needs to be taken as the unit trace and positivity requirements

need to be fulfilled so simple clopping of the density matrix would not be a proper choice. Kurzyński [96] has shown that a three-level system can be described by three Bloch vectors each of which relating a pair ouf of three levels. I suggest using the Bloch vector for the logical states to describe two-level logical information of three-level system, and I think this is a good choice as the Bloch vector description satisfies the unit trace and positivity requirements and the purity of the extracted state is bounded by the trace of the logical two-level part of the original density matrix.

### One Qutrit

Here I will describe the usage of the two-level system Bloch vector to extract the two-level information out of three-level system[96]. The basic idea is to regard the first two levels only to obtain the Bloch vector and adjust the trace value to the unity. For the density matrix of a three level system where the first two states are the basis for the logical qubit state,

$$\rho = \begin{pmatrix} \rho_{00} & \rho_{01} & \rho_{0e} \\ \rho_{10} & \rho_{11} & \rho_{1e} \\ \rho_{e0} & \rho_{e1} & \rho_{ee} \end{pmatrix}$$

The first two levels are taken:

$$\rho = \begin{pmatrix} \rho_{00} & \rho_{01} \\ \rho_{10} & \rho_{11} \end{pmatrix}$$

and $(1 - \rho_{00} - \rho_{11})\frac{I}{2}$ is added to finally obtain

$$\rho = \begin{pmatrix} \frac{1+\rho_{00}-\rho_{11}}{2} & \rho_{01} \\ \rho_{10} & \frac{1-\rho_{00}+\rho_{11}}{2} \end{pmatrix}$$

The description is equivalent to constructing Bloch vector elements

$$n_x = \rho_{01} + \rho_{10}, n_y = i(\rho_{01} - \rho_{10}), n_z = \rho_{00} - \rho_{11}$$

For instance, from

$$\begin{pmatrix} 0.5 & 0 & 0 \\ 0 & 0 & 0 \\ 0 & 0 & 0.5 \end{pmatrix}$$

we extract $\frac{0.5I+0.5\sigma_z}{2}$

$$\begin{pmatrix} 0.5 & 0 \\ 0 & 0 \end{pmatrix}$$

and adjust it to $\frac{I+0.5\sigma_z}{2}$ so that it has the unit trace.

$$\begin{pmatrix} 0.75 & 0 \\ 0 & 0.25 \end{pmatrix}$$

The final result maintains the quantum coherence as it has non-zero Bloch vector element along z-direction, and it is reasonably not a pure state as the original state involves non-zero third state element $\rho_{22}$.

This method would disregard the coherence of the logical states with the leakage state, whose benefit for quantum computation has not been investigated yet. The amount of loss would be negligible if the size of leakage is small ($\rho_{ee} \ll 1$) [97].

### $N$ Qutrits

The idea of chopping the density matrix can be applied to multi-partite states. For instance, the state of two three-level states (qubits) is described by $9 \times 9$ density matrix, and the two-level $4 \times 4$ part is extracted

$$n_{Iz} = \rho_{00,00} - \rho_{01,01} + \rho_{10,10} - \rho_{11,11}, n_{zI} = \rho_{00,00} + \rho_{01,01} - \rho_{10,10} - \rho_{11,11}$$

$$n_{zz} = \rho_{00,00} - \rho_{01,01} - \rho_{10,10} + \rho_{11,11}$$

$$n_{Ix} = \rho_{00,01} + \rho_{01,00} + \rho_{10,11} + \rho_{11,10}, n_{xI} = \rho_{00,10} + \rho_{10,00} + \rho_{01,11} + \rho_{11,01}$$

$$n_{zx} = \rho_{00,01} + \rho_{01,00} - \rho_{10,11} - \rho_{11,10}, n_{xz} = \rho_{00,10} - \rho_{01,11} + \rho_{10,00} - \rho_{11,01}$$

$$n_{Iy} = i(\rho_{00,01} - \rho_{01,00} + \rho_{10,11} - \rho_{11,10}), n_{yI} = i(\rho_{00,10} + \rho_{01,11} - \rho_{10,00} - \rho_{11,01})$$

$$n_{zy} = i(\rho_{00,01} - \rho_{01,00} - \rho_{10,11} + \rho_{11,10}), n_{yz} = i(\rho_{00,10} - \rho_{01,11} - \rho_{10,00} + \rho_{11,01})$$

$$n_{xy} = i(\rho_{00,11} - \rho_{01,10} + \rho_{10,01} - \rho_{11,00}), n_{yx} = i(\rho_{00,11} + \rho_{01,10} - \rho_{10,01} - \rho_{11,00})$$

$$n_{xx} = \rho_{00,11} + \rho_{01,10} + \rho_{10,01} + \rho_{11,00}, n_{xx} = -\rho_{00,11} + \rho_{01,10} + \rho_{10,01} - \rho_{11,00}$$

to construct the Bloch tensor for a two qubit system $\rho = \frac{\sum_{a\in\{0,1,2,3\}^{\otimes 2}} n_a\sigma_a}{4}$ and take $n_{II} = 1$ so that the trace of $\rho$ would be 1. This can be readily generalized to $N$-qubit case to construct $\rho_N = \frac{\sum_{a\in\{0,1,2,3\}^{\otimes N}} n_a\sigma_a}{2^N}$ with $n_{II} = 1$ to meet the unit trace requirement.

## 5.4 One-Qubit Operation

One-qubit operation in silicon quantum dot systems has been investigated [22–25]. Koh *et al.* has suggested the ideal point of the detuning $\epsilon$ to perform one-qubit x-rotate and z-rotate gate operations for double quantum dot qubit [87]. In its implementation of double quantum dot qubit, one-qubit z-rotation is implemented using the energy gap between the two logical qubit states, $J_1 = \Delta E$, which, in the far-detuned regime $\epsilon \ll -g$, is approximately $\frac{2g^2}{|\epsilon|}$. On the other hand, the charge noise decoherence rate $\tilde{\Gamma}$ in Eq.(5.6) depends on the derivative of the energy gap which is approximately $s(\epsilon) \sim \frac{2g^2}{|\epsilon|^2}$ in the far-detuned regime $\epsilon \ll -g$. The operation time for a $\pi$ z-rotation $\tau_{operation} \sim \frac{\hbar\pi}{J_1} \propto |\epsilon|$, together with the decoherence rate $\tilde{\Gamma} = \Gamma_{max}s(\epsilon)$ decides the amount of decoherence by $\tilde{\Gamma}\tau_{operation} \propto \frac{1}{|\epsilon|}$.

So decoherence for one-qubit operations can be suppressed by pushing the detuning $\epsilon$ to far left regime until another, non-charge noise decoherence effect kicks in. The impact of non-charge noise decoherence is independent of the detuning value so pushing $\epsilon$ to left worsens the decoherence effect by elongating the operation time while the non-charge noise decoherence rate is kept constant. The optimal middle point taking into account the competing effect of both noise sources had been suggested [87]. (Figure 5.2) It needs to be noted that this argument depends on the implementation of the gate operation. Recently, one-qubit operation with hybrid qubit (with three electrons in double quantum dots) was demonstrated to take advantage of its different energy spectrum to reduce the decoherence [25].

## 5.5 Two-Qubit Operation

To the best of my knowledge, the implementations for one-qubit operation were performed in the regime where $\epsilon < 0$ [22–25]. As shown in Section (5.4), the reason is that as the detuning

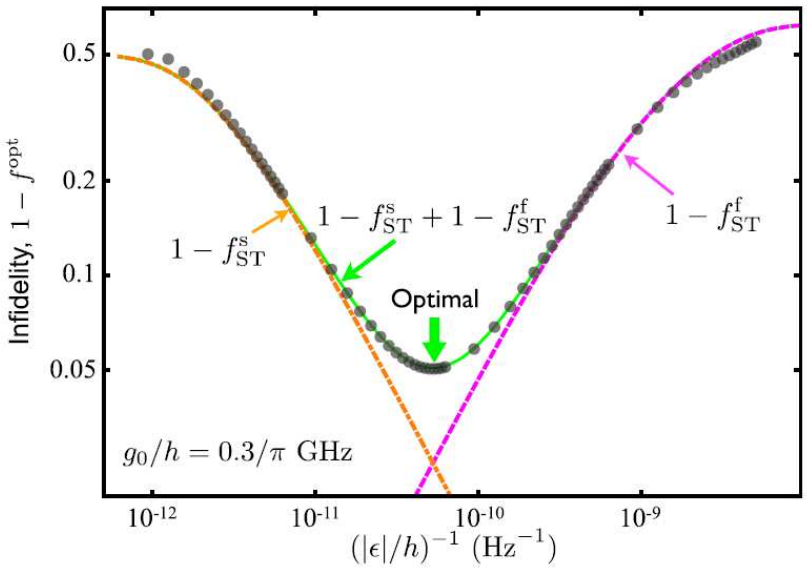


Figure 5.2: (Figure adapted from Koh *et al.* [87]) The infidelities (1 - fidelity) as the detuning $\epsilon$ changes. $f^f_{ST}$ (purple line) is the result with the charge noise only, $f^s_{ST}$ (orange line) is the one with the non-charge noise only. The optimal value is of $\epsilon$ is obtained when both charge- and non-charge- noises are taken into account.

$\epsilon$ increases, the charge-noise decoherence rate increases fast enough to offset the shortened operation time. In this section, I will demonstrate that two-qubit capacitive interaction scales differently from the one-qubit interaction as the detuning $\epsilon$ is pushed toward right due to the fact that it is dipole-dipole interaction and suggest how to perform a two-qubit operation.

### The Procedure

I will base the discussion of two-qubit operation on the experimental result of Shulman *et al.* [91] where a procedure involving a two-qubit operation was demonstrated and resultant non-zero entanglement between two qubits was shown. I will introduce two double quantum dots and the interaction between them. The Hamiltonian of two double quantum dots has one-qubit Hamiltonian parts for each qubit and in addition it has the interaction term

$$H_{12} = H_1 \otimes I + I \otimes H_2 + J_{12} \left|0\right\rangle \left\langle 0\right| \otimes \left|0\right\rangle \left\langle 0\right|$$

Here $J_{12}$ is the two-qubit interaction that causes quantum correlation between two qubits and conditionally works only on state where the condition on both qubits is met (both in $|0\rangle$ state). The circuit diagram 5.8 describes the procedure.

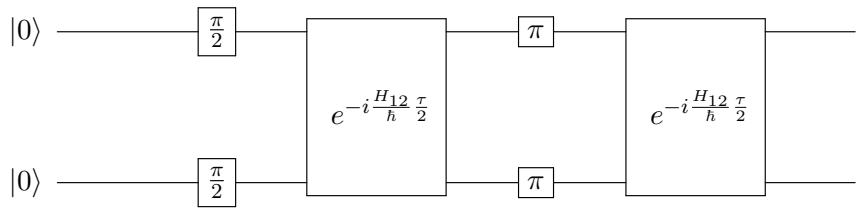


(5.8)

The initial state is prepared in $|\Psi_1\rangle$ $|0\rangle|0\rangle$. Then $|\Psi_2\rangle$ $\frac{\pi}{2}$ pulse is applied $|\Psi_3\rangle$ to change the state to $|\Psi_4\rangle$

$$|\psi_1\rangle = \frac{1}{\sqrt{2}}(|0\rangle - i\,|1\rangle) \otimes \frac{1}{\sqrt{2}}(|0\rangle - i\,|1\rangle) = \frac{1}{2}(|0\rangle\,|0\rangle - i\,|0\rangle\,|1\rangle - i\,|1\rangle\,|0\rangle - |1\rangle\,|1\rangle)$$

Then the detuning $\epsilon$ of both qubits changes concurrently to turn on the two-qubit coupling $J_{12}$ for the period of $\frac{\tau}{2}$, which results in

$$|\psi_2\rangle = \frac{1}{2}(e^{i\frac{-J_1-J_2}{2}\frac{\tau}{2}}\,|0\rangle\,|0\rangle - ie^{i\frac{-J_1+J_2}{2}\frac{\tau}{2}}\,|0\rangle\,|1\rangle - ie^{i\frac{J_1-J_2}{2}\frac{\tau}{2}}\,|1\rangle\,|0\rangle - e^{i\frac{J_1+J_2}{2}\frac{\tau}{2}}e^{-iJ_{12}\frac{\tau}{2}}\,|1\rangle\,|1\rangle)$$

Then $J_{12}$ is turned off and $\pi$ pulse is applied to flip the logical value of state ($|0\rangle \to -i\,|1\rangle$, $|1\rangle \to -i\,|0\rangle$) to give

$$|\psi_3\rangle = \frac{1}{2}(e^{i\frac{J_1+J_2}{2}\frac{\tau}{2}}e^{-iJ_{12}\frac{\tau}{2}}\,|0\rangle\,|0\rangle) + ie^{i\frac{J_1-J_2}{2}\frac{\tau}{2}}\,|0\rangle\,|1\rangle + ie^{i\frac{-J_1+J_2}{2}\frac{\tau}{2}}\,|1\rangle\,|0\rangle - e^{i\frac{-J_1-J_2}{2}\frac{\tau}{2}}\,|1\rangle\,|1\rangle$$

Finally $J_{12}$ is turned on for another $\frac{\tau}{2}$ evolution, which gives

$$\begin{aligned} |\psi_4\rangle = \quad & \frac{1}{2}(e^{-iJ_{12}\frac{\tau}{2}}\,|0\rangle\,|0\rangle) + i\,|0\rangle\,|1\rangle + i\,|1\rangle\,|0\rangle - e^{-iJ_{12}\frac{\tau}{2}}\,|1\rangle\,|1\rangle \\ = \quad & -\frac{1}{2}(1 - e^{-iJ_{12}\frac{\tau}{2}})\,|{+}{+}\rangle_y + (1 + e^{-iJ_{12}\frac{\tau}{2}})\frac{1}{2}(1)\,|{-}{-}\rangle_y \end{aligned}$$

where $|\pm\rangle_y = \frac{1}{\sqrt{2}}(|0\rangle \pm i\,|1\rangle)$. In case $\tau = \frac{\hbar\pi}{J_{12}}$, the final state $|\psi_4\rangle$ is:

$$|\psi_4\rangle = -e^{i\frac{\pi}{4}\sigma_y}\frac{1}{\sqrt{2}}(|{+}{+}\rangle_y - |{-}{-}\rangle_y)$$

We will assume that the two double quantum dots operate symmetrically so $\epsilon_1 = \epsilon_2 = \epsilon$, $g_1 = g_2 = g$.

### Quantum Correlation And Two-Qubit Operation

I will consider the concurrence [98, 99] to measure the quantum correlation of the two qubits created from a two-qubit operation. For simplicity, I will consider a two-qubits system prepared initially as

$$\frac{1}{2}(e^{-i\phi_0}|00\rangle + |01\rangle + |10\rangle + |11\rangle)$$

with $\phi_0 = 0$. With the two-qubit interaction $H_{12} = J_{12}|00\rangle\langle 00|$, the state evolves to

$$\frac{1}{2}(e^{-i(\phi(t)\equiv\phi_0+J_{12}t)}|00\rangle + |01\rangle + |10\rangle + |11\rangle) \tag{5.9}$$

The initial state with $\phi(t) = 0$ is separable $\frac{1}{\sqrt{2}}(|0\rangle + |1\rangle) \otimes \frac{1}{\sqrt{2}}(|0\rangle + |1\rangle)$ and when $\phi(t) = \pi$, fully entangled $\frac{1}{\sqrt{2}}|0\rangle \otimes \frac{-|0\rangle+|1\rangle}{\sqrt{2}} + \frac{1}{\sqrt{2}}|1\rangle \otimes \frac{|0\rangle+|1\rangle}{\sqrt{2}}$. The concurrence for the state of Eq.(5.9) can be calculated as

$$Con(t) = |\sin(\frac{\phi(t)}{2})|$$

As mentioned in Section 5.2, the Markovian noise affects the system to reduce the off-diagonal elements of the states with different charge profiles. If $|0\rangle = \cos(\theta)|S(1,1)\rangle + \sin(\theta)|S(0,2)\rangle$ and $|1\rangle = |T(1,1)\rangle$, charge noise rate would be effectively $\tilde{\Gamma} \equiv \Gamma \sin^2(\theta) = \Gamma s(\epsilon)$ and the charge noise would decay off-diagonal elements of the density matrix in a similar fashion as in Eq. 5.3. The density matrix of the state would evolve as

$$\rho = \begin{pmatrix} \rho_{00,00} & e^{-\tilde{\Gamma}t}\rho_{10,00} & e^{-\tilde{\Gamma}t}\rho_{01,00} & e^{-2\tilde{\Gamma}t}\rho_{11,00} \\ e^{-\tilde{\Gamma}t}\rho_{00,10} & \rho_{10,10} & e^{-2\tilde{\Gamma}t}\rho_{01,10} & e^{-\tilde{\Gamma}t}\rho_{11,10} \\ e^{-\tilde{\Gamma}t}\rho_{00,01} & e^{-2\tilde{\Gamma}t}\rho_{10,01} & \rho_{01,01} & e^{-\tilde{\Gamma}t}\rho_{11,01} \\ e^{-2\tilde{\Gamma}t}\rho_{00,11} & e^{-\tilde{\Gamma}t}\rho_{10,11} & e^{-\tilde{\Gamma}t}\rho_{01,11} & \rho_{11,11} \end{pmatrix}$$

And as there are two qubits, a factor of $e^{-\tilde{\Gamma}t}$ is introduced in the off-diagonal terms with different charge setting from each qubit, *e.g.* the $\rho_{11,00}$ element has $e^{-2\tilde{\Gamma}t}$ factor. The concurrence of the above state with the decoherence can be calculated as

$$Con(t) = \max\{e^{-\tilde{\Gamma}t}(|\sin(\frac{\phi(t)}{2})| - \sinh(\tilde{\Gamma}t)), 0\}$$

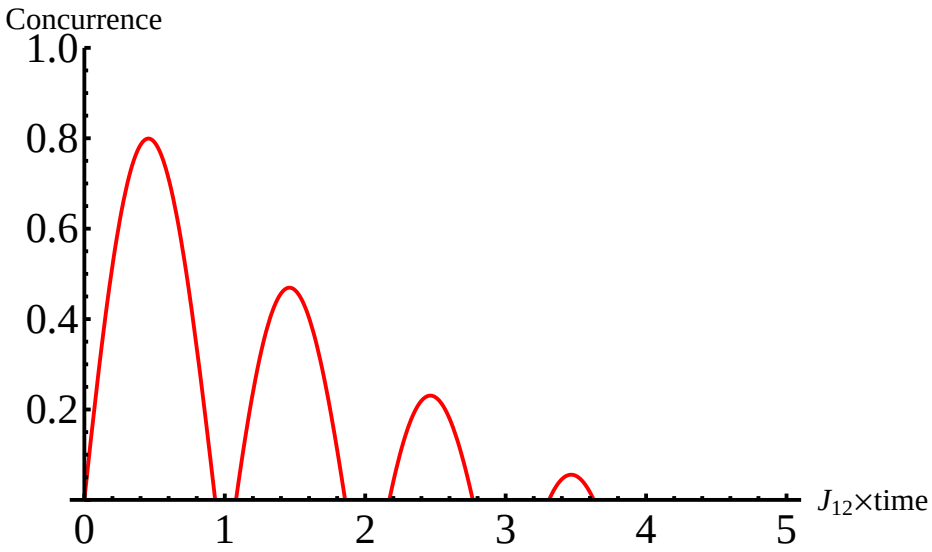


Figure 5.3: The concurrence of the state with decoherence ($J_{12,max} = 5$ GHz and $\Gamma_{M,max} = 1$ GHz, ignoring the slow noise).

As discussed in the Sec. 5.2, in addition to the Markovian noise, we have additional Gaussian decay factor from quasi-static slow noise with $1/f$ frequency spectrum caused by slow charge fluctuation discussed in Chapter 2. The decaying factor is altered to give

$$Con(t) = D(|\sin(\frac{\phi(t)}{2})| - \frac{D^{-1} - D}{2})$$

with $D = e^{-\tilde{\Gamma}_M t} e^{-(\tilde{\Gamma}_G t)^2}$. It is worthy noting that there is a competition between $J_{12}$ coupling to cause concurrence and the decoherence rate to quench it by getting rid of quantum coherence. For instance, the condition $\frac{dCon}{dt}(t = 0) > 0$ leads to $\frac{J_{12}}{\tilde{\Gamma}_M} > \frac{2(1+\sin(\phi_0))}{\cos(\phi_0)}$ which means there is a threshold value of $\frac{J_{12}}{\tilde{\Gamma}_M}$ so that additional concurrence would not be produced if the coupling $J_{12,max}$ is not as strong. It also needs to be noted that the concurrence of the system has the 'recurrence' behavior that it disappears to zero and revives, which was displayed as one of the general behaviors of quantum entanglement [67]. The concurrence dynamics is shown in Figure 5.3. Due to the decoherence, the envelope of the oscillations decays and the maximum value of the concurrence is obtained at the first peak. The following peaks have smaller values because of the decay.

### Parameter For Two-Qubit Operation

Now I will talk about how two-qubit interaction changes as the detuning $\epsilon$ changes. The largest dipole moment is generated in each qubit in the $\epsilon \gg g$ limit as the lowest energy state $|0\rangle$ approaches $|S(0,2)\rangle$ while the second lowest energy state $|1\rangle$ is kepts at $|T(1,1)\rangle$ as it does not mix with $|e\rangle$. In general, the energy shift by the small change of potential gap $\frac{d\Delta E}{d\epsilon}$ is proportional to the dipole moment, which gives us

$$J_{12}(\epsilon) \propto p_1(\epsilon)p_2(\epsilon) \propto s(\epsilon)^2$$

$$J_{12}(\epsilon) = J_{12,max}s(\epsilon)^2$$

where $s(\epsilon)$ is the slope of the energy splitting between $|0\rangle$ and $|1\rangle$,

$$s(\epsilon) = (\epsilon + \sqrt{\epsilon^2 + 8g^2})/(2\sqrt{\epsilon^2 + 8g^2}) = \sin(\theta)^2$$

where the mixing angle $\theta$ between $|S(0,1)\rangle$ and $|S(0,2)\rangle$ is given in Eq.(5.2). As a result, as the detuning increases, the polarization is obtained whose maximum value is achieved when $|0\rangle = |S(0,2)\rangle$. The operation time for the suggested two-qubit operation is the time to reach the first peak of concurrence $\tau \sim \frac{\hbar\pi}{J_{12}}$. This is an estimation as the actual time would be shorter due to the decay from decoherence. And the amount of decoherence is decided by $\tilde{\Gamma}_M\tau + \tilde{\Gamma}_G^2\tau^2 = \tilde{\Gamma}_{M,max}\frac{\hbar\pi}{J_{12,max}}\frac{1}{s(\epsilon)} + \tilde{\Gamma}_G^2(\frac{\hbar\pi}{J_{12,max}})^2\frac{1}{s(\epsilon)^2}$. Thus, without considering other restrictions, the two-qubit operation can be best performed where $s(\epsilon)$ obtains the maximum value of 1 ($\epsilon \gg g$). Numerical result in Figure 5.4 shows that the maximum concurrence during the process increases as $\epsilon$ (so $\frac{d\Delta E}{d\epsilon}$) increases for a fixed value of $J_{12,max}$.

### Restrction From Pulse Rise-time

However, this simple scaling argument for the two-qubit coupling has not taken into account the realistic restrictions such as pulse rise-time and one-qubit operations which are necessary to implement the whole algorithm. In this section, I will consider the pulse rise-time, which is of $\tau_{min} = 100ps$ [22]. For simplicity, I will only consider the Markovian decoherence rate.

Without considering the pulse rise-time, the optimal operation time would be how long it takes to achieve the first peak of concurrence, $\tau_{operation} = \tau_{optimal} \sim \frac{\hbar\pi}{J_{12,max}}$ (so that $\phi(t) \sim \pi$

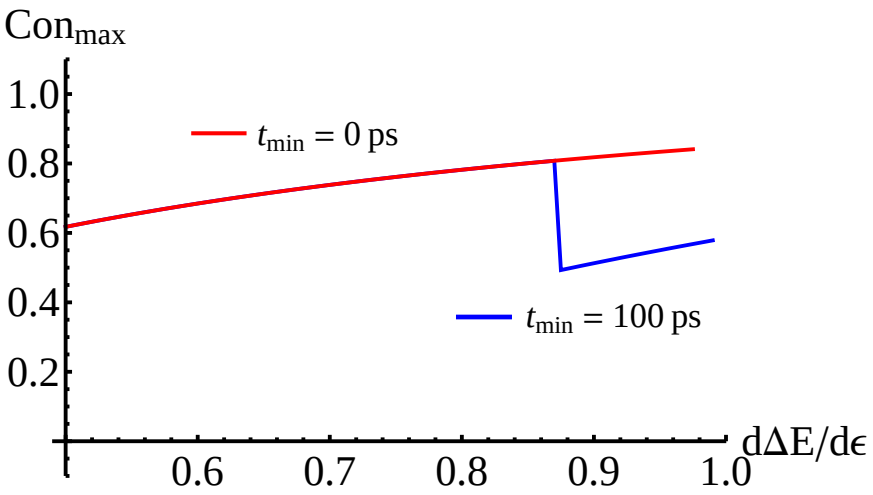


Figure 5.4: The maximum concurrence increases as the detuning value $\epsilon$ is pushed toward $\epsilon \gg g$ when $t_{min} = 0$ (blue line. $\epsilon$ at which the value drops is the optimal value of operation). However, when $t_{min} = 100ps$, increasing $\epsilon$ causes $J_{12}(\epsilon)$ large enough so that the first peak of the concurrence is found before $t_{min}$ and the maximum concurrence after $t_{min}$ is the second peak with lower value (red line). (with $J_{12,max} = 5$ GHz)

while the actual time would be shorter because of the decay from decoherence). And the amount of decoherence, as shown in Section 5.5, is decided by the size of $\tilde{\Gamma}_G \tau_{operation} \propto \frac{1}{s(\epsilon)}$ so that having large $s(\epsilon)$ value lowers the amount of decoherence and getting $\epsilon \gg g$ is a good choice. However, if $\tau_{optimal} < \tau_{min}$, then $\tau_{operation} = \tau_{min}$ as the procedure involves an application of $\pi$ pulse and the operation time $\tau_{operation}$ of the process can not be shorter than the pulse rise-time $\tau_{min}$. And the amount of decoherence is decided by $\tilde{\Gamma}_G \tau_{operation} = \Gamma_{G,max} s(\epsilon) \tau_{min}$ so getting large slope $s(\epsilon)$ actually makes the decoherence worse in this case. The comparison between the case with $t_{min} = 0$ and the case with $t_{min} = 100ps$ is shown in Figure 5.5.

On the other hand, as Gaussian noise is introduced, $e^{-(\tilde{\Gamma}_G t)^2}$ factor is added in addition to $e^{-\tilde{\Gamma}_M t}$ and the same argument as above might be applied. However, as Gaussian decoherence rate $\sim 10$ GHz is dominantly large, the first peak of the concurrence is significantly suppressed. Figure 5.6

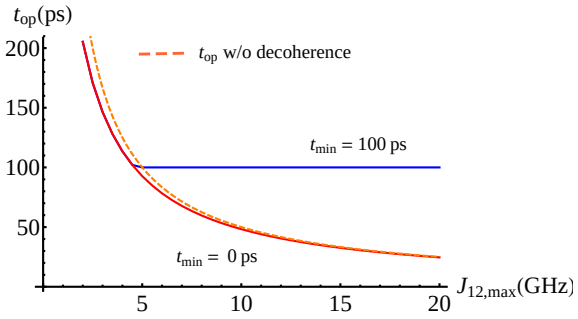


(a) $t_{op} vs.\ J_{12,max}$

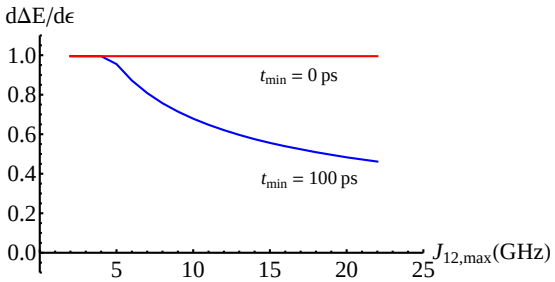


(b) slope($\epsilon$) $vs.\ J_{12,max}$

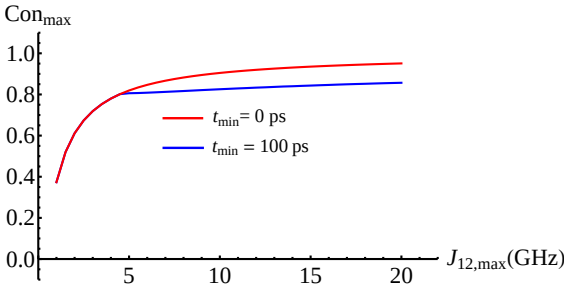


(c) $Con_{max}\ vs.\ J_{12,max}$

Figure 5.5: (a) As the coupling $J_{12,max}$ gets strong, the optimal operation time $t_{optimal}$ where the first peak of concurrence occurs decreases. Once $t_{optimal}$ hits $t_{min}$, the process can not be shortened further. The dashed line shows the first peak position without decoherence, $\frac{\hbar\pi}{J_{12,max}}$ and is shown to match the one with decoherence. (b) The slope $s(\epsilon) \equiv \frac{d\Delta E}{d\epsilon}$ value is shown where the optimal detuning $\epsilon$ is chosen. $s(\epsilon)$ has its maximum value 1 when $\epsilon$ is pushed toward $\epsilon \gg g$ and 1/2 when $\epsilon = 0$. In ideal situation ($t_{min} = 0$), the optimal operation always done with the maximum charge dispaity, but with non-zero $t_{min} = 100ps$, $\epsilon$ has to be adjusted to minimize the decoherence during the opeartion time $t_{operation} = t_{min}$. (c) In ideal situation with $t_{min} = 0$, the operation can be done arbitrarily quickly as long as the coupling strength allows. Due to the nature of the coupling, large charge disparity allows the operation time be shortened enough to offset the increased charge noise rate and higher concurrence can be achieved with stronger coupling $J_{12,max}$. With non-zero $t_{min}$, the improvement from stronger $J_{12,max}$ is hampered as the operation time $t_{operation}$ should be kept at $t_{min}$. (Only Markovian noise with $\Gamma_{M,max} = 1$ GHz is considered)

## 5.6 Summary

I have investigated a two-qubit operation that induces quantum coherence using capacitive coupling. Based on how the decoherence rate and coupling scale differently as the charge

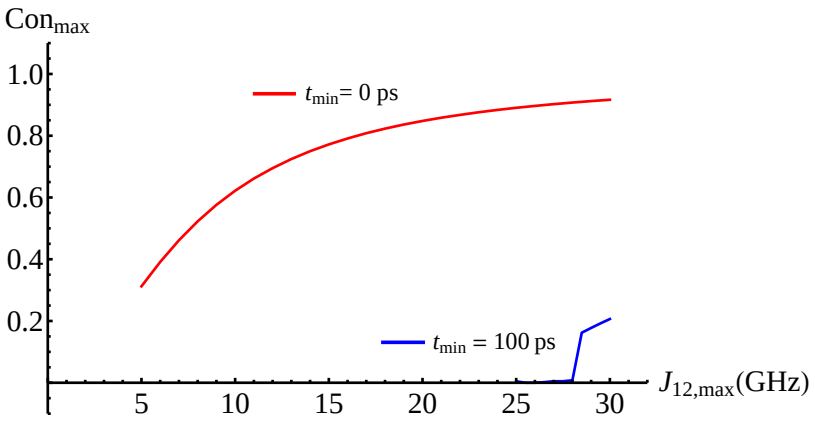


Figure 5.6: With the slow noise with $\Gamma_{G,max} = 10$ GHz, the maximum concurrence value is supressed due to the large decoherence rate comparing to Figure 5.5(c) ($\Gamma_{M,max} = 1$ GHz). With the pulse rise-time of $\tau_{min} = 100$ ps introduced (blue line), no first peak of concurrence can be obtained until $J_{12,max} \sim 27$ GHz.

distribution changes, I demonstrated that the two-qubit operations, unlike one-qubit counterpart, can, in the ideal case, be more efficiently done when we have large charge disparity between dots.

However, this improved performance is hampered when pulse-rise time is taken into account. Indeed, at a certain point the large charge disparity makes the decoherence rate larger while the operation time does not get shorter. Hence when the rise time is taken into account an optimal detuning value can be found. Even this calculation may be too simple as the detuning value may change during the pulsing duration so a really accurate description would require a more sophisticated analysis of the pulsing scheme.

On the experimental side it has been shown that the decoherence rate due to the slowly varying quasi-static noise would be $\sim 10$ GHz [22, 24] and it turns out this noise eliminates a substantial part of the quantum coherence so that the maximum concurrence with $J_{12,max} = 5$ GHz is only $\sim 0.3$. This suggests stronger coupling and echo techniques to remove the slow noise can improve the performance. In fact the procedure described in this chapter includes the application of a $\pi$ pulse which can function as a low frequency noise filter. An optimal pulse sequence should be designed which takes all of these factors into account, and we would expect that an experimental implementation using such a sequence would give

better performance.

# Chapter 6

# Conclusion

Correlation in quantum computing certainly plays important roles. In this thesis, I investigated correlations in the noise source and in the qubit system. Noise in quantum computing is the unwanted interaction between the qubit system and its environment. Noise correlation, which causes noises on distinct qubits to happen concurrently is generally thought to be harmful as error correction scheme can handle error occurring on up to certain number qubits. This is confirmed in the leading order calculation of the fidelity. However, in a classical noise correlation model that I suggested, it was shown that the correlation of classical telegraph noise might actually lead to improved performance.

On the other hand, quantum correlation between qubits seems to be a crucial part of quantum speed-up. Although the role of entanglement cannot be overlooked in quantum computation, its minimal involvement in certain quantum algorithms [1] suggests that it is not always an integral part of quantum computation, which led to the suggestion of the new type of quantum correlation, quantum discord. Like quantum entanglement, the operational meaning of quantum discord for quantum computation is not generally known, although the quantitative relation was shown for some algorithms [11]. One issue regarding quantum discord is that its definition involves optimization to extract maximum amount of classical correlation, making its calculation challenging. To investigate quantum discord calculation in multi-qubit systems, I used an altered version of quantum discord, geometric

global quantum discord. I proposed the use of the generalized Bloch vector for calculation of quantum discord as it makes calculation easier for previously known cases and provides some useful insights on quantum correlation. I showed that the calculation of the geometric global quantum discord is an NP-hard problem by transforming another NP-hard problem, MAX-k-SAT, into the calculation of geometric global quantum discord. I also conjecture that the calculation of quantum discord with non-geometric measure is NP-hard, but it appears to be significantly more difficult to prove the corresponding statements since they involve more complicated non-polynomial functions. For certain states of the form of Eq.(3.17), I suggested a numerical method to calculate geometric global quantum discord, which appears to give good results for many interesting models.

One property of quantum discord that separates it from quantum entanglement is that it persists longer under noisy environment than quantum entanglement and in some cases even stays constant until it suddenly changes its behavior and starts to decay (sudden transition) [2, 3]. The condition for this behavior had been shown for two-qubit Bell diagonal states[2], and I showed that the similar condition holds for the multi-partite state for whose Bloch tensor high order singular value decomposition can be applied. The point is that certain singular values are preserved by the symmetry of the system-environment interaction. In the case of small mixing, I showed the preserved part and the other parts should not mix significantly blurring the sharp transition. In general case, I propsed a model where the contribution of preserved part for the initial state decides if the crossing would occur during the decoherence process. Randomly chosen 2-qubit states have only a small chance to observe the sudden transition and it becomes exponentially rarer as the number of qubits increases as the number of conditions to meet the symmetry condition for the phenomenon rises rapidly.

Finally, I have investigated a two-qubit operation that induces quantum coherence using capacitive coupling. I suggested that two-qubit operation based on capacitive coupling might be done more efficiently in a parameter regime previously not explored. The point is that the decoherence rate and coupling strength scale differently as the charge distribution

changes, in the way that favors large charge disparity. But the two-qubit operation is not expected to perform sufficiently well as more realistic restrictions such as slow quasi-static $1/f$ noise and finite pulse rise-time are introduced.

For the future work, various aspects of the classical noise correlation model need to be tested for physical validity. Beneficial effects of quantum environment had also been shown before [46] but they did not go further than phenomenological demonstrations and further analysis is required. Also, an efficient way to handle non-geometric discord is needed. In order to separate quantum discord from quantum entanglement, I believe a careful exploration of quantum algorithms originally suggested with pure state but performed with mixed state would lead to a connection between the performance of quantum algorithms and quantum discord. In the two-qubit operation demonstrated in the thesis, as the slow noise is dominant source of decoherence, an experimental procedure involving echo-like sequence would improve the performance. And obviously stronger two-qubit capacitive coupling would be helpful. Also, I think the exchange coupling can be explored further as a candidate for multi-qubit gates [27].

# Appendix A

# Decoherence In Spin Boson Model

This section describes the derivation of Eq.(2.11), the fidelity of a system in quantum environment described with bosonic degree of freedome (spin boson model). It is based on the calculation given by Reina *et al.* [38]. I will omit $\hbar$ for simplicity. The Hamiltonian in this model is given as

$$\begin{aligned} H &= H_{sys} + H_{env} + V \\ &= H_{sys} + \sum_k \omega_k b_k^+ b_k + \sum_{n,k} \sigma_{z,n}(g_{k,n} b_k^+ + g_{k,n}^* b_k) \end{aligned}$$

where $H_{sys}, H_{env}, V$ are the parts describing the system, environment and interaction between them. $b_k^+, b_k$ are creation, annihilation operators for the mode $k$ with the frequency $\omega$. Now I will switch to the interaction picture as the change of basis of environment does not change the result after the environment traced out. The subscript $I$ stands for the interaction picture.

$$\begin{aligned} V_I &= \sum_{n,k} \sigma_{z,n}(g_{k,n} e^{i\omega_k t} b_k^+ + g_{k,n}^* e^{-i\omega_k t} b_k) \\ &\equiv \sum_k g_k(e^{i\omega_k t} b_k^+ \sigma_{z,k} + e^{-i\omega_k t} b_k \sigma_{z,k}^+) \end{aligned}$$

with $g_{k,n} = g_k e^{-i\vec{k}\cdot\vec{r}_n}$, $\sigma_{z,k} \equiv \sum_n e^{-i\vec{k}\cdot\vec{r}_n}\sigma_{z,n}$ (I will use the indices $m, n$ to indicate qubit $m, n$ positioned at $\vec{r}_m$, $\vec{r}_n$ and $k$ for boson mode).

Now I will calculate the interaction picture time evolution operator $U_I(t) = Te^{-i\int_{t_0'=0}^{t} dt' V_I(t')}$ where $T$ is the time ordering operator [31].

$$U_I(t) = T\exp(-i\int_{t_0'=0}^{t} dt' \sum_k g_k(e^{i\omega_k t'} b_k^+ \sigma_{z,k} + e^{-i\omega_k t'} b_k \sigma_{z,k}^+))$$

With $\phi(t) \equiv -i\int_0^{t'} dt' e^{i\omega_k t'} = \frac{1-e^{i\omega_k t}}{\omega_k}$, it can be written as following [31]

$$U_I(t) = e^{\sum_k A_k^+(t)} T\exp(-i\int_0^t dt' \sum_k e^{-A_k^+(t)}(g_k e^{-i\omega_k t'}\sigma_{z,k}^+ b_k)e^{A_k^+(t)})$$

$$= e^{\sum_k g_k\phi_k(t)\sigma_{z,k}b_k^+} T\exp(-i\int_0^t dt' \sum_k e^{-i\omega_k t'} e^{-(g_k\phi_k(t)\sigma_{z,k}b_k^+)}(g_k\sigma_{z,k}^+ b_k)e^{(g_k\phi_k(t)\sigma_{z,k}b_k^+)})$$

Using $e^{-B}Ae^B = A + [A,B] + \cdots$,

$$U_I(t) = e^{\sum_k g_k\phi_k(t)\sigma_{z,k}b_k^+} e^{-\sum_k g_k\phi_k(t)^*\sigma_{z,k}^+ b_k} \exp(-i\int_0^t dt' \sum_k |g_k|^2\sigma_{z,k}\sigma_{z,k}^+\phi_k(t')e^{-i\omega_k t'})$$

Using $e^{A+B} = e^A e^B e^{-\frac{1}{2}[A,B]}$,

$$\begin{aligned} U_I(t) &= e^{i\Phi(t)} e^{\sum_k (A_k^+(t) - A_k(t))} \\ &\equiv e^{i\Phi(t)} e^{i\sum_n B_n(t)\sigma_{z,n}} \end{aligned}$$

where

$$\begin{aligned} \Phi(t) &\equiv \sum_k |g_k|^2\sigma_{z,k}\sigma_{z,k}^+ \frac{\omega_k t - \sin(\omega_k t)}{\omega_k^2} = \sum_{m,n}\sum_k |g_k|^2 e^{i\vec{k}\cdot\vec{r}_{mn}}\sigma_{z,m}\sigma_{z,n}\frac{\omega_k t - \sin(\omega_k t)}{\omega_k^2} \\ &=_{m\leftrightarrow n} \sum_{m,n}\sum_k |g_k|^2\cos(\vec{k}\cdot\vec{r}_{mn})\sigma_{z,m}\sigma_{z,n}s(\omega_k,t) \end{aligned}$$

where $s(\omega_k,t) \equiv \frac{\omega_k t - \sin(\omega_k t)}{\omega_k^2}$. This is where the $D(t)$ in Eq.(2.10) comes from after integrating the angular part of $\vec{k}$. And

$$B_n(t) \equiv \sum_k (-i) g_k\big(\phi_k(t) b_k^+ e^{-i\vec{k}\cdot\vec{r}_n} - \phi_k^*(t) b_k e^{i\vec{k}\cdot\vec{r}_n}\big)$$

It is worthy noting that $i\sum_n B_n(t) = -i\int_0^t dt' V_I(t')$ (so $B_n(t)$ is a Hermitian operator) and the factor $e^{i\Phi(t)}$ appears due to the time ordering operator $T$. As $[iB_m(t), iB_n(t)] = -\sum_k g_k^2|\phi_k|^2 2i\sin(\vec{k}\cdot\vec{r}_{mn})$, it can be written as

$$e^{i\Phi(t)} e^{i\sum_{m<n}\sum_k g_k^2|\phi_k|^2\sigma_{z,m}\sigma_{z,n}}\Pi_n e^{iB_n(t)\sigma_{z,n}}$$

$$\equiv e^{i\Phi(t)+iC(t)}\Pi_n e^{iB_n(t)\sigma_{z,n}} \equiv e^{i\Phi_{mn}(t)\sigma_{z,m}\sigma_{z,n}+iC_{mn}(t)\sigma_{z,m}\sigma_{z,n}}\Pi_n e^{iB_n(t)\sigma_{z,n}}$$

where $\Phi_{mn} = \sum_k |g_k|^2 \cos(\vec{k} \cdot \vec{r}_{mn}) s(\omega_k, t)$ and $C_{mn} = \sum_k g_k^2 |\phi_k|^2$. This is where $D_{mn} \equiv \Phi_{mn} + C_{mn}$ in Eq. 2.6 is obtained.

Now apply the time evolution operator to a state $|\vec{a}\rangle = \otimes_{n=1}^{N} |a_n\rangle$ where $a_n \in \{0, 1\}$ and to $|\vec{b}\rangle$.

$$U_I(t) |\vec{a}\rangle = e^{i \sum_{m,n} \sum_k |g_k|^2 \cos(\vec{k} \cdot \vec{r}_{mn}) a_m a_n s(\omega_k, t)} e^{i \sum_n B_n(t) a_n} |\vec{a}\rangle$$
$$\langle \vec{b}| U_I^+(t) = \langle \vec{b}| e^{-i \sum_{m,n} \sum_k |g_k|^2 \cos(\vec{k} \cdot \vec{r}_{mn}) b_m b_n s(\omega_k, t)} e^{-i \sum_n B_n(t) b_n}$$

Using $e^A e^B = e^{A+B} e^{\frac{1}{2}[A,B]}$,

$$U_I(t) |\vec{a}\rangle \langle \vec{b}| U_I(t)^+ = |\vec{a}\rangle \langle \vec{b}| e^{i \sum_k |g_k|^2 \sum_{m,n} \cos(\vec{k} \cdot \vec{r_{mn}}) (a_m a_n - b_m b_n) s(\omega_k, t)} e^{i \sum_n B_n(t)(a_n - b_n)}$$
$$\left(e^{\frac{1}{2}[i \sum_n B_n(t)(-b_n), i \sum_n B_n(t) a_n]} = e^{\frac{1}{2}(|g_k|^2 |\phi_k|^2 2i \sin(\vec{k} \cdot \vec{r}_{mn}) b_n a_m)}\right)$$
$$= |\vec{a}\rangle \langle \vec{b}| e^{i \sum_k |g_k|^2 \left( \sum_{m,n} \cos(\vec{k} \cdot \vec{r_{mn}}) (a_m a_n - b_m b_n) s(\omega_k, t) + |\phi_k|^2 2 \sin(\vec{k} \cdot \vec{r}_{nm}) b_n a_m \right)} e^{i \sum_n B_n(t)(a_n - b_n)}$$

And because $\int d\Omega_k \sin(\vec{k} \cdot \vec{r}_{mn}) = 0$,

$$= |\vec{a}\rangle \langle \vec{b}| e^{i \sum_k |g_k|^2 \left( \sum_{m,n} \cos(\vec{k} \cdot \vec{r_{mn}}) (a_m a_n - b_m b_n) s(\omega_k, t) \right)} e^{i \sum_n B_n(t)(a_n - b_n)}$$

The state of the system and environment is

$$\rho = \sum_{\vec{a}, \vec{b}} \sum_{\vec{k}, \vec{k}'} \rho_{|\vec{a}, \vec{k}\rangle |\vec{b}, \vec{k}'\rangle} |\vec{a}, \vec{k}\rangle \langle \vec{b}, \vec{k}'|$$

The state of the system only can be calculated by tracing out the environemnt and its element $\rho_{sys, \vec{a}, \vec{b}}$ can be calculated as

$$Tr_{env}(U_I(t) \langle \vec{a}| \rho |\vec{b}\rangle U_I^+(t))$$
$$= e^{i \sum_k |g_k|^2 \sum_{m,n} \cos(\vec{k} \cdot \vec{r_{mn}}) (a_m a_n - b_m b_n) s(\omega_k, t)} Tr_{env}(\rho_{env} e^{i \sum_n B_n(t)(a_n - b_n)})$$

Where the tracing out can be done as following

$$
\begin{aligned}
&Tr_{env}\big(\rho_{env}e^{i\sum_n B_n(t)(a_n-b_n)}\big)\\
&= Tr_{env}\big(\rho_{env}(1+\sum_{k,n}(-i)g_k\big(\phi_k(t)b_k^+e^{-i\vec{k}\cdot\vec{r}_n}-\phi_k^*(t)b_ke^{i\vec{k}\cdot\vec{r}_n}\big)(a_n-b_n)\\
&+\frac{1}{2}\sum_{k,k'}\sum_{m,n}g_kg_{k'}\big(\phi_k(t)b_k^+e^{-i\vec{k}\cdot\vec{r}_n}-\phi_k^*(t)b_ke^{i\vec{k}\cdot\vec{r}_n}\big)\\
&\big(\phi_{k'}(t)b_{k'}^+e^{-i\vec{k'}\cdot\vec{r}_n}-\phi_{k'}^*(t)b_{k'}e^{i\vec{k'}\cdot\vec{r}_n}\big)(a_n-b_n)(a_m-b_m)+\cdots)\big)\\
&= 1+0\\
&+\frac{1}{2}\sum_k\sum_{m,n}|g_k(t)\phi_k(t)|^2(-1)\,Tr_{env}(b_k^+b_ke^{-i\vec{k}\cdot\vec{r}_{mn}}+b_kb_k^+e^{i\vec{k}\cdot\vec{r}_{mn}})(a_n-b_n)(a_m-b_m)+\cdots\\
&= 1+0+\frac{1}{2}\sum_k\sum_{m,n}|g_k(t)\phi_k(t)|^2(-1)\cos(\vec{k}\cdot\vec{r}_{mn})\,Tr_{env}(\{b_k,b_k^+\})\\
&+i\sin(\vec{k}\cdot\vec{r}_{nm})\,Tr_{env}(\big[b_k,b_k^+\big])(a_n-b_n)(a_m-b_m)+\cdots\\
&= 1-\sum_k|g_k(t)|^2\frac{1-\cos(\omega_kt)}{\omega_k^2}\coth(\frac{\omega_k}{2kT})\sum_{m,n}\cos(\vec{k}\cdot\vec{r}_{mn})+\cdots
\end{aligned}
$$

where $<\{b_k,b_k^+\}>_{env}=2\coth(\frac{\omega_k}{2kT})$. In general the term of odd power of $B_n(t)$ is traced out to be 0, while the ones of even power $2p$ has the coefficient of $\frac{1}{2p!}2^p(2p-1)!!=\frac{1}{p!}$ where $(2p-1)!!$ is the number of ways of making $p$ pairs from $2p$ $b_k,b_k^+$ operators and $2^p$ is from $p$ factors of 2 in $|\phi_k(t)|^2=2\frac{1-\cos(\omega_kt)}{\omega_k^2}$. So above expression becomes

$$
\begin{aligned}
&=\sum_{p=0}\frac{1}{p!}\big(-\sum_k|g_k(t)|^2\frac{1-\cos(\omega_kt)}{\omega_k^2}\coth(\frac{\omega_k}{2\tau})\sum_{m,n}\cos(\vec{k}\cdot\vec{r}_{mn})(a_n-b_n)(a_m-b_m)\big)^p\\
&=\Pi_k\exp(\big(-|g_k(t)|^2\frac{1-\cos(\omega_kt)}{\omega_k^2}\coth(\frac{\omega_k}{2\tau})\sum_{m,n}\cos(\vec{k}\cdot\vec{r}_{mn})(a_n-b_n)(a_m-b_m)\big)
\end{aligned}
$$

Eq.(2.8) is obtained from the expression above.

# Appendix B

# Transfer Matrix Method For Classical Noise

This section describes the derivation of the dephasing factor $\zeta$ of Eq.(2.15) of spin fluctuator model using transfer matrix method [41–43]. The basic idea is to extend the system states $\rho_{sys}$ to include the state of the fluctuators, each of which has two values (up and down) so can be described using a two-dimensional vector $\vec{p}$. Also, as the ensemble average is supposed to be calculated, the state vector of fluctuator represents the probability. The time evolution of the qubit system is described by unitary evolution $\frac{d}{dt}\rho_{sys} = \frac{i}{\hbar}[\rho_{sys}, H]$ while the time evolution of the fluctuator probability distribution $\vec{p}$ is given by the transfer matrix $\frac{d}{dt}\vec{p} = V\vec{p}$. $V$ is a $2 \times 2$ matrix

$$V = (-\gamma I + \gamma\sigma_x) = \begin{pmatrix} -\gamma & \gamma \\ \gamma & -\gamma \end{pmatrix}$$

where $\gamma$ is the flip rate of the fluctuator. Here I assumed that the fluctuator is unbiased. The Hamiltonian of the qubit system is

$$H = -\frac{1}{2}(B_0 + gs(t))\sigma_z$$

With this Hamiltonian, the time evolution of the quantum part is given as

$$
\begin{aligned}
i\left[|0\rangle\langle 0|, H\right] &= i\left[|1\rangle\langle 1|, H\right] = 0 \\
i\left[|0\rangle\langle 1|, H\right] &= +i(B_0 + gs(t))\,|0\rangle\langle 1| \\
i\left[|1\rangle\langle 0|, H\right] &= -i(B_0 + gs(t))\,|1\rangle\langle 0|
\end{aligned}
$$

For simplicity, I will assume $B_0 = 0$. The time evolution of the qubit system and classical environment together can be described as following

$$
\begin{aligned}
\frac{d}{dt}\{\vec{p}, |0\rangle\langle 0|\} &= \{V\vec{p}, |0\rangle\langle 0|\} = \{V, I\}\{\vec{p}, |0\rangle\langle 0|\} \\
\frac{d}{dt}\{\vec{p}, |1\rangle\langle 1|\} &= \{V\vec{p}, |1\rangle\langle 1|\} = \{V, I\}\{\vec{p}, |1\rangle\langle 1|\} \\
\frac{d}{dt}\{\vec{p}, |0\rangle\langle 1|\} &= \{V\vec{p}, |0\rangle\langle 1|\} + ig\{\sigma_z\vec{p}, |0\rangle\langle 1|\} = \{((-\gamma I + \gamma\sigma_x) - ig\sigma_z), I\}\{\vec{p}, |0\rangle\langle 1|\} \\
&= -i\{(i(-\gamma I + \gamma\sigma_x) - g\sigma_z), I\}\{\vec{p}, |0\rangle\langle 1|\} \equiv \{H_{quasi,+}, I\}\{\vec{p}, |0\rangle|1\rangle\} \\
\frac{d}{dt}\{\vec{p}, |1\rangle\langle 0|\} &= -i\{(i(-\gamma I + \gamma\sigma_x) + g\sigma_z), I\}\{\vec{p}, |1\rangle\langle 0|\} \equiv \{H_{quasi,-}, I\}\{\vec{p}, |1\rangle|0\rangle\}
\end{aligned}
$$

For the system with $N$ qubits, the time evolution of the quantum part would be described as

$$
i\left[|\mu\rangle\langle\nu|, H\right] = i\sum_{i=1}^{N} S_{\mu_i,\nu_i}(B_0 + gs_i(t))\,|\mu\rangle\langle\nu|
$$

If the noise on each qubit is independent, $s_i(t)$ for each $i$ is independent random variable. In case where the $N$ fluctuators are fully correlated, they share the same value altogether, $s_i(t) = s(t)$, and

$$
i\left[|\mu\rangle\langle\nu|, H\right] = i\sum_{i=1}^{N}(B_0 + g_{\mu,\nu}s_i(t))\,|\mu\rangle\langle\nu|
$$

where $S_{\mu_i,\nu_i} = 1$ if $(\mu_i, \nu_i) = (0, 1)$, $-1$ if $(\mu_i, \nu_i) = (1, 0)$, and 0 otherwise. And $g_{\mu,\nu} \equiv \sum_{i=1}^{N} S_{\mu_i,\nu_i} g$ is as given in Eq.(2.15).

$H_{quasi,\pm}$ can be diagonalized because it is a symmetric matrix.

$$
H_{quasi,\pm} = \sum_{i=1}^{2} \lambda_{\pm,i}\Pi_{\pm,i}
$$

It needs to be noted that as $H_{quasi,\pm}$ is not Hermitian, the inner products of its eigenvectors $\{\vec{v}_{\pm,i}\}$ is supposed to done with the transpose of one of them, not with the Hermitian conjugate which can be shown as following.

$$\begin{aligned}\vec{v}_2^T\vec{v}_1 &= \frac{1}{\lambda_1}\vec{v}_2^T(H_{quasi}\vec{v}_1)\\ &= \frac{1}{\lambda_1}(H_{quasi}^T\vec{v}_2)^T\vec{v}_1 = \frac{1}{\lambda_1}(H_{quasi}\vec{v}_2)^T\vec{v}_1 = \frac{\lambda_2}{\lambda_1}\vec{v}_2\vec{v}_1 = 0 \ (if\ \lambda_1 \neq \lambda_2).\end{aligned}$$

I will assume that the fluctuator is initially at the equalibrium, so $\vec{p}_i = \{\frac{1}{2}, \frac{1}{2}\}$. And I will average over the inital value of the fluctuator, which can be done by taking an inner product of $\vec{p}_f = \{1, 1\}$ and the final value of $\{\vec{p}, |\mu\rangle\langle\nu|\}$. $\vec{p}_i$ and $\vec{p}_f$ can be spanned by the eigenvectors of $H_{quasi,\pm}$

$$\begin{aligned}\vec{p}_i &= \sum_i c_{\pm,i}\vec{v}_{\pm,i}\\ \vec{p}_f &= \sum_i 2c_{\pm,i}\vec{v}_{\pm,i}\end{aligned}$$

The time evolution of the whole system can be

$$\begin{aligned}\{\vec{p_i}, |0\rangle\langle 1|\}(t) &= \{e^{-iH_{quasi,+}t}, I\}\{\vec{p_i}, |0\rangle\langle 1|\} = \sum_{i=1}^{2}\{e^{-i\lambda_{+,i}t}, I\}c_{+,i}\{\vec{v}_{+,i}, |0\rangle\langle 1|\}\\ \{\vec{p_i}, |1\rangle\langle 0|\}(t) &= \{e^{-iH_{quasi,-}t}, I\}\{\vec{p_i}, |1\rangle\langle 0|\} = \sum_{i=1}^{2}\{e^{-i\lambda_{-,i}t}, I\}c_{-,i}\{\vec{v}_{-,i}, |1\rangle\langle 0|\}\\ \{\vec{p_i}, |0\rangle\langle 0|\}(t) &= e^{Vt}\{\vec{p_i}, |0\rangle\langle 0|\} = \{\vec{p_i}, |0\rangle\langle 0|\}\\ \{\vec{p_i}, |1\rangle\langle 1|\}(t) &= e^{Vt}\{\vec{p_i}, |1\rangle\langle 1|\} = \{\vec{p_i}, |1\rangle\langle 1|\}\end{aligned}$$

Finally, the average value of the fluctuator value is taken by applying taking the inner product with $\vec{p}_f$.

$$\begin{aligned}\zeta(t) = \{\vec{p}_f^T, I\}\{\vec{p_i}, |0\rangle\langle 1|\}(t) &= \sum_{i=1}^{2} c_{+,i}^2 e^{-i\lambda_{+,i}t}\\ = \{\vec{p}_f^T, I\}\{\vec{p_i}, |1\rangle\langle 0|\}(t) &= \sum_{i=1}^{2} c_{-,i}^2 e^{-i\lambda_{-,i}t}\\ = e^{-\gamma t}\big(\cos(t\sqrt{g^2-\gamma^2}) &+ \frac{\gamma\sin(t\sqrt{g^2-\gamma^2})}{\sqrt{(g^2-\gamma^2)}}\big)\end{aligned}$$

which produces the result of Eq.(2.15).

# Bibliography

[1] Datta Animesh, Flammia Steven T., and Caves Carlton M. Entanglement and the power of one qubit. *Phys. Rev. A*, 72(4):042316, October 2005.

[2] Maziero J., Cèleri L. C., Serra R. M., and Vedral V. Classical and quantum correlations under decoherence. *Phys. Rev. A*, 80(4):044102, October 2009.

[3] Mazzola L., Piilo J., and Maniscalco S. Sudden transition between classical and quantum decoherence. *Phys. Rev. Lett.*, 104(20):200401, May 2010.

[4] Yuri Manin. Vychislimoe i nevychislimoe (computable and noncomputable). *Sov.Radio.*, page 13–15, 1980.

[5] Feynman Richard P. Simulating physics with computers. *Int. Jour. Theo. Phys.*, 21:467–488, 1982.

[6] Feynman Richard P. There's plenty of room at the bottom, 1959. the annual meeting of the AmericanPhysical Society at the CaliforniaInstitute of Technology (Caltech).

[7] Cleve R. and Buhrman H. Substituting quantum entanglement for communication. *Phys. Rev. A*, 56(2):1201, 1997.

[8] Prevedel R., Lu Y., Matthews W., Kaltenbaek R., and Resch K. J. Entanglement-enhanced classical communication over a noisy classical channel. *Phys. Rev. Lett.*, 106(11):110505, March 2011.

[9] Jozsa R. and Linden N. On the role of entanglement in quantum-computational speed-up. *R. Soc. London, Ser. A*, 459(2036):2011, August 2003.

[10] Vidal Guifrè. Efficient classical simulation of slightly entangled quantum computations. *Phys. Rev. Lett.*, 91(14):147902, October 2003.

[11] Gu Mile, Chrzanowski Helen M., Assad Syed M., Symul Thomas, Modi Kavan, Ralph Timothy C., Vedral Vlatko, and Lam Ping Koy. Observing the operational significance of discordconsumption. *Nature Physics*, 8(9):671–675, August 2012.

[12] Michael E., Peskin and Dan V., Schroeder. *An Introduction To Quantum Field Theory*. Westview Press, reprint edition edition, 1995.

[13] Farhi Edward, Goldstone Jeffrey, Gutmann Sam, and Sipser Michael. Quantum computation by adiabatic evolution. *arXiv preprint*, 2000.

[14] Boixo Sergio, Rønnow Troels F., Isakov Sergei V., Wang Zhihui, Wecker David, Lidar Daniel A., Martinis John M., and Troyer Matthias. Evidence for quantum annealing with more than one hundred qubits. *Nature Physics*, 10:218–224, 2014.

[15] Rønnow Troels F., Wang Zhihui, Job Joshua, Boixo Sergio, Isakov Sergei V., Wecker David, Martinis John M., Lidar Daniel A., and Troyer Matthias. Defining and detecting quantum speedup. *arXiv preprint*, 2014.

[16] Michael A., Nielsen and Isaac L., Chuang. *Quantum Computation and Quantum Information*. Cambridge University Press, 10th anniversary edition edition, 2011.

[17] Abrams D. S. and Lloyd S. Quantum algorithm providing exponential speed increase for finding eigenvalues and eigenvectors. *Phys. Rev. Letters*, 83(24):5162–5165, 1999.

[18] Jakóbczyk L. and Siennicki M. Geometry of bloch vectors in two-qubit system. *Phys. Lett. A*, 286:383–390, 2001.

[19] Hawking S. The quantum state of the universe. *Nuc. Phys. B*, 239:257–276, 1984.

[20] Ángel, Rivas and Susana F., Huelga. *Open Quantum Systems*. Springer, 2012.

[21] Zurek Wojciech. Decoherence and the transition from quantum to classical. *arXiv preprint*, 2003.

[22] Dovzhenko Y., Stehlik J., Petersson K. D., Petta J. R., Lu H., and Gossard A. C. Nonadiabatic quantum control of a semiconductor charge qubit. *Phys. Rev. B*, 84:161302, 2011.

[23] Petta J. R., Johnson A. C., Taylor J. M., Laird E. A., Yacoby A., Lukin M. D., Marcus C. M., Hanson M. P., and Gossard A. C. Coherent manipulation of coupled electron spins in semiconductor quantum dots. *Science*, 309:2180, 2005.

[24] Shi Zhan, Simmons C. B., Ward Daniel R., Prance J. R., Mohr R. T., Koh Teck Seng, Gamble John King, Wu Xian, Savage D. E., Lagally M. G., Friesen Mark, Coppersmith S. N., and Eriksson M. A. Coherent quantum oscillations and echo measurements of a si charge qubit. *Phys. Rev. B*, 88:075416, 2013.

[25] Shi Zhan, Simmons C. B., Ward Daniel R., Prance J. R., Wu Xian, Koh Teck Seng, Gamble John King, Savage D. E., Lagally M. G., Friesen Mark, Coppersmith S. N., and Eriksson M. A. Fast coherent manipulation of three-electron states in a double quantum dot. *Nature Communications*, 5:3020, 2014.

[26] Loss Daniel and DiVincenzo David P. Quantum computation with quantum dots. *Phys. Rev. A*, 57:120, 1998.

[27] Michielis Marco De, Ferraro Elena, Fanciulli Marco, and Prati Enrico. Universal set of quantum gates for double-dot exchange-only spin qubits with intradot coupling. *arXiv preprint*, 2014.

[28] Weperen I. van, Armstrong B. D., Laird E. A., Medford J., Marcus C. M., Hanson M. P., and Gossard A. C. Charge-state conditional operation of a spin qubit. *Phys. Rev. Lett.*, 107:030506, 2011.

[29] Fedichkin L., Fedorov A., and Privman V. Measures of decoherence. In *Proceedings of SPIE*, volume 5105, pages 243–254, 2003.

[30] Preskill J. Fault-tolerant quantum computation. *Introduction to quantum computation and information*, pages 213–269, 1998.

[31] Mahan Gerald. *Many-Particle Physics (Physics of Solids and Liquids)*. Springer, 2nd edition, 2000.

[32] Paladino E., Faoro L., Falci G., and Fazio R. Decoherence and 1/f noise in josephson qubits. *Phys. Rev. Letters*, 88(22):228304, 2002.

[33] Schriefl J., Makhlin Y., Shnirman A., and Schon G. Decoherence from ensembles of two-level fluctuators. *New Journal of Physics*, 8(1):1, 2006.

[34] Bergli J., Galperin Y. M., and Altshuler B. L. Decoherence in qubits due to low-frequency noise. *New Journal of Physics*, 11(2):025002, 2009.

[35] Bergli J., Galperin Y. M., and Altshuler B. L. Decoherence of a qubit by non-gaussian noise at an arbitrary working point. *Phys. Rev. B*, 74(2), July 2006.

[36] Muller C., Shnirman A., and Makhlin Y. Relaxation of josephson qubits due to strong coupling to two-level systems. *Phys. Rev. B*, 80(13):134517, 2009.

[37] Zhou D. *Decoherence and disentanglement due to classical noise*. Ph.d. dissertation, University of Wisconsin - Madison, 1150 University Ave. Madison, WI, 53706, US, May 2011.

[38] Reina J. H., Quiroga L., and Johnson N. F. Decoherence of quantum registers. *Phys. Rev. A*, 65(3):032326, 2002.

[39] G. Massimo, Palma, Kalle-Antti, Suominen, and Artur K., Ekert. Quantum computers and dissipation. *Proc. R. Soc. Lond. A*, 452:567–584, 1996.

[40] Duan L. M. and Guo G. C. Reducing decoherence in quantum-computer memory with all quantum bits coupling to the same environment. *Phys. Rev. A*, 57(2):737, 1998.

[41] Nghiem D. and Joynt R. Exact solution of qubit decoherence models by a transfer matrix method. *Phys. Rev. A*, 73(3):032333, 2006.

[42] Joynt R., Zhou D., and Wang Q. H. Quasi-hamiltonian method for computation of decoherence rates. *International Journal of Modern Physics B*, 25(16):2115–2134, 2011.

[43] Cheng B., Wang Q. H., and Joynt R. Transfer matrix solution of a model of qubit decoherence due to telegraph noise. *Phys. Rev. A*, 78(2):022313, 2008.

[44] Zhou D., Lang A., and Joynt R. Disentanglement and decoherence from classical non-markovian noise: random telegraph noise. *Quantum Information Processing*, 9(6):727–747, 2010.

[45] Hu Y., W. Zho Z., Cai J. M., and Guo G. C. Decoherence of coupled josephson charge qubits due to partially correlated low-frequency noise. *Phys. Rev. A*, 75(5):052327, 2007.

[46] Shabani A. Correlated errors can lead to better performanof quantum codes. *Phys. Rev. A*, 77(2):022323, 2008.

[47] Eisntein Albert, Podolsky Boris, and Rosen Nathan. Can quantum-mechanical description of physical reality be considered complete? *Phys. Rev.*, 47:777, 1935.

[48] John Bell. On the einstein podolsky rosen paradox. *Physics*, 3:195, 1964.

[49] Deutsch D. and Jozsa R. Rapid solution of problems by quantum computation. *R. Soc. London, Ser. A*, 439(1907):553, 1992.

[50] BrußD. and Macchiavello C. Multipartite entanglement in quantum algorithms. *Phys. Rev. A*, 83(5):052313, May 2011.

[51] Lloyd S. Quantum search without entanglement. *Phys. Rev. A*, 61(1):010301, 1999.

[52] Meyer D. A. Sophisticated quantum search without entanglement. *Phys. Rev. Lett.*, 85(9):2014, 2000.

[53] Ollivier Harold and Zurek Wojciech H. Quantum discord: A measure of the quantumness of correlations. *Phys. Rev. Lett.*, 88(1):017901, December 2001.

[54] Datta Animesh, Shaji Anil, and Caves Carlton M. Quantum discord and the power of one qubit. *Phys. Rev. Lett.*, 100(5):050502, February 2008.

[55] Passante G., Moussa O., and Laflamme R. Measuring geometric quantum discord using one bit of quantum information. *Phys. Rev. A*, 85(3):032325, 2012.

[56] Rulli C. C. and Sarandy M. S. Global quantum discord in multipartite systems. *Phys. Rev. A*, 84(4):042109, October 2011.

[57] Modi Kavan, Paterek Tomasz, Son Wonmin, Vedral Vlatko, and Williamson Mark. Unified view of quantum and classical correlations. *Phys. Rev. Lett.*, 104(8):080501, February 2010.

[58] Luo Shunlong and Fu Shuangshuang. Geometric measure of quantum discord. *Phys. Rev. A*, 82(3):034302, September 2010.

[59] Xu Jianwei. Geometric measure of quantum discord over two-sided projective measurements. *Phys. Lett. A*, 376(4):320–324, January 2012.

[60] Xu Jianwei. Geometric global quantum discord. *J. Phys. A-Math. Theor.*, 45(40):405304, October 2012.

[61] Grover Lov. A fast quantum mechanical algorithm for database search. *28th ACM Symp. Theory of Comp.*, pages 212–219, 1996.

[62] Knill E. and Laflamme R. Power of one bit of quantum information. *Phys. Rev. Lett.*, 81(25):5672, 1998.

[63] Davide Girolami and Gerardo Adesso. Quantum discord for general two-qubit states: Analytical progress. *Phys. Rev. A*, 83(5):052108, May 2011.

[64] Bellomo Bruno, Giorgi Gian L., Galve Fernando, Franco Rosario L., Compagno Giuseppe, and Zambrini Roberta. Unified view of correlations using the square-norm distance. *Phys. Rev. A*, 85:032104, 2012.

[65] Nguyen Nga and Joynt Robert. Topology of quantum discord. *arXiv preprint*, 2013.

[66] Byrd M. S. and Khaneja N. Characterization of the positivity of the density matrix in terms of the coherence vector representation. *Phys. Rev. A*, 68(6):062322, 2003.

[67] Zhou Dong and Joynt Robert. Disappearance of entanglement: a topological point of view. *Quantum Inf. Process.*, 11(2):571–583, August 2012.

[68] Harrow Aram W. and Montanaro Ashley. Testing product states, quantum merlin-arthur games and tensor optimisation. *arXiv preprint*, 2012.

[69] Shunlong Luo. Quantum discord for two-qubit systems. *Phys. Rev. A*, 77(4):042303, April 2008.

[70] Ali Mazhar, Rau A. R. P., and Alber G. Quantum discord for two-qubit x states. *Phys. Rev. A*, 81(4):042105, April 2010.

[71] Dakić Borivoje, Vedral Vlatko, and Brukner Časlav. Necessary and sufficient condition for nonzero quantum discord. *Phys. Rev. Lett.*, 105(19):190502, November 2010.

[72] Bellomo B., Franco R. Lo, and Compagno G. Dynamics of geometric and entropic quantifiers of correlations in open quantum systems. *Phys. Rev. A.*, 86:012312, 2012.

[73] Franco Rosario, Bellomo Bruno, Masniscalco Sabrina, and Compagno Giuseppe. Dynamics of quantum correlations in two-qubit systems within non-markovian environments. *Int. J. Mod. Phys. B*, 27:1245053, 2013.

[74] Lang Matthias D. and Caves Carlton M. Quantum discord and the geometry of bell-diagonal states. *Phys. Rev. Lett.*, 105(15):150501, October 2010.

[75] Caves Rüdiger, Schackand Carlton M. Explicit product ensembles for separable quantum states. *J. Mod. Optic*, 47(2-3):387–399, February 2000.

[76] Braunstein S. L., Caves C. M., Jozsa R., Linden N., Popescu S., and Schack R. Separability of very noisy mixed states and implications for NMR quantum computing. *Phys. Rev. Lett.*, 83(5):1054, 1999.

[77] Gurvits Leonid and Barnum Howard. Separable balls around the maximally mixed multipartite quantum states. *Phys. Rev. A*, 68(4):042312, October 2003.

[78] Bergqvist G. and Larsson Erik. The higher-order singular value decomposition: Theory and an application [lecture notes. *IEEE Signal Proc. Mag.*, 27(3):151–154, May 2010.

[79] Lathauwer L. De, Moor B. De, and Vandewalle J. A multilinear singular value decomposition. *SIAM J. Matrix. Anal. A*, 21(4):1253–1278, 2000.

[80] Streltsov Alexander, Kampermann Hermann, and BrußDagmar. Simple algorithm for computing the geometric measure of entanglement. *Phys. Rev. A*, 84(2):022323, August 2011.

[81] Thoft-Christensen Palle and Murotsu Yoshisada. The branch-and-bound method. In *Application of Structural Systems Reliability Theory*, pages 215–265. Springer Berlin Heidelberg, Berlin, Heidelberg, 1986.

[82] Ferraro A., Aolita L., Cavalcanti D., Cucchietti F. M., and Acìn A. Almost all quantum states have nonclassical correlations. *Phys. Rev. A*, 81(5):052318, May 2010.

[83] Yu Chang-shui, Li Bo, and Fan Heng. The witness of sudden change of geometric quantum correlation. *Quantum info. and comp.*, 14(5,6):0454–0466, 2013.

[84] Pinto João, Karpat Göktuǒ, and Fanchini Felipe. Sudden change of quantum discord for a system of two qubits. *Phys. Rev. A*, 88:034304, 2013.

[85] Taylor J. M., Petta J. R., Johnson A. C., Yacoby A., Marcus C. M., and Lukin M. D. Relaxation, dephasing, and quantum control of electron spins in double quantum dots. *Phys. Rev. B*, 76:035315, 2007.

[86] DiVincenzo David P. The physical implementation of quantum computation. *arXiv preprint*, 2000.

[87] Koh T., Coppersmith S., and Friesen M. High-fidelity gates in quantum dot spin qubits. *Proc. of Nat. Acad. of Sci.*, 110:19695, 2013.

[88] Koh T., Gamble J., Friesen M., Eriksson M., and Coppersmith S. Pulse-gated quantum-dot hybrid qubit. *Phys. Rev. Lett.*, 109:250503, 2012.

[89] Shi Zhan, Simmons C. B., Prance J. R., Gamble John King, Koh Teck Seng, Shim Yun-Pil, Hu Xuedong, Savage D. E., Lagally M. G., Eriksson M. A., Friesen Mark, and Coppersmith S. N. Fast hybrid silicon double-quantum-dot qubit. *Phys. Rev. Lett.*, 108:140503, 2012.

[90] DiVincenzo D. P., Bacon D., Kempe J., Burkard G., and Whaley K. B. Universal quantum computation with the exchange interaction. *Nature*, 408:339–342, 2000.

[91] Shulman M., Dial O., Harvey S., Bluhm H., Umansky V., and Yacoby A. Demonstration of entanglement of electrostatically coupled singlet-triplet qubits. *Science*, 336:202–205, 2012.

[92] Trifunovic Luka, Dial Oliver, Trif Mircea, Wootton James R., Abebe Rediet, Yacoby Amir, and Loss Daniel. Long-distance spin-spin coupling via floating gates. *Phys. Rev. X*, 2:011006, 2012.

[93] Hu Xuedong and Sarma S. Das. Charge-fluctuation-induced dephasing of exchange-coupled spin qubits. *Phys. Lett. Lett.*, 96:100501, 2006.

[94] Lindblad G. On the generators of quantum dynamical semigroups. *Commun. Math. Phys.*, 48:119–130, 1976.

[95] Hayashi T., Fujisawa T., Cheong H. D., Jeong Y. H., and Hirayama Y. Coherent manipulation of electronic states in a double quantum dot. *Phys. Rev. Lett.*, 91:226804, 2003.

[96] Kurzynski P. Multi-block vector rrepresentation of the qutrit. *Quantum Inf. Comp.*, 11:361, 2011.

[97] Medford J., Beil J., Taylor J. M., Bartlett S. D., Doherty A. C., Rashba E. I., DiVincenzo D. P., Lu H., Gossard A. C., and Marcus C. M. Self-consistent measurement and state tomography of an exchange-only spin qubit. *Nature Nanotechnology*, 8:654–659, 2013.

[98] Hill S. and Wootters W. K. Entanglement of a pair of quantum bits. *Phys. Rev. Lett.*, 78(26):5022, 1997.

[99] Wootters W. K. Entanglement of formation of an arbitrary state of two qubits. *Phys. Rev. Lett.*, 80(10):2245, 1998.